

**MECHANISMS OF PLANT IMMUNE RECEPTOR RPM1 AND ITS ASSOCIATED  
PROTEINS IN DISEASE RESISTANCE**

**Eui-Hwan Chung**

A dissertation submitted to the faculty of the  
University of North Carolina at Chapel Hill in partial fulfillment of  
the requirements for the degree of Doctor of Philosophy in the  
Department of Biology

Chapel Hill  
2011

Approved by:

Professor Jeffrey L. Dangl, Advisor

Professor Joseph J. Kieber, Reader

Professor Jason W. Reed, Reader

Professor Sarah Liljegren, Reader

Professor Sarah R. Grant, Reader

## **ABSTRACT**

Eui-Hwan Chung: Mechanisms of plant immune receptor RPM1 and its associated proteins in disease resistance  
(Under the direction of Jeffrey L. Dangl)

Plants evolved an immune system to recognize specific pathogens, like animals. Recognition of pathogens in plants results in series of outputs such as generation of reactive oxygen species (ROS), cell wall lignification, and a type of programmed cell death (PCD) called the Hypersensitive Response (HR). Plant immune receptor proteins, disease resistance (R) proteins, are the necessity for this recognition process. The R proteins mediate the plant immune response through “direct” or “indirect” recognition of pathogen effector proteins. Our previous works proposed an “indirect” mode of recognition explaining that R proteins can monitor the host targets (guardees) by “guarding” them and sense the host targets modification by pathogen effector proteins. Here I present evidence that the Arabidopsis R protein RPM1 and its interacting protein RIN4 form protein complexes in the plant in the presence/absence of bacterial effector proteins implicating that the immune response regulated by R proteins can be controlled via immune complexes. I demonstrate data for RPM1 or RIN4 containing protein complexes by size exclusion chromatography (SEC). I also present data for putative RPM1 interactors by coimmunoprecipitation-coupled liquid chromatography (LC) / mass spectrometry (MS) / MS. With the known RPM1-interacting partner, RIN4, I defined the specific

mechanisms of the RPM1-mediated immune response in Arabidopsis through the phosphorylation of the residue threonine 166 in RIN4 triggered by two evolutionarily unrelated bacterial effector proteins, AvrRpm1 and AvrB. Furthermore, I found that an important residue in RIN4, phenylalanine 169, is a key for physical interaction between RPM1 and RIN4 resultant in full accumulation and activation of RPM1 in Arabidopsis.

## **ACKNOWLEDGEMENTS**

First of all, I thank to God for His guidance in the whole life.

I am deeply grateful to my wife, Miji Lee, for her extraordinary support and love. To my beloved daughter and son, Kaylee and Nathan, they opened the wonderful world of family life, growing as a beautiful princess-loving girl and a smiling boy. It is a pleasure to thank my parents and parents-in-law for their unconditional love and support. I am also grateful to my brother-in-law, who is always clapping every step of my way.

My advisor, Jeff Dangl, has made me grown with all steps in science from the infant to the toddler now. He has taught me how to be a good scientist in every step by mentoring and understanding my ups and downs and provided all resources necessary for the research. Most of all, I thank to his extreme patience with me when I missed things in a thought process or struggled to build up ideas. It is a great honor of me to work as a citizen in Dangl-Grant lab.

I'm also grateful to Sarah Grant for her great inspiration and supportiveness to the lab every time including me. She also provided a chance to be a teaching assistant in the class that provided a good experience and made me learn more concepts for Genetics. Her smile in every place let me and others always feel happy.

Terry Law has been a constant good friend and made sure that I had everything that I needed to get my works done with great expense to her time and

efforts. She has also advised me how to be a good dad for my kids with sharing her great experiences. There is no way to express my appreciation for her.

A special thanks to past and current colleagues over the years in Dangl-Grant Lab who have discussed and developed ideas to make progress. Thanks to Ai-Jiuan Wu, Karen Cherkis, Luis da Cunha and David Mackey for the achievement of paper based on the chapter 3. Thanks to Zhiyong Gao for helping me finish works at late night. Thanks to Petra Epple, Mindy Roberts and Erica Washington for their critical and careful reading of each chapter to make each sentence much better than I originally wrote. I would like to thank all other members in Dangl-Grant lab. Everyone provided me much easier and delightful life in both science and daily base in his/her own way. It was a great experience to share my time and space with all of you.

Finally to my committee members, Joe Kieber, Jason Reed, and Sarah Liljegren, your help has always been invaluable for my graduate works. I have respectfully appreciated your suggestions and guidance with full of encouragement.

## **DEDICATION**

Dedicated to the holy God

For His guidance in my life,

Dedicated to my family, Miji Lee, Kaylee and Nathan Chung,

For their sacrifice and love,

Dedicated to my parents, Jeegyo Chung and Keumsook Yang,

For their unconditional love,

Dedicated to my parents-in-law, Dongkeun Lee and Byungok Cheon,

For their encouragement and love,

I love you all!

## TABLE OF CONTENTS

LIST OF TABLES.....	ix
LIST OF FIGURES.....	x
CHAPTER	
I. INTRODUCTION.....	1
Abstract.....	1
References.....	10
II. PROTEIN COMPLEXES ASSOCIATED WITH THE ARABIDOPSIS IMMUNE RECEPTOR RPM1.....	15
Abstract.....	15
Introduction.....	17
Results.....	20
Discussion.....	41
Materials and Methods.....	54
References.....	58
III. SPECIFIC THREONINE PHOSPHORYLATION OF A HOST TARGET MEDIATED BY TWO UNRELATED TYPE III EFFECTOR PROTEINS RESULTS IN ACTIVATION A HOST INNATE IMMUNE RECEPTOR IN PLANTS.....	64
Preface.....	64
Abstract.....	64

Introduction.....	66
Results.....	70
Discussion.....	102
Materials and Methods.....	107
References.....	114
IV. CONCLUSIONS AND FUTURE DIRECTIONS.....	118
Background and Significance.....	118
Future Directions.....	122
References.....	130

## LIST OF TABLES

### TABLE

2.1. Proteins identified at least three different conditions .....	40
2.2. Protein IDs identified under medium stringency washing condition.....	45
3.1. Summary of RIN4 BBS for interaction and function with effector Proteins and RPM1.....	101

## LIST OF FIGURES

### FIGURE

2.1.	Normalization of size exclusion chromatography (SEC) .....	21
2.2.	Distribution of RPM1 and RIN4 in different buffer conditions.....	23
2.3.	Distribution of RPM1 and RIN4 in harsh extraction conditions.....	25
2.4.	Distribution of RPM1 and RIN4 in response to bacterial effectors.....	27
2.5.	Distribution of RPM1 and RIN4 in effector-expressing transgenic plants.....	29
2.6.	RIN4 distribution is unchanged in <i>rps2</i> .....	31
2.7.	Self-association of RPM1 in Arabidopsis.....	32
2.8.	Schematic diagram depicting the isolation of plant protein Complexes by coimmunoprecipitation.....	34
2.9.	Coimmunoprecipitation of RIN4 with RPM1 or AvrRpm1.....	35
2.10.	Proteins identified by LC/MS/MS analysis from Co-IPs performed using three different washing conditions. ....	38
3.1.	The C-terminal NOI of RIN4 is required for RPM1 function .....	71
3.2.	Point mutations in RIN4 BBS residues that contact AvrB alter interaction with AvrB in Yeast Two-hybrid system.....	74
3.3.	RPM1-dependent HR triggered by AvrB and mediated by RIN4 can be reconstructed in <i>Nicotiana benthamiana</i> using Agrobacterium-mediated transient gene expression.....	75
3.4.	RIN4 T166D is required for AvrB-mediated RPM1-dependent HR in <i>Nicotiana benthamiana</i> and a phosphomimic of this residue confers effector independent RPM1 activation.....	79
3.5.	RIN4 T166D activity is dependent on RPM1 P-loop function in <i>Nicotiana benthamiana</i> .....	80
3.6.	RIN4 T166D does not confer RPM1-independent HR.....	83

3.7.	RIN4 T166D retains cleavage by AvrRpt2 in <i>Nicotiana benthamiana</i> .....	85
3.8.	RIN4 T166 contributes to AvrRpm1-dependent RPM1-mediated HR in <i>N. benthamiana</i> .....	87
3.9.	RIN4 T166D drives ectopic cell death and elevated PR-1 expression in the presence of RPM1.....	89
3.10.	RIN4 T166 is required for AvrB-, and contributes to AvrRpm1-dependent, RPM1-mediated HR in Arabidopsis.....	92
3.11.	RIN4 BBS residues contribute to effector activation of RPM1 HR ....	93
3.12.	RIN4 T166 residue is phosphorylated by AvrB and AvrRpm1 <i>in planta</i> .....	95
3.13.	Differential coimmunoprecipitation of RPM1 with RIN4 BBS mutants identifies residues required for interaction and RPM1 accumulation.....	98
4.1.	Working model of RPM1-mediated HR with RIN4 phosphorylation on T166.....	121
4.2.	RPM1 complexes in an “inactive” and “active” state in Arabidopsis .....	123
4.3.	PAMP-triggered phenotype of RIN4 phosphorylation mutants.....	126
4.4.	Phenotypes of autoactive RPM1 alleles with RIN4 and RIN4 mutants.....	129

## **CHAPTER 1**

### **INTRODUCTION**

#### **ABSTRACT**

In the past few years, several important publications have significantly enhanced the understanding of plant defense mechanisms. The most important discoveries involve the so-called “guard hypothesis”, which provides one possibility of how disease resistance (R) proteins mediate immune responses in plants. This theory suggests that indirect interaction of pathogen-derived proteins and plant resistance proteins of the nucleotide-binding, leucine rich repeat (NB-LRR) protein family is mediated by binding and recognition of modification of host target proteins by these NB-LRRs to initiate host defense mechanisms. The critical domains in NB-LRR proteins for this initial perception of pathogen attack, with or without host target proteins, were determined in many different experimental systems. This insight demonstrates how plants, with a limited set of NB-LRR proteins are able to respond to a wide variety of pathogen virulence factors. In addition, the Guard Hypothesis proposed that intra- or inter-molecular interactions of NB-LRR proteins may function as a mode of signaling

control, shifting the defense response system from the “inactive” to “active” state. There is also a significant body of emerging evidence suggesting that pathogen proteins target and modify these same host proteins to benefit the pathogen by suppressing plant defense signaling pathways. Host target proteins also interact and cooperate with NB-LRRs to determine the specificity for recognition of pathogen and initiation of immune response.

## **INTRODUCTION**

Plants utilize a two-layer, innate immune system to prevent the invasion and growth of pathogens. The primary level of defense uses membrane-localized receptors that detect pathogen-associated molecular patterns (PAMPs) (Chisholm et al., 2006; Dangl and Jones, 2001; Dangl and McDowell, 2006; Jones and Dangl, 2006). To overcome PAMP-triggered immunity (PTI) from plants, pathogens have evolved effector proteins and injected them into plant cells through type III secretion systems (T3SS). Co-evolution between pathogens and plants led to effector-triggered immunity (ETI), to overcome PTI suppression by employing disease resistance (R) proteins. ETI results in robust host defense responses such as the hypersensitive response (HR), massive production of reactive oxygen species (ROS), and transcriptional reprogramming (Heath, 2000).

Pathogenic bacteria deliver a mixture of effector proteins directly into plant cells via the type III secretion system (T3SS), a pilus-like structure (Cunnac et al., 2004; Lindeberg et al., 2004; Zwiesler-Vollick et al., 2002). Bacterial effectors are diverse among even closely related strains and are key components to determine host range (Stavrinos et al., 2008). Effectors dampen a variety of cellular processes in the host defense system. Recently, extensive biochemical and functional studies have been performed to determine how T3SS effectors support the successful growth of bacteria by suppressing the host immune system. One well characterized function of some effectors is protease activity, which directly cleaves

host target proteins (Axtell and Staskawicz, 2003; Chisholm et al., 2005; Nimchuk et al., 2007; Shao et al., 2003). The T3SS effector protein AvrPphE in *P. syringae* acts as a cysteine protease with a conserved N-terminus catalytic triad (Nimchuk et al., 2007). AvrPphB also proteolyzes PBS1 and other PBS1-like (PBL) kinases in Arabidopsis leading to suppression of FLS2, a well-characterized PAMP receptor (Shao et al., 2003; Zhang et al., 2010). AvrRpt2 can cleave the host target RIN4, increasing the virulence of *P. syringae* in an SA-independent manner (Chen et al., 2004). Additionally, AvrRpt2 cleaves RIN4-like proteins in Arabidopsis which contain conserved cleavage sites for the cysteine protease recognition and cleavage (Chisholm et al., 2005; Wu and Dangl, unpublished data).

Some bacterial effectors can modify host target proteins through phosphorylation/dephosphorylation or ubiquitination (Bretz et al., 2003; Espinosa et al., 2003; Janjusevic et al., 2006; Mackey et al., 2002; Nomura et al., 2006). AvrRpm1 and AvrB trigger phosphorylation of host target RIN4 (Chung et al., 2011; Mackey et al., 2002). Interestingly, AvrB can induce phosphorylation of MPK4 (mitogen activated protein kinase 4), a negative regulator of basal defense, and perturbs hormonal signaling of the host to enhance susceptibility (Cui et al., 2010). Conversely, HopPtoD2 suppresses HR and defense gene expression via tyrosine phosphatase activity, indicating that dephosphorylation of HopPtoD2 may suppress MAP kinase signaling, a well-characterized pathway of PTI (Espinosa and Alfano, 2004; Petnicki-Ocwieja et al., 2002). HopF2 disrupts Arabidopsis innate immunity by blocking PTI mediated by MAPKs through MKK5 (MAP kinase kinase 5) with ADP-ribosyltransferase activity (Wang et al., 2010). HopF2 also hinders phosphorylation

of BIK1, a plasma membrane-associated cytoplasmic kinase, induced by PAMPs (Lu et al., 2010). AvrPtoB containing a C-terminal E3-ligase suppresses PTI mediated by the receptor-like kinase, FLS2, in tomato through E3-ligase activity (Abramovitch et al., 2006; Janjusevic et al., 2006). In Arabidopsis, HopM1 suppresses callose deposition, an output of PTI (DebRoy et al., 2004), causing proteasome-dependent degradation of multiple proteins (Nomura et al., 2006). Many other effectors are involved in increasing the virulence effect of bacteria via their functions as transcription factors (Fujikawa et al., 2006; Kearney and Staskawicz, 1990) and glycerolphosphoryl diester phosphodiesterases (Swords et al., 1996) in another phytopathogen, *Xanthomonas campestris*.

The structures of the majority of R proteins are highly conserved, with a diverse N-terminal region and both nucleotide-binding (NB) and leucine-rich repeat (LRR)-domains. Plant NB-LRR proteins are structurally and functionally conserved and similar to animal NLR innate immune receptors (Ting et al., 2008). The structure-function relationships of NB-LRR proteins have been intensively investigated. The CC or TIR N-terminal variable regions likely serve as a platform for homodimerization in signal transduction allowing for the perception of signal (Ade et al., 2007; Burch-Smith et al., 2007; Shen et al., 2007). The NB domain is composed of an ATP-binding site known as P-loop, a Walker-B motif for ATP hydrolysis, and a MHD motif (Tameling et al., 2006; van Ooijen et al., 2007). ATP binding and hydrolysis are considered as a common feature of NB-LRR activation in I-1 and Mi-1 (Tameling et al., 2002). Currently, it has been proposed that the NB domain may function as a switch for NB-LRR activation. In the active state after perceiving

pathogen invasion, ATP binds to an NB-LRR leading to ATP-hydrolysis to initiate the NB-LRR mediated defense responses. The LRR domains are necessary for recognition specificity as well as direct effector interaction in several cases (Dodds et al., 2006; Krasileva et al., 2010). In the inactive state, NB-LRR proteins form intramolecular interactions with N- and C-terminal domains (Leister et al., 2005; Moffett et al., 2002; Rairdan and Moffett, 2006). Inter-molecular associations of NB-LRRs have been observed through the N-terminal variable region and/or NB domains (Ade et al., 2007; Gutierrez et al., 2010; Mestre and Baulcombe, 2006).

The involvement of the N-terminal region of NB-LRR proteins has been investigated despite the role of LRR domains for pathogen specificity via receptor-ligand binding (Hwang et al., 2000; Luck et al., 2000; Mucyn et al., 2006). In tomato, the NB-LRR protein Prf is required for disease resistance against *Pseudomonas syringae* expressing AvrPto and AvrPtoB. This interaction is mediated by the tomato protein kinase Pto. A unique extended N-terminus of Prf interacts with Pto which recognizes AvrPtoB, indicating that alteration or modification of Pto initiates the molecular switch of Prf through its N-terminal domain (Mucyn et al., 2006). Also, the N-terminus of RPS5 in Arabidopsis and N in tobacco interact with PBS1 and TMV p50 helicases, respectively, which supports that the initial binding to interactors with the N-terminal domain of NB-LRR has a pivotal function to elicit NB-LRR activation (Ade et al., 2007; Burch-Smith et al., 2007). The CC domain of MLA10, an NB-LRR protein in barley (*Hordeum vulgare*), interacts with HvWRKY1 and HvWRKY2 *in vitro* and *in planta* with the virulence effector AvrA10 to trigger immune responses (Shen et al., 2007). Moreover, Rx, a CC-NB-LRR protein, functions via interaction with a

Ran GTPase-Activating protein2 (RanGAP2), through the CC domain to recognize the viral coat protein of Potato virus X (PVX) in the potato immune system (Tameling and Baulcombe, 2007).

In Arabidopsis, RPS5 forms a complex with PBS1 through its CC domain to trigger immune responses to bacteria containing the protease effector protein AvrPphB (Ade et al., 2007). RPM1 interacts with RIN4 *in vitro* and *in planta* (Chung et al., 2011; Holt III et al., 2002; Mackey et al., 2002) and consistent with other examples, the CC (1-176) domain of RPM1 interacts with RIN4 *in vitro* (Holt III et al., 2002). A recent study of Pi-ta, a rice NB-LRR protein which confers resistance to rice blast fungus, found that it interacts with the rice GTPase OsRac1 on the plasma membrane via the NB domain of Pi-ta to contribute to HR and ROS generation (Kawano et al., 2010). Importantly, the LRR domain is also sufficient for interaction and recognition of pathogen attack. Pi-ta binds directly to its effector protein (AvrPi-ta) dependent on its LRR domain in rice (Jia et al., 2000). The recognition and function of a flax rust resistance (L) protein requires the LRR domain to determine specificity (Ellis et al., 2007). The interplay of N-terminus and LRR domain for NB-LRR recognition has been reported in the N protein of tobacco (*Nicotiana tabacum*). The N interacts with p50, a subunit of tobacco mosaic virus replicase, through NRIP1 resulting in a series of binding to and recognition by the LRR domain of N (Caplan et al., 2008). Overall, the diversity of recognition to pathogen proteins requires specific protein domains such as the N-terminus, NB, or LRR, which must recognize host target proteins. Inter-molecular Interactions among these domains in NB-LRR proteins are required for a strong immune response.

RPM1, a CC-NB-LRR protein in Arabidopsis, interacts with RIN4 (Boyes et al., 1998; Mackey et al., 2002). RPM1 initiates immune responses by recognizing RIN4 modification, which is mediated by one of two unrelated T3SS effectors, AvrRpm1 and AvrB (Mackey, 2002). Both AvrRpm1 and AvrB also localize to the host plasma membrane by acylation after delivery (Nimchuk et al., 2000) and phosphorylate RIN4 at threonine 166 for full or partial activation of RPM1 for AvrB or AvrRpm1, respectively (Chung et al., 2011). RIN4 is required for full accumulation of RPM1 on the plasma membrane and functions as a negative regulator for PTI (Boyes et al., 1998; Kim et al., 2005). Two other different bacterial effectors target RIN4 in different ways. AvrRpt2 in *P. syringae* induces RPS2-mediated immune responses in Arabidopsis via cleavage of RIN4 (Axtell and Staskawicz, 2003; Mackey et al., 2003). Recently, HopF2 was shown to interact with RIN4 *in vitro* and *in vivo*. HopF2 enhances growth of *P. syringae* indicating the virulence function of HopF2 through RIN4 (Wilton et al., 2010), possibly by ADP-ribosylation (Wang et al., 2010). RIN4 is also important for PTI, as MPK4 interacts and phosphorylates RIN4 in response to flg22, a flagellin PAMP peptide (Cui et al., 2010). Potential phosphorylation sites of RIN4 by flg22 treatment have been identified (Benschop et al., 2007; Nuhse et al., 2007; Nuhse et al., 2004). A receptor-like cytoplasmic kinase RIPK (RIN4 interacting protein kinase), a subfamily of PBS1 which mediates RPS5-dependent immune response in Arabidopsis, phosphorylates RIN4 at threonine 21, serine 160, and threonine 166 residue. RIPK interacts with RIN4 competing with AvrB and leading to the phosphorylation of RIN4 and AvrB, and functions as a negative regulator for ETI and PTI (Liu et al., 2011).

The function and mechanism of activation of several NB-LRRs has been extensively studied, though no general model has emerged. In our lab, a detailed mode of action for RPM1 has not been clearly uncovered, although it has been found to share structural homology with other mechanistically well-characterized CC-NB-LRR proteins. These similarities include the homodimerization of RPM1, possession of domains necessary for dimerization, the fine-tuned activation of RPM1 through host target RIN4, AvrRpm1- and AvrB-dependent immune responses of RPM1, and the role of ATP binding and hydrolysis in proper RPM1 function. Although the regulation of RIN4 by phosphorylation with multiple candidate kinases has been defined in great detail, further elucidation is needed for 1) whether AvrB-induced phosphorylation of MPK4 can induce the phosphorylation of RIN4, if so, 2) what residues are phosphorylated on RIN4 by AvrB through MPK4 activation, 3) what is the role of phosphorylated residues on RIN4 induced by RIPK in PTI and 4) what different phosphorylation can be induced by effector (AvrB) and PAMP (flg22). The efforts to answer these questions will broaden our understanding of how plants response to biotic stresses triggered by pathogens.

## **REFERENCES**

- Abramovitch, R.B., Janjusevic, R., Stebbins, C.E., and Martin, G.B. (2006). Type III effector AvrPtoB requires intrinsic E3 ubiquitin ligase activity to suppress plant cell death and immunity. *Proceedings of the National Academy of Sciences of the United States of America* *103*, 2851-2856.
- Ade, J., DeYoung, B.J., Golstein, C., and Innes, R.W. (2007). Indirect activation of a plant nucleotide binding site-leucine-rich repeat protein by a bacterial protease. *Proc Natl Acad Sci U S A* *104*, 2531-2536.
- Axtell, M.J., and Staskawicz, B.J. (2003). Initiation of *RPS2*-specified disease resistance in Arabidopsis is coupled to the AvrRpt2-directed elimination of RIN4. *Cell* *112*, 369-377.
- Benschop, J.J., Mohammed, S., O'Flaherty, M., Heck, A.J., Slijper, M., and Menke, F.L. (2007). Quantitative phosphoproteomics of early elicitor signaling in Arabidopsis. *Mol Cell Proteomics* *6*, 1198-1214.
- Boyes, D.C., Nam, J., and Dangl, J.L. (1998). The Arabidopsis thaliana RPM1 disease resistance gene product is a peripheral plasma membrane protein that is degraded coincident with the hypersensitive response. *Proc Natl Acad Sci U S A* *95*, 15849-15854.
- Bretz, J.R., Mock, N.M., Charity, J.C., Zeyad, S., Baker, C.J., and Hutcheson, S.W. (2003). A translocated protein tyrosine phosphatase of *Pseudomonas syringae* pv. tomato DC3000 modulates plant defence response to infection. *Mol Microbiol* *49*, 389-400.
- Burch-Smith, T.M., Schiff, M., Caplan, J.L., Tsao, J., Czymmek, K., and Dinesh-Kumar, S.P. (2007). A novel role for the TIR domain in association with pathogen-derived elicitors. *PLoS Biol* *5*, e68.
- Caplan, J.L., Mamillapalli, P., Burch-Smith, T.M., Czymmek, K., and Dinesh-Kumar, S.P. (2008). Chloroplastic protein NRIP1 mediates innate immune receptor recognition of a viral effector. *Cell* *132*, 449-462.
- Chen, Z., Kloek, A.P., Cuzick, A., Moeder, W., Tang, D., Innes, R.W., Klessig, D.F., McDowell, J.M., and Kunkel, B.N. (2004). The *Pseudomonas syringae* type III effector AvrRpt2 functions downstream or independently of SA to promote virulence on Arabidopsis thaliana. *Plant J* *37*, 494-504.
- Chisholm, S.T., Coaker, G., Day, B., and Staskawicz, B.J. (2006). Host-Microbe Interactions: Shaping the Evolution of the Plant Immune Response. *Cell* *124*, 803-814.
- Chisholm, S.T., Dahlbeck, D., Krishnamurthy, N., Day, B., Sjolander, K., and Staskawicz, B.J. (2005). Molecular characterization of proteolytic cleavage sites of the *Pseudomonas syringae* effector AvrRpt2. *PNAS* *102*, 2087-2092.
- Chung, E.H., da Cunha, L., Wu, A.J., Gao, Z., Cherkis, K., Afzal, A.J., Mackey, D., and Dangl, J.L. (2011). Specific Threonine Phosphorylation of a Host Target by Two Unrelated Type III Effectors Activates a Host Innate Immune Receptor in Plants. *Cell Host & Microbe* *9*, 125-136.

Cui, H., Wang, Y., Xue, L., Chu, J., Yan, C., Fu, J., Chen, M., Innes, R.W., and Zhou, J.M. (2010). *Pseudomonas syringae* effector protein AvrB perturbs Arabidopsis hormone signaling by activating MAP kinase 4. *Cell Host Microbe* 7, 164-175.

Cunnac, S., Occhialini, A., Barberis, P., Boucher, C., and Genin, S. (2004). Inventory and functional analysis of the large Hrp regulon in *Ralstonia solanacearum*: identification of novel effector proteins translocated to plant host cells through the type III secretion system. *Mol Microbiol* 53, 115-128.

Dangl, J.L., and Jones, J.D. (2001). Plant pathogens and integrated defence responses to infection. *Nature* 411, 826-833.

Dangl, J.L., and McDowell, J.M. (2006). Two modes of pathogen recognition by plants. *Proc Natl Acad Sci U S A* 103.

DebRoy, S., Thilmony, R., Kwack, Y.-B., Nomura, K., and He, S.Y. (2004). A family of conserved bacterial effectors inhibits salicylic acid-mediated basal immunity and promotes disease necrosis in plants. *Proc Natl Acad Sci U S A* 101, 9927-9932.

Dodds, P.N., Lawrence, G.J., Catanzariti, A.-M., Teh, T., Wang, C.-I.A., Ayliffe, M.A., Kobe, B., and Ellis, J.G. (2006). Direct protein interaction underlies gene-for-gene specificity and coevolution of the flax resistance genes and flax rust avirulence genes. *Proc Natl Acad Sci U S A* 103, 8888-8893.

Ellis, J.G., Dodds, P.N., and Lawrence, G.J. (2007). Flax rust resistance gene specificity is based on direct resistance-avirulence protein interactions. *Annu Rev Phytopathol* 45, 289-306.

Espinosa, A., and Alfano, J.R. (2004). Disabling surveillance: bacterial type III secretion system effectors that suppress innate immunity. *Cellular Microbiology* 6, 1027-1040.

Espinosa, A., Guo, M., Tam, V.C., Fu, Z.Q., and Alfano, J.R. (2003). The *Pseudomonas syringae* type III-secreted protein HopPtoD2 possesses protein tyrosine phosphatase activity and suppresses programmed cell death in plants. *Mol Microbiol* 49, 377-387.

Fujikawa, T., Ishihara, H., Leach, J.E., and Tsuyumu, S. (2006). Suppression of defense response in plants by the *avrBs3/pthA* gene family of *Xanthomonas* spp. *Molecular plant-microbe interactions : MPMI* 19, 342-349.

Gutierrez, J.R., Balmuth, A.L., Ntoukakis, V., Mucyn, T.S., Gimenez-Ibanez, S., Jones, A.M., and Rathjen, J.P. (2010). Prf immune complexes of tomato are oligomeric and contain multiple Pto-like kinases that diversify effector recognition. *The Plant journal : for cell and molecular biology* 61, 507-518.

Heath, M.C. (2000). Hypersensitive response-related death. *Plant Mol Biol* 44, 321-334.

Holt III, B.F., Boyes, D.C., Ellerstrom, M., Siefers, N., Wiig, A., Kauffman, S., Grant, M.R., and Dangl, J.L. (2002). An evolutionarily conserved mediator of plant disease resistance gene function is required for normal Arabidopsis development. *Dev Cell* 2, 807-817.

Hwang, C.-F., Bhakta, A.V., Truesdell, G.M., Pudlo, W., and Williamson, V.M. (2000). Evidence for a role of the N terminus and leucine-rich repeat region of the *Mi* gene product in regulation of localized cell death. *Plant Cell* 12, 1319-1329.

Janjusevic, R., Abramovitch, R.B., Martin, G.B., and Stebbins, C.E. (2006). A bacterial inhibitor of host programmed cell death defenses is an E3 ubiquitin ligase. *Science* 311, 222-226.

Jia, Y., McAdams, S.A., Bryan, G.T., Hershey, H.P., and Valent, B. (2000). Direct interaction of resistance gene and avirulence gene products confers rice blast resistance. *EMBO J* 19, 4004-4014.

Jones, J.D., and Dangl, J.L. (2006). The plant immune system. *Nature* 444, 323-329.

Kawano, Y., Akamatsu, A., Hayashi, K., Housen, Y., Okuda, J., Yao, A., Nakashima, A., Takahashi, H., Yoshida, H., Wong, H.L., *et al.* (2010). Activation of a Rac GTPase by the NLR family disease resistance protein Pit plays a critical role in rice innate immunity. *Cell Host & Microbe* 7, 362-375.

Kearney, B., and Staskawicz, B.J. (1990). Widespread distribution and fitness contribution of *Xanthomonas campestris* avirulence gene *avrBs2*. *Nature* 346, 385-386.

Kim, M.-G., da Cunha, L., Belkadir, Y., DebRoy, S., Dangl, J.L., and Mackey, D. (2005). Two *Pseudomonas syringae* type III effectors inhibit RIN4-regulated basal defense in *Arabidopsis*. *Cell* 121, 749-759.

Krasileva, K.V., Dahlbeck, D., and Staskawicz, B.J. (2010). Activation of an Arabidopsis resistance protein is specified by the in planta association of its leucine-rich repeat domain with the cognate oomycete effector. *The Plant Cell* 22, 2444-2458.

Leister, R.T., Dahlbeck, D., Day, B., Li, Y., Chesnokova, O., and Staskawicz, B.J. (2005). Molecular genetic evidence for the role of SGT1 in the intramolecular complementation of Bs2 protein activity in *Nicotiana benthamiana*. *Plant Cell* 17, 1268-1278.

Lindeberg, M., Stavrinides, J., Chang, J.H., Alfano, J.R., Collmer, A., Dangl, J.L., Greenberg, J.T., Mansfield, J.W., and Guttman, D.S. (2004). Unified nomenclature and phylogenetic analysis of extracellular proteins delivered by the type III secretion system of the plant pathogenic bacterium *Pseudomonas syringae*. unpublished.

Liu, J., Elmore, J.M., Lin, Z.J., and Coaker, G. (2011). A Receptor-like Cytoplasmic Kinase Phosphorylates the Host Target RIN4, Leading to the Activation of a Plant Innate Immune Receptor. *Cell Host & Microbe* 9, 137-146.

Lu, D., Wu, S., Gao, X., Zhang, Y., Shan, L., and He, P. (2010). A receptor-like cytoplasmic kinase, BIK1, associates with a flagellin receptor complex to initiate plant innate immunity. *Proceedings of the National Academy of Sciences of the United States of America* 107, 496-501.

Luck, J.E., Lawrence, G.J., Dodds, P.N., Shepherd, K.W., and Ellis, J.G. (2000). Regions outside of the leucine-rich repeats of Flax Rust resistance proteins play a role in specificity determination. *Plant Cell* 12, 1367-1377.

- Mackey, D., Belkhadir, Y., Alonso, J.M., Ecker, J.R., and Dangl, J.L. (2003). Arabidopsis RIN4 is a target of the type III virulence effector AvrRpt2 and modulates RPS2-mediated resistance. *Cell* 112, 379-389.
- Mackey, D., Holt, B.F., 3rd, Wiig, A., and Dangl, J.L. (2002). RIN4 interacts with *Pseudomonas syringae* type III effector molecules and is required for RPM1-mediated resistance in Arabidopsis. *Cell* 108, 743-754.
- Mestre, P., and Baulcombe, D.C. (2006). Elicitor-mediated oligomerization of the tobacco N disease resistance protein. *Plant Cell* 18, 491-501.
- Moffett, P., Farnham, G., Peart, J., and Baulcombe, D.C. (2002). Interaction between domains of a plant NBS-LRR protein in disease resistance-related cell death. *Embo J* 21, 4511-4519.
- Mucyn, T.S., Clemente, A., Andriotis, V.M., Balmuth, A.L., Oldroyd, G.E., Staskawicz, B.J., and Rathjen, J.P. (2006). The tomato NBARC-LRR protein Prf interacts with Pto kinase in vivo to regulate specific plant immunity. *Plant Cell* 18, 2792-2806.
- Nimchuk, Z., Marois, E., Kjemtrup, S., Leister, R.T., Katagiri, F., and Dangl, J.L. (2000). Eukaryotic fatty acylation drives plasma membrane targeting and enhances function of several type III effector proteins from *Pseudomonas syringae*. *Cell* 101, 353-363.
- Nimchuk, Z.L., Fisher, E.J., Desveaux, D., Chang, J.H., and Dangl, J.L. (2007). The HopX (AvrPphE) family of *Pseudomonas syringae* type III effectors require a catalytic triad and a novel N-terminal domain for function. *Mol Plant Microbe Interact* 20, 346-357.
- Nomura, K., Debroy, S., Lee, Y.H., Pumplin, N., Jones, J., and He, S.Y. (2006). A bacterial virulence protein suppresses host innate immunity to cause plant disease. *Science* 313, 220-223.
- Nuhse, T.S., Bottrill, A.R., Jones, A.M., and Peck, S.C. (2007). Quantitative phosphoproteomic analysis of plasma membrane proteins reveals regulatory mechanisms of plant innate immune responses. *Plant J* 51, 931-940.
- Nuhse, T.S., Stensballe, A., Jensen, O.N., and Peck, S.C. (2004). Phosphoproteomics of the Arabidopsis plasma membrane and a new phosphorylation site database. *Plant Cell* 16, 2394-2405.
- Petnicki-Ocwieja, T., Schneider, D.J., Tam, V.C., Chancey, S.T., Shan, L., Jamir, Y., Schechter, L.M., Janes, M.D., Buell, C.R., Tang, X., *et al.* (2002). Genomewide identification of proteins secreted by the Hrp type III protein secretion system of *Pseudomonas syringae* pv. tomato DC3000. *Proc Natl Acad Sci U S A* 99, 7652-7657.
- Rairdan, G.J., and Moffett, P. (2006). Distinct Domains in the ARC Region of the Potato Resistance Protein Rx Mediate LRR Binding and Inhibition of Activation 10.1105/tpc.106.042747. *Plant Cell*, tpc.106.042747.
- Shao, F., Golstein, C., Ade, J., Stoutemyer, M., Dixon, J.E., and Innes, R.W. (2003). Cleavage of Arabidopsis PBS1 by a bacterial type III effector. *Science* 301, 1230-1233.

Shen, Q.-H., Saijo, Y., Mauch, S., Biskup, C., Bieri, S., Keller, B., Seki, H., Ulker, B., Somssich, I.E., and Schulze-Lefert, P. (2007). Nuclear Activity of MLA Immune Receptors Links Isolate-Specific and Basal Disease-Resistance Responses [10.1126/science.1136372](https://doi.org/10.1126/science.1136372). *Science* *315*, 1098-1103.

Stavrinos, J., McCann, H.C., and Guttman, D.S. (2008). Host-pathogen interplay and the evolution of bacterial effectors. *Cell Microbiol* *10*, 285-292.

Swords, K.M.M., Dahlbeck, D., Kearney, B., Roy, M., and Staskawicz, B.J. (1996). Spontaneous and induced mutations in a single open reading frame alter both virulence and avirulence in *Xanthomonas campestris* pv. *vesicatoria* *avrBs2*. *J Bacteriol* *178*, 4661-4669.

Tameling, W.I., and Baulcombe, D.C. (2007). Physical association of the NB-LRR resistance protein Rx with a Ran GTPase-activating protein is required for extreme resistance to Potato virus X. *The Plant Cell* *19*, 1682-1694.

Tameling, W.I.L., Elzinga, S.D.J., Darmin, P.S., Vossen, J.H., Takken, F.L.W., Haring, M.A., and Cornelissen, B.J.C. (2002). The tomato *R* gene products I-2 and Mi-1 are functional ATP-binding proteins with ATPase activity. *Plant Cell* *14*, 2929-2939.

Tameling, W.I.L., Vossen, J.H., Albrecht, M., Lengauer, T., Berden, J.A., Haring, M.A., Cornelissen, B.J.C., and Takken, F.L.W. (2006). Mutations in the NB-ARC Domain of I-2 That Impair ATP Hydrolysis Cause Autoactivation [10.1104/pp.105.073510](https://doi.org/10.1104/pp.105.073510). *Plant Physiol* *140*, 1233-1245.

Ting, J.P., Lovering, R.C., Alnemri, E.S., Bertin, J., Boss, J.M., Davis, B.K., Flavell, R.A., Girardin, S.E., Godzik, A., Harton, J.A., *et al.* (2008). The NLR gene family: a standard nomenclature. *Immunity* *28*, 285-287.

van Ooijen, G., van den Burg, H.A., Cornelissen, B.J., and Takken, F.L. (2007). Structure and function of resistance proteins in solanaceous plants. *Annu Rev Phytopathol* *45*, 43-72.

Wang, Y., Li, J., Hou, S., Wang, X., Li, Y., Ren, D., Chen, S., Tang, X., and Zhou, J.M. (2010). A *Pseudomonas syringae* ADP-ribosyltransferase inhibits Arabidopsis mitogen-activated protein kinase kinases. *Plant Cell* *22*, 2033-2044.

Wilton, M., Subramaniam, R., Elmore, J., Felsensteiner, C., Coaker, G., and Desveaux, D. (2010). The type III effector HopF2Pto targets Arabidopsis RIN4 protein to promote *Pseudomonas syringae* virulence. *Proc Natl Acad Sci U S A* *107*, 2349-2354.

Zhang, J., Li, W., Xiang, T., Liu, Z., Laluk, K., Ding, X., Zou, Y., Gao, M., Zhang, X., Chen, S., *et al.* (2010). Receptor-like cytoplasmic kinases integrate signaling from multiple plant immune receptors and are targeted by a *Pseudomonas syringae* effector. *Cell Host Microbe* *7*, 290-301.

Zwiesler-Vollick, J., Plovanich-Jones, A.E., Nomura, K., Bandyopadhyay, S., Joardar, V., Kunkel, B.N., and He, S.Y. (2002). Identification of novel hrp-regulated genes through functional genomic analysis of the *Pseudomonas syringae* pv. *tomato* DC3000 genome. *Mol Microbiol* *45*, 1207-1218.

## CHAPTER 2

### Protein complexes associated with the Arabidopsis immune receptor RPM1

#### ABSTRACT

The majority of plant disease resistance (R) genes involved in the plant immune system contain Nucleotide-Binding site and Leucine Rich Repeat domains (NB-LRR). There is a paucity of knowledge regarding where NB-LRR proteins are localized in the plant cell and how they are activated by pathogen-encoded proteins during the initiation of disease resistance responses. Plant pathogenic bacteria deliver virulence factors through the evolutionarily conserved type III secretion system; these are termed type III effector proteins. Some type III effector proteins are the genetic determinants of plant disease resistance; in these instances they are termed avirulence (Avr) proteins. Here, I used size exclusion chromatography (SEC) to analyze the effect of two different type III effector proteins, AvrRpm1 and AvrB, from the bacterial pathogen *Pseudomonas syringae*, on the Arabidopsis target RIN4 (RPM1 interacting protein 4) and on the RPM1. I found that RPM1 can be found in complexes ranging from 500 kDa to high apparent molecular weight (HMW

complexes partly via homotypic association, while RIN4 can be found mainly in 200-300 kDa protein complexes independent of RPM1. AvrRpm1 and phosphorylated RIN4 were detected in about 300 kDa protein complexes. RIN4 is associated with RPM1 or AvrRpm1 in the microsomal fraction. By Co-IP coupled mass spectrometry analysis from microsomal extracts, putative interacting proteins of the RPM1 immune complex were identified with two different epitope tags (c-Myc and hemagglutinin) and three different experimental conditions.

## **INTRODUCTION**

Plants express a finely tuned immune system. Recognition specificity resides in a limited number of protein families, the largest of which contains N-terminal signaling domains, a central nucleotide-binding (NB) domain and Leucine-Rich Repeats (LRRs) of various lengths (Dangl and Jones, 2001; Jones and Dangl, 2006). There are roughly 150 NB-LRR genes in the complete *Arabidopsis thaliana* genome predicted to encode intracellular proteins (Meyers et al., 2003). Each NB-LRR allele is typically activated by a single signal, usually a protein, encoded by particular alleles of pathogen genes. Thus, this branch of the plant immune system exhibits specificity (Nimchuk et al., 2003). Phytopathogenic bacteria like *Pseudomonas syringae* pv *tomato* (Pto) DC3000 possess an evolutionarily conserved type III secretion system (TTSS) to transit type III effector proteins into the host cytosol (Alfano and Collmer, 1997). These prokaryotic proteins can be re-directed by the eukaryotic cellular addressing machinery to sites where they can act as virulence factors contributing to disease (Abramovitch et al., 2003; Nguyen et al., 2010; Nimchuk et al., 2000). Type III effector proteins, and presumably other virulence factors, can contribute to disease by dampening the host's basal defense response to pathogen associated molecular patterns (PAMPs) (Gomez-Gomez and Boller, 2002; Hauck et al., 2003; Jamir et al., 2004; Lu et al., 2010) and potentially by providing a more nourishing micro-niche for the growing pathogen colony or contributing to pathogen dispersal. Thus, the bacterial type III effector proteins, and

by extension, virulence factors from other pathogens, are likely targets for recognition by the intracellular NB-LRR receptors (Rathjen and Moffett, 2003).

However, most attempts to show direct interaction between an NB-LRR protein and its genetically defined nominal ligand have ended in frustration. An alternative, the “guard hypothesis”, posits that virulence factor function at a host target would trigger “recognition” of that action by the corresponding plant NB-LRR protein (Jones and Dangl, 2006; Nishimura and Dangl, 2010; Rathjen and Moffett, 2003). In mechanistic terms, the NB-LRR protein might be 1) part of a multi-protein target complex which it monitors for the action of a given virulence factor, or 2) part of a signaling complex into which a virulence factor-host target complex is recruited. In either scenario, assembly of at least three components is necessary to initiate successful disease resistance responses. Studies with the NB-LRR proteins RPM1 and RPS2 in *Arabidopsis* revealed that specific activation by the respective type III effector proteins AvrRpm1 (or AvrB) and AvrRpt2, is mediated through RIN4, a small plasma membrane associated protein of unknown biochemical function (Axtell and Staskawicz, 2003; Mackey et al., 2003; Mackey et al., 2002). RIN4 is therefore a host target of three unrelated type III effector proteins. Another excellent example of the guard hypothesis is provided by the molecular trio of the AvrPphB type III effector, its host target, the *Arabidopsis* PBS1 protein kinase, and the NB-LRR protein RPS5 (Shao et al., 2003; Simonich and Innes, 1995). Here, AvrPphB is an active cysteine protease whose activity on PBS1 is required for RPS5 activation. However, a clear mechanistic understanding of the cell biological processes leading to any NB-LRR activation event is lacking. Targeting of host protein machines by

different virulence factors necessitates both an understanding of how NB-LRR proteins are activated, and how the virulence factors in question, here phytopathogenic type III effector proteins, influence host cell responses via manipulation of one or more targets (Collier and Moffett, 2009; da Cunha et al., 2007).

Dynamic changes of protein complexes are essential for the functions of many proteins. Tandem affinity purification (TAP) (Puig et al., 2001) is used widely for purification of protein complexes from bacteria (Gavin and Superti-Furga, 2003) and mammals (Burckstummer et al., 2006; Gregan et al., 2007). A modified TAP tag method that lacks a nuclear localization signal in the CBP domain was developed for protein complex purification from plants (Rohila et al., 2004; Rohila et al., 2009). Recently, application of this modified TAP tag to identify RPS2-containing complexes was successful (Qi and Katagiri, 2009). Furthermore, Co-IP coupled mass spectrometry (MS) of the RIN4 complex was performed and identified interacting partners (Liu et al., 2009).

This chapter describes an effort to monitor the immune complexes containing RPM1 and/or RIN4 through size exclusion chromatography (SEC) and to identify associated proteins with Co-IP coupled MS analysis.

## **RESULTS**

### **RPM1 and RIN4 are in distinct protein complexes.**

RPM1 and RIN4, a RPM1-interacting protein localize to the plant plasma membrane (Boyes et al., 1998). To monitor whether RPM1 and RIN4 can form protein complexes in vivo, microsomal fractions from Arabidopsis plants expressing RPM1:myc under the control of its native promoter were extracted using the mild, non-ionic detergent dodecyl maltoside (DDM), which preserves the integrity of protein complexes (Knol et al., 1998; Le Maire et al., 2000). The size of RPM1/RIN4 protein complexes was analyzed by size exclusion chromatography. The initial void volume ( $V_0$ ) was determined by running Blue dextran in column running buffer (150 mM NaCl). The  $V_0$  was noted in fractions 9 and 10 with (Figure 2.1A left) or without plant microsomal extract (Figure 2.1A right). The relative molecular weight of each fraction was determined by flowing thyroglobulin (669kDa), ferritin (440kDa), catalase (232kDa) and aldolase (158kDa) together with the plant microsomal extract (Figure 2.1C). RPM1 (110 kDa) isolated from uninfected plants migrated in an apparent size range of  $500-1.5 \times 10^3$  kDa (fractions 10-17), presumably as part of a protein complex confirmed by breaking down complexes with harsh conditions such as boiling and 6M urea treatment (see below). This signal is not present in extracts isolated from the isogenic mutant *rpm1-3* (Figure 2.1C top). Under the same conditions, RIN4 (23 kDa), was eluted with an apparent size of 100-300 kDa, and there was a second peak indicating a high molecular weight of over 700kDa (Figure

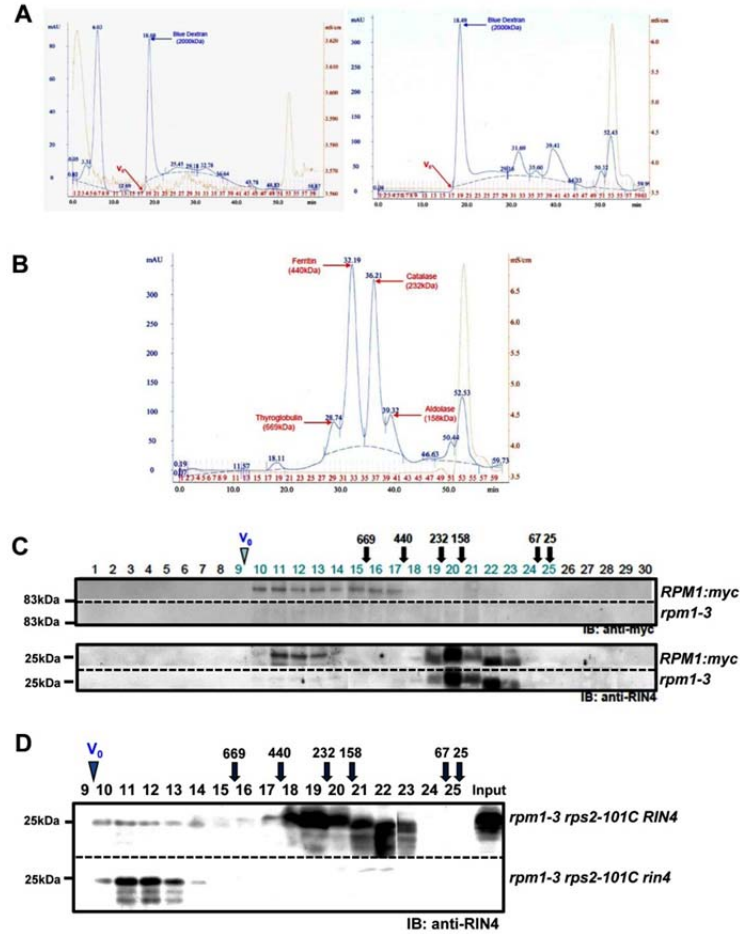


**Figure 2.1. Normalization of size exclusion chromatography (SEC)**

- (A) Determination of void volume ( $V_0$ ). Blue dextran was run in 150 mM NaCl without (left) and with (right) microsomal extracts demonstrating no change in  $V_0$  in both cases. Standard proteins including thyroglobulin (669 kDa), ferritin (440 kDa), catalase (232 kDa) and aldolase (158 kDa) were run with and without plant microsomal extract to validate elution profiles based on the size. Preparation of enriched microsomal fractions is shown in right panel (see Materials and Methods for detail). The peak represents UV absorption (280 nm) in absorption units (mAU) on the y-axis of the fractions.
- (B) The apparent molecular weight of each fraction. Molecular weight standard proteins described in (A) were mixed with microsomal extracts and run through a Superose 6L column.
- (C) RPM1- and RIN4-containing protein complexes. The elution profile of RPM1:myc and RIN4 was determined after running microsomal extracts through a Superose 6L column. The mutant *rpm1* (*rpm1-3*) was used as a negative control for RPM1:myc. Immunoblot with anti-myc and anti-RIN4 was performed to detect target proteins in each fraction.
- (D) Microsomal proteins were extracted from a *rin4* mutant (*rpm1 rps2-101C rin4*) and compared to RIN4 wild type extracts (*rpm1 rps2-101C RIN4*). Equal volumes of each column fraction were separated by SDS-PAGE and subjected to immunoblot (IB) with anti-RIN4.

2.1C bottom). A very small proportion of RIN4 eluted in the same fraction as RPM1 (fraction 18) consistent with the previously published finding that less than 5% of RIN4 is associated with RPM1 (Mackey et al., 2002). RIN4 was also eluted in the high molecular weight complex with RPM1 in fractions between 10 and 14 which can be considered as non-specific signal from RIN4 anti-serum (Figure 2.1D). To prove that RIN4 existed in apparent high molecular weight complexes, microsomal protein extracts isolated from the *rin4* mutant (*rpm1 rps2 rin4*) was used for SEC and compared to RIN4 wild type (*rpm1 rps2*). The fractions from 17 to 23 which represented the majority of RIN4 distribution in previous figures were absent in *rin4* mutant background, whereas detected RIN4 in the higher molecular weight (HMW) fractions were still detected suggesting that there must be cross-reactivity of RIN4 antiserum (Figure 2.1D). Together, RPM1 and RIN4 forms protein complex *in planta* although I did not clearly detect fractions where both RPM1 and RIN4 were eluted.

The size of many signaling protein complexes cannot be defined accurately because of the nature and variability of protein-protein and/or protein-lipid interactions (Knol et al., 1998). The conformation and the apparent size of protein complexes are influenced by ionic and hydrophobic conditions. As a control, different concentrations from 1% to 5% of DDM were applied, demonstrating that increasing DDM concentration had no adverse effects on the general elution properties of RPM1 and RIN4 (Figure 2.2A). Additionally, a different type of non-ionic detergent, Triton X-100, was used at a concentration of 0.2%. RPM1 eluted in a fraction of approximately 670 kDa and its detection was less efficient (Figure 2.2A top),

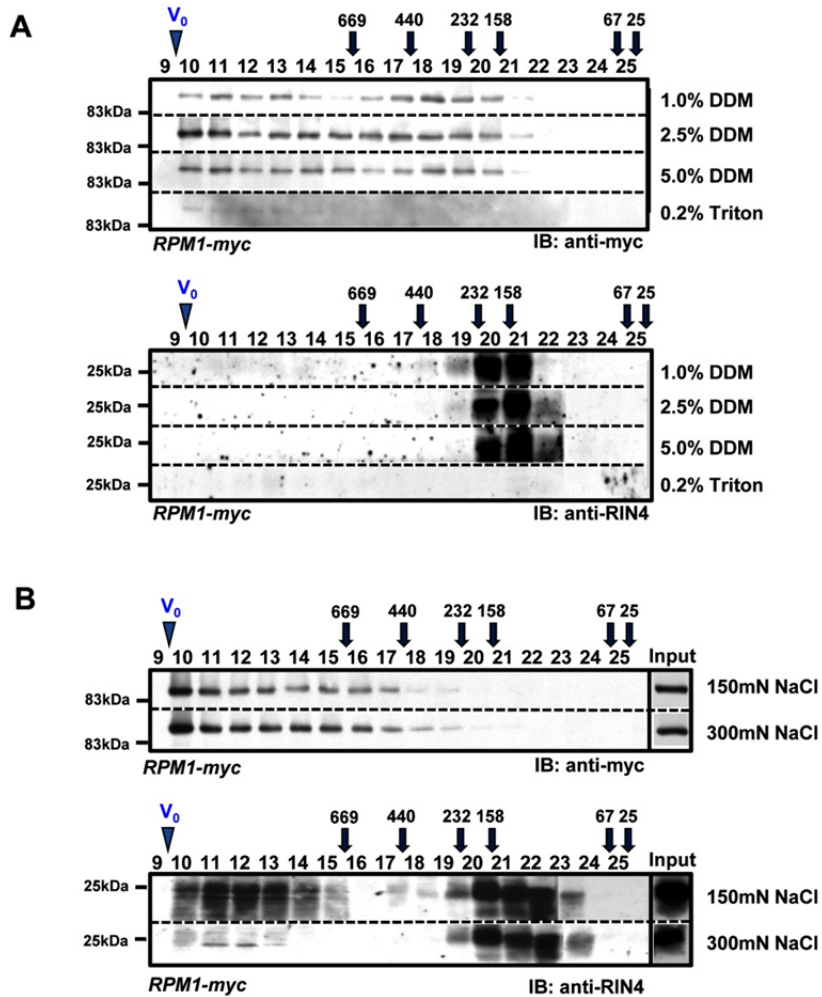


**Figure 2.2. Distribution of RPM1 and RIN4 in different buffer conditions**

- (A) Elution pattern of RPM1 and RIN4 in different detergent conditions. The non-ionic detergent, dodecyl-D-maltoside (DDM) was used to extract microsomes with different concentrations. Triton X-100 was used to compare the efficiency of extraction with DDM. Higher percentage of DDM did not affect RPM1 and RIN4 protein complexes.
- (B) Elution pattern of RPM1 and RIN4 in different salt conditions. High salt conditions (300 mM NaCl) are not limiting for RPM1 and RIN4 complexes. Extraction of microsome complexes was performed with DDM-containing buffer with different salt concentration.

consistent with the different extraction ability between DDM and Triton (Knol et al., 1998). Similarly, RIN4 distribution was altered and its extraction much less efficient in this detergent condition (Figure 2.2A bottom). Increasing salt concentrations from 150 mM to 300 mM also exhibited no adverse effect on RPM1 distribution with DDM (Figure 2.2B top). The elution properties of RIN4 in high salt concentrations (300 mM NaCl) were slightly altered (Figure 2-2B bottom).

To exclude the possibility of non-specific interaction caused by aggregation, elution profiles for RPM1 and RIN4 were monitored under harsh conditions such as boiling and treatment with 6M urea. By boiling, both RPM1 and RIN4 proteins were degraded (Figure 2-3A). Urea treatment led to a shift of RPM1 to lower molecular fractions (13-20) (Figure 2-3B top). The elution property of RIN4 was changed accordingly (Figure 2-3B bottom). Thus, both RPM1 and RIN4 are associated in protein complexes in native conditions, implying that the immune response induced by RPM1 with RIN4 could be modulated as protein complexes. Thus, data using the DDM buffer yields RPM1 and RIN4 elution profiles that 1) suggest preservation of the possible RPM1- and/or RIN4-containing protein complexes, 2) are reproducible by ionic conditions and changes in detergent and dissociation by harsh conditions, and 3) that are not merely the result of micelle or “salting in” effects (Wang et al., 2009). Therefore, all SEC data shown in this chapter are from microsomal extracts with 150mM NaCl and 1% DDM to solubilize microsome.

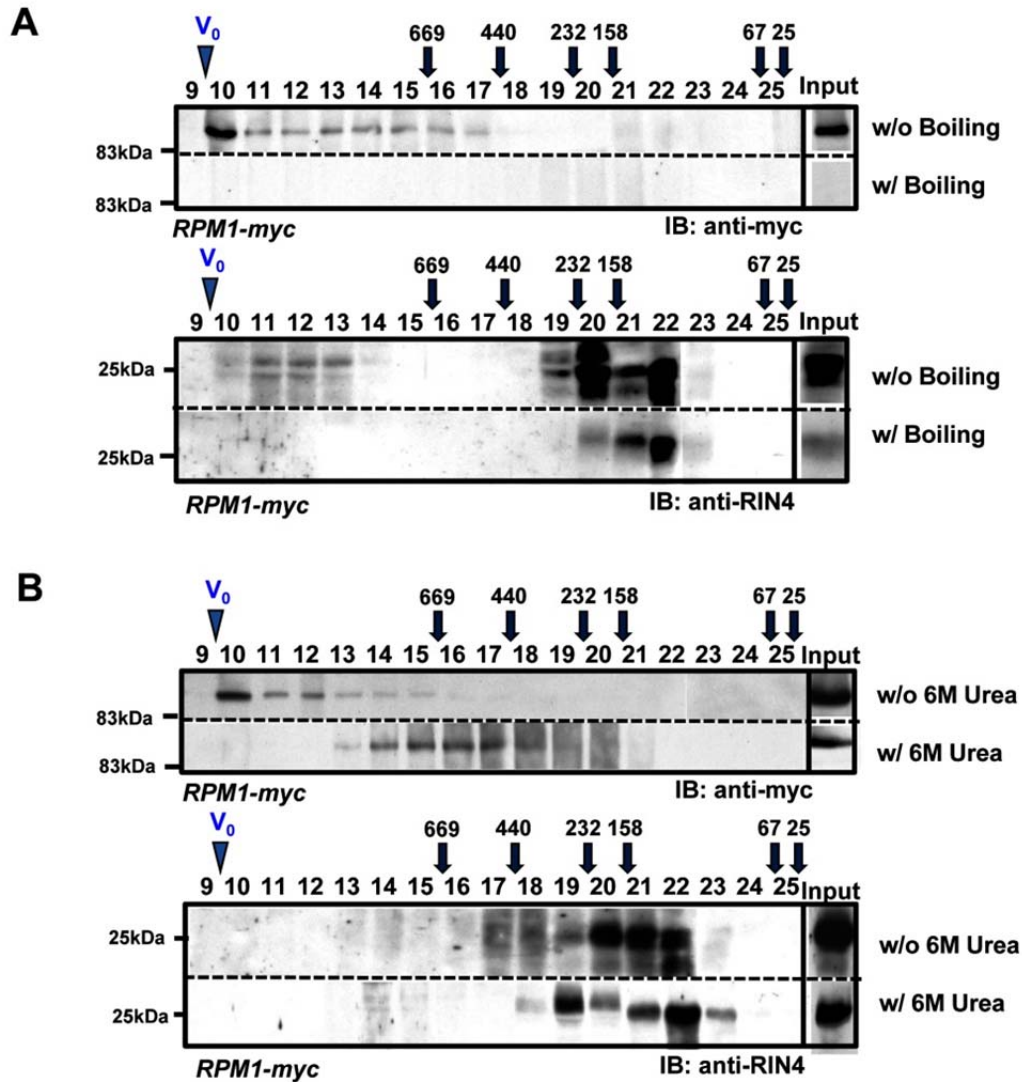


**Figure 2.3. Distribution of RPM1 and RIN4 in harsh extraction conditions**

- (A) Elution pattern of RPM1 and RIN4 after boiling. Microsomal extracts from RPM1:myc plants were boiled for 30min and subsequently run through a Superose 6L column. Boiling abolished both RPM1 and RIN4-associated protein complexes.
- (B) Elution pattern of RPM1 and RIN4 after treatment with 6M Urea. Microsomal extracts from RPM1:myc plants were solubilized with a 6M Urea column running buffer with DDM before SEC. The apparently high molecular weight complexes of RPM1 were disrupted (top). RIN4-associated complexes (fractions 18-21) were shown (bottom).

**No dynamic re-distribution of RPM1 and RIN4 by type III effector proteins correlated with RPM1 activation.**

The dynamics of RPM1 and/or RIN4-containing protein complexes after challenge with *Pto* DC3000 expressing the type III effector proteins AvrRpm1 and AvrB, which trigger RPM1-mediated responses, were investigated (Mackey et al., 2002). The profile of RPM1 distribution was monitored over time (in hours post-inoculation; hpi) after delivery of AvrRpm1 and AvrB by hand infiltration (Figure 2.4). The RPM1-containing complex did not display discernable changes (Figure 2.4A top). The overall distribution of RIN4 was not altered by delivery of AvrRpm1 (Figure 2.4A bottom). Delivery of AvrB did not result in change of RPM1 distribution (Figure 2.4B top). No discernable alteration of RPM1 distribution was observed by the virulent strain *Pto* DC3000(EV) either (Figure 2.4B bottom).

RIN4 can be phosphorylated by both AvrB and AvrRpm1 resulting in recognition by RPM1 and subsequent triggering of HR (Grant et al., 1995; Mackey et al., 2002). The phosphorylation of RIN4 was confirmed by one-dimensional mobility shift assays (Mackey et al., 2002) and direct detection with a phospho-RIN4 specific antibody (Chung et al., 2011). The RIN4 elution patterns demonstrated that phosphorylated RIN4 distributed in fractions 18 to 20 (200 to 400kDa MW), suggesting that phosphorylated RIN4 might associate with RPM1. This is consistent with the result that a RIN4 phospho-mimic mutant (T166D) interacted with RPM1 (Chung et al., 2011)

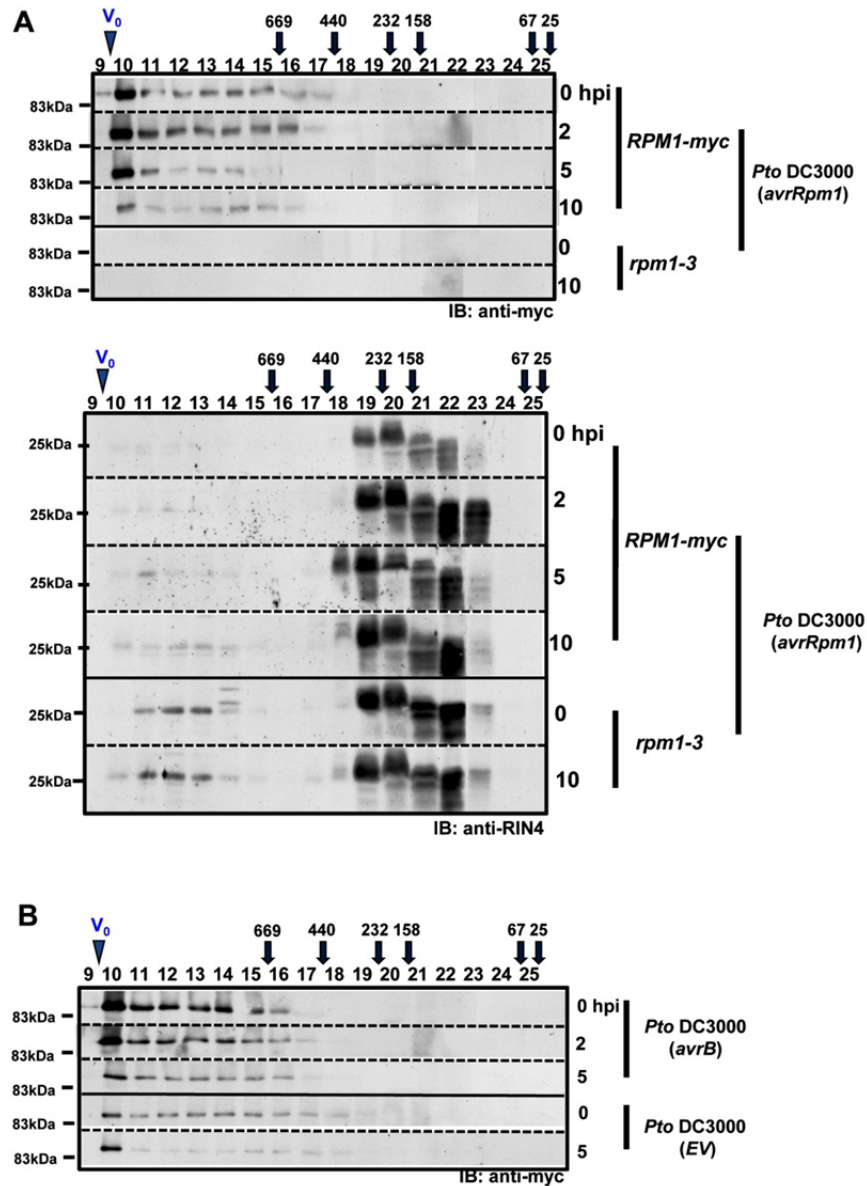


**Figure 2.4. Distribution of RPM1 and RIN4 in response to bacterial effectors.**

- (A) Distribution of RPM1 and RIN4 following delivery of AvrRpm1 was not clearly altered. Transgenic plants expressing RPM1:myc were inoculated with *Pto* DC3000(*avrRpm1*) at  $5 \times 10^7$  cfu/ml and leaves were harvested at the indicated time points. Microsomal membrane proteins were extracted and fractionated by gel-filtration chromatography as described in previous figures. The RPM1 profile exhibited a shift of proteins toward higher molecular weight and a marked disappearance of RPM1 protein was observed by 10 hpi (top). The elution profile of RIN4 was not changed by AvrRpm1. The possibly phosphorylated RIN4 (shifted band) was detected in fractions 18-20 (bottom).
- (B) Distribution of RPM1 after challenge with virulent *Pto* DC3000 (EV) and avirulent *Pto* DC3000(*avrB*).

To address whether AvrRpm1 distributed to the same fractions as RIN4 and RPM1, transgenic plants expressing *AvrRpm1-HA* under the conditional, Dexamethasone inducible (DEX) promoter in *RPM1:myc* and *rpm1-3* backgrounds were tested by SEC (Figure 2.5). AvrRpm1 distributed mainly in fractions 18 and 20 around 200 kDa in both *RPM1:myc* and *rpm1-3* backgrounds (Figure 2.5A). Elution patterns of both RPM1 (Figure 2.5B) and RIN4 (Figure 2.5C) were unchanged when compared to elution patterns obtained after inoculation with bacteria (Figure 2.4), indicating that conditionally overexpressed AvrRpm1 behaved like the natural effector protein and did not affect RPM1 and RIN4 distribution. Interestingly, the main fractions (fractions 19 and 20) of both AvrRpm1 and RIN4 overlap implying that the protein complex of just over 200 kDa may contain both AvrRpm1 and RIN4, consistent with the previously published coimmunoprecipitation of AvrRpm1 and RIN4 *in vivo* (Chung et al., 2011; Mackey et al., 2002).

To monitor whether AvrRpm1 distribution can be affected by RIN4, we analyzed by SEC conditionally expressed AvrRpm1 in a *rin4* mutant background (*rpm1 rps2 rin4*). AvrRpm1 eluted in *rin4* in the same fractions (18-20) as in RIN4 wt, suggesting that AvrRpm1 distribution is independent of RIN4 (Figure 2.5D).

The results in Figure 2.4 and 2.5 demonstrate that RPM1 exists in protein complexes with molecular weights ranging from 500 kDa to an apparently high molecular weight (HMW). Neither RPM1 nor RIN4 elution patterns changed during effector activated RPM1-mediated defense responses. AvrRpm1 and RIN4 may exist in the same complex of 200 kDa, allowing AvrRpm1 to phosphorylate RIN4 which then results in RPM1-mediated HR.

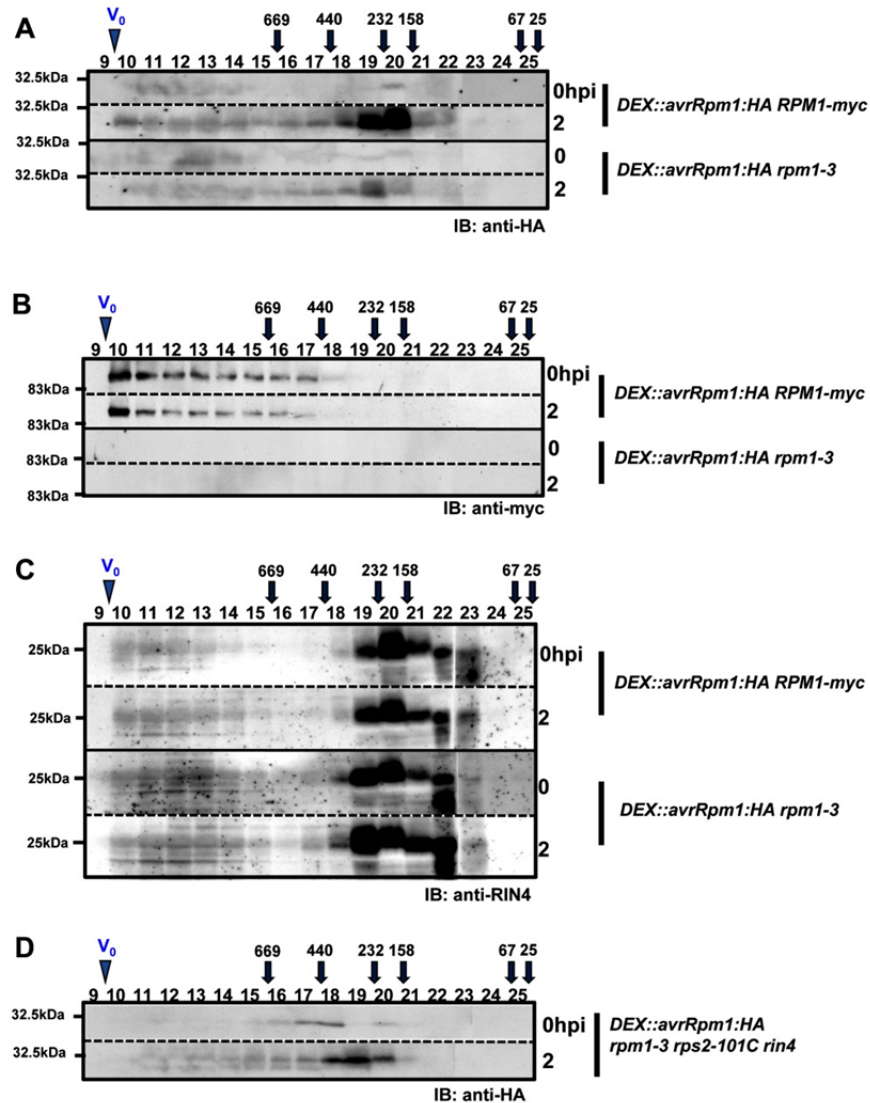


**Figure 2.5. Distribution of RPM1 and RIN4 in effector-expressing transgenic plants.**

- (A) AvrRpm1 detected mainly in fraction 19 and 20. Transgenic plants expressing Dexamethasone (Dex) inducible AvrRpm1:HA in RPM1:myc or rpm1-3 backgrounds were treated with 20  $\mu$ M Dex. Tissue was collected at the indicated time points. AvrRpm1 was detected by immunoblotting with an anti-HA antibody.
- (B) RPM1 distribution is unchanged after expression of AvrRpm1 in plants. RPM1 was detected by immunoblotting with anti-myc antibodies from the same fractions as shown in (A).
- (C) RIN4 distribution is unchanged after expression of AvrRpm1 in plants. RIN4 was detected by immunoblotting with anti-RIN4 antibodies.
- (D) Distribution of AvrRpm1 is independent of RPM1 and RIN4. Microsomes from transgenic plants expressing AvrRpm1 under the Dex-inducible promoter in the *rpm1 rps2 rin4* mutant background were used for SEC. AvrRpm1 was detected by immunoblotting with anti-HA antibodies.

## **RIN4 distribution in the presence of *Pto* DC3000(*avrRpm1*) does not require RPM1 or RPS2.**

RIN4 coimmunoprecipitates with RPM1 and plays a role in RPM1 stabilization (Mackey et al., 2002). RIN4 also interacts with the NB-LRR R-gene RPS2, and is cleaved by AvrRpt2, a cysteine protease, resulting in RPS2-dependent HR (Axtell and Staskawicz, 2003; Chisholm et al., 2005; Kim et al., 2005; Mackey et al., 2003). Thus RIN4 complexes might contain both or either RPM1 or RPS2 *in planta*. Hence, dynamics of RIN4 complexes were monitored after expressing conditionally inducible AvrRpm1 in the *rpm1 rps2* mutant background. AvrRpm1 expression did not change the RIN4 elution profile (Figure 2.6A and 6B). These findings suggested that RPM1-mediated HR could be activated independently of RPS2, although RIN4 associates with both RPM1 and RPS2 *in planta*.

## **RPM1 is “self-associated” *in planta***

NB-LRR proteins can undergo homotypic association with or without pathogen infection. The CC-NB-LRR protein RPS5 and the N-terminal domain-Solanaceous Domain(SD)-CC-NB-LRR protein Prf form homotypic associations without elicitation (Ade et al., 2007; Gutierrez et al., 2010), while the TIR-NB-LRR protein N forms homotypic interactions only after activation by the viral protein p50 (Mestre and Baulcombe, 2006). Therefore, the homotypic association of RPM1 was monitored by coimmunoprecipitation from extracts of *RPM1:myc RPM1:GFP rpm1 (R1:myc R1:GFP)* plants which is functional as wild type (Eitas and Dangl, unpublished data).

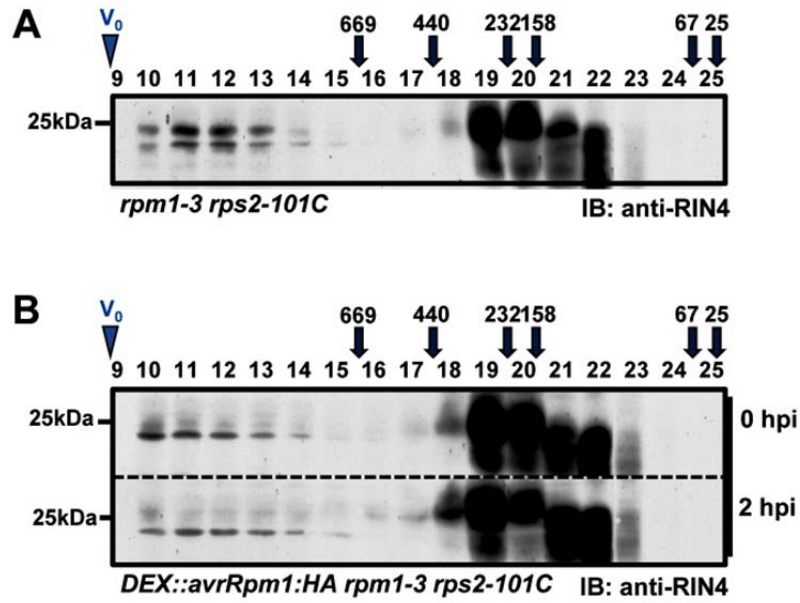


**Figure 2.6. RIN4 distribution is unchanged in *rps2***

Dex-inducible AvrRpm1 was expressed in the *rps2* mutant. Microsome extraction and SEC was performed as described in previous figures. RIN4 was detected with anti-RIN4 antibodies.

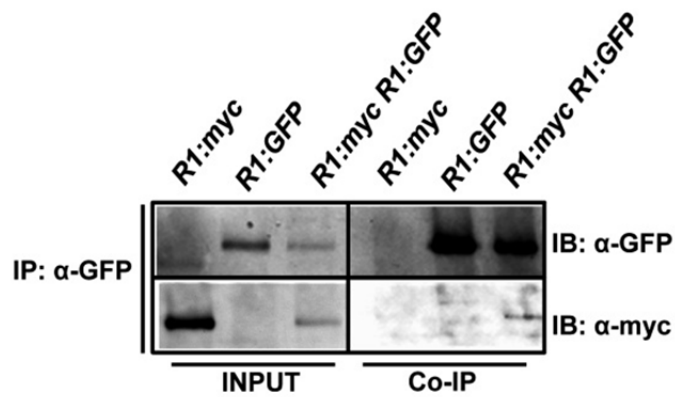


**Figure 2.7. Self-association of RPM1 in Arabidopsis**

RPM1:myc (R1:myc) and RPM1:GFP (R1:GFP) transgenic lines were crossed to generate RPM1:myc RPM1:GFP-containing plants (R1:myc R1:GFP) in *rpm1-3* mutant. Microsomal extracts from stable homozygous F3 plants were immunoprecipitated with anti-GFP. Coimmunoprecipitation of RPM1:myc was detected with the anti-myc antibody.

*RPM1:myc* (*R1:myc*) and *RPM1:GFP* (*R1:GFP*) plants were used as controls. *RPM1:myc* was co-immunoprecipitated by *RPM1-GFP*, demonstrating that *RPM1* can associate in a homotypic manner (Figure 2.7). This homotypic association occurred in the absence of bacterial effector proteins. Hence, *RPM1* can form dimers or oligomers *in planta* in an inactive status, as has been shown for *RPS5* as well (Ade et al., 2007). The *RPM1* homotypic interaction may also contribute to the *RPM1* distribution presented in previous figures independent of effector proteins.

### **RIN4 interacts with *RPM1* and *AvrRpm1* in the microsomal fraction**

The interaction between *RPM1* and *RIN4* *in planta* was observed by co-immunoprecipitation from total protein extracts (Mackey et al., 2002). Both proteins localize to the plasma membrane (Boyes et al., 1998). To clarify the interaction of *RPM1* and *RIN4* or *AvrRpm1* and *RIN4* on the plasma membrane, co-immunoprecipitation (Co-IP) was performed from microsomal fractions, using low, medium and high stringency washing conditions (Figure 2.8). To test the interaction between *RPM1* and *RIN4* before and after activation of *RPM1*, *RPM1:myc* plants conditionally expressing *AvrRpm1* with Dex-treatment were used as “activated samples” (*RPM1+AvrRpm1*). Samples were pooled 2, 5, and 7 hours after *AvrRpm1*-induction. The *rpm1 rps2 rin4* triple mutant was used as a negative control (Figure 2.9).

With low (50 mM NaCl) and medium (150 mM NaCl) stringency washing conditions, *RIN4* and *RPM1* were coimmunoprecipitated from the microsomal

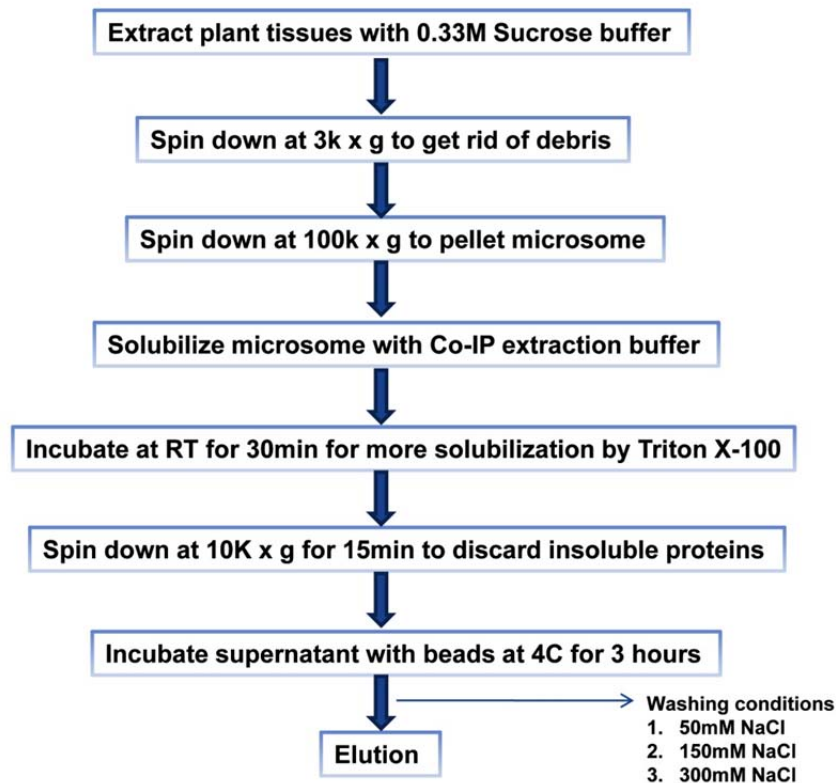


**Figure 2.8. Schematic diagram depicting the isolation of plant proteins complexes by coimmunoprecipitation.**

Microsomal extraction were performed as described in Materials and Methods. For Co-IPs, microsomal extracts from 10 g of plant tissue were collected and solubilized in Co-IP buffer. The solubilized microsomes were recovered from the supernatant after centrifugation at 20,000 x g for 15 min at 4 °C. Three different washing conditions (50, 150 and 300 mM NaCl) were employed to provide low, medium and high stringency washing conditions.

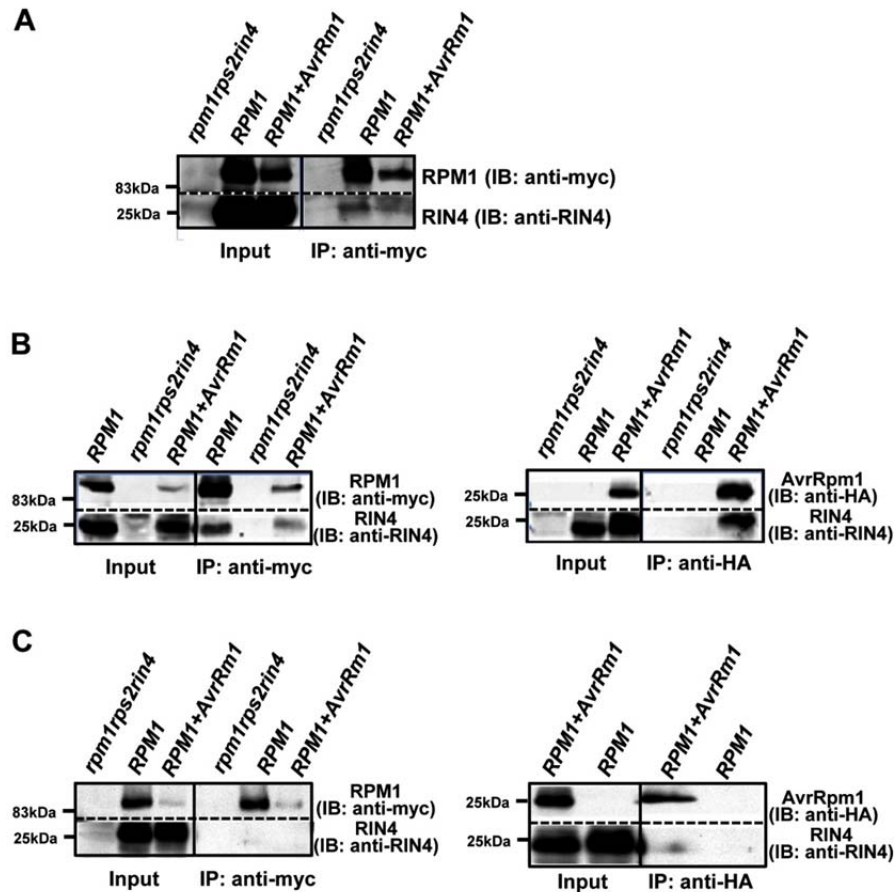


**Figure 2.9. Coimmunoprecipitation of RIN4 with RPM1 or AvrRpm1**

- (A) Association between RPM1 and RIN4 under low stringent washing conditions. Interaction of RPM1 with RIN4 was monitored in *RPM1:myc* (inactive) and AvrRpm1-expressing *RPM1:myc* (active) plants. The *rpm1 rps2 rin4* mutant was used as a negative control for RPM1 and RIN4. Co-IP with anti-myc was confirmed with microsomes from each genotype followed by immunoblotting with anti-RIN4. Bound proteins were washed three times with washing buffer containing 50 mM NaCl.
- (B) Association of RIN4 with RPM1 or AvrRpm1 under medium stringency washing conditions. All experimental procedures were the same as in (A), except for washing with 150 mM NaCl-containing washing buffer. In addition, AvrRpm1 was immunoprecipitated with anti-HA antibodies. Co-immunoprecipitation of RIN4 was detected with the anti-RIN4 antibody.
- (C) Association between RPM1 and RIN4 under high stringency washing conditions. The Co-IP with anti-myc and anti-HA was performed as described in (B), except for using a 300 mM NaCl-containing washing buffer.

fraction (Figure 2.9A and 2.9B left). This interaction was disrupted by high (300 mM NaCl) stringency washing (Figure 2.9C left). Consistent with the fact that samples were pooled before and after onset of HR (4-5 hpi), we observed a decrease in RPM1 accumulation correspondent to the published disappearance of RPM1 after its activation (Boyse, 1998). Interestingly, phosphorylated RIN4 coimmunoprecipitated with RPM1, indicating that phosphorylated RIN4 might still associate with RPM1 after RPM1 activation. This finding is also consistent with the result that a phospho-mimic RIN4 (T166D) interacts with RPM1, which itself exhibited low accumulation caused by activation (Chung et al., 2011; see Chapter 3).

The interaction between RIN4 and AvrRpm1 was monitored by co-immunoprecipitation from microsomal fractions under medium and high stringency washing conditions. As shown for the interaction of RPM1 and RIN4, interaction of RIN4 and AvrRpm1 was observed under medium stringency washing conditions (Figure 2.9B right), and abolished under high stringency conditions (Figure 2.9C right). Collectively, we provide evidence for a plasma membrane localized interaction between RIN4 and AvrRpm1 or RIN4 and RPM1.

### **Identification of RPM1-interacting proteins by Mass Spectrometry**

Coimmunoprecipitated proteins performed as in Figure 2.9 was analyzed LC/MS/MS. By comparing MS profiles from three different washing conditions performed as in Figure 2.9, protein profiles from three different washing conditions were described in Figure 2.10. Coimmunoprecipitation under low stringency washing conditions using

microsomal fractions from *Dex:avrRpm1:HA RPM1:myc* and *RPM1-myc* plants, yielded 73 (*RPM1-myc*) and 138 (*Dex:avrRpm1:HA RPM1:myc*) proteins based on peptide sequencing. 53 proteins were isolated in common from both microsomal fractions. 20 and 85 proteins, respectively, were uniquely detected from each (Figure 2.10A). The same microsomal fractions were tested under medium stringency washing conditions. Additionally, we added samples derived from anti-HA coimmunoprecipitated microsomal fractions from AvrRpm1-HA-induced *RPM1:myc* plants. This allowed us to directly compare protein profiles of anti-myc and anti-HA Co-IPs from the same plants. 146 (*RPM1:myc*) and 55 (*Dex:avrRpm1:HA RPM1:myc*) proteins were recovered from coimmunoprecipitation using anti-myc. 147 proteins (*Dex:avrRpm1:HA RPM1:myc*) were found in Co-IP with anti-HA; 25 proteins were commonly detected in all three categories (Figure 2.10B) Under high stringency washing conditions a dramatic decrease of detected proteins was observed, consistent with our finding that the "control" interaction of RIN4 with RPM1 or AvrRpm1 was disrupted as well (Figure 2.9). Only 15, 13 and 26 proteins were detected from Co-IPs with anti-myc in *RPM1:myc* and *Dex:avrRpm1:HA RPM1:myc* and Co-IP with anti-HA in *Dex:avrRpm1:HA RPM1:myc*, respectively (Figure 2.10C).

Total proteins from each washing conditions were compared and shown in Figure 2.10D. Based on the loss of interaction of RIN4 with RPM1 or AvrRpm1 (Figure 2.9), it can be considered that proteins identified under the high stringent washing condition might be false positives caused by non-specific aggregation during Co-IP. Approximately 68% of proteins detected under high

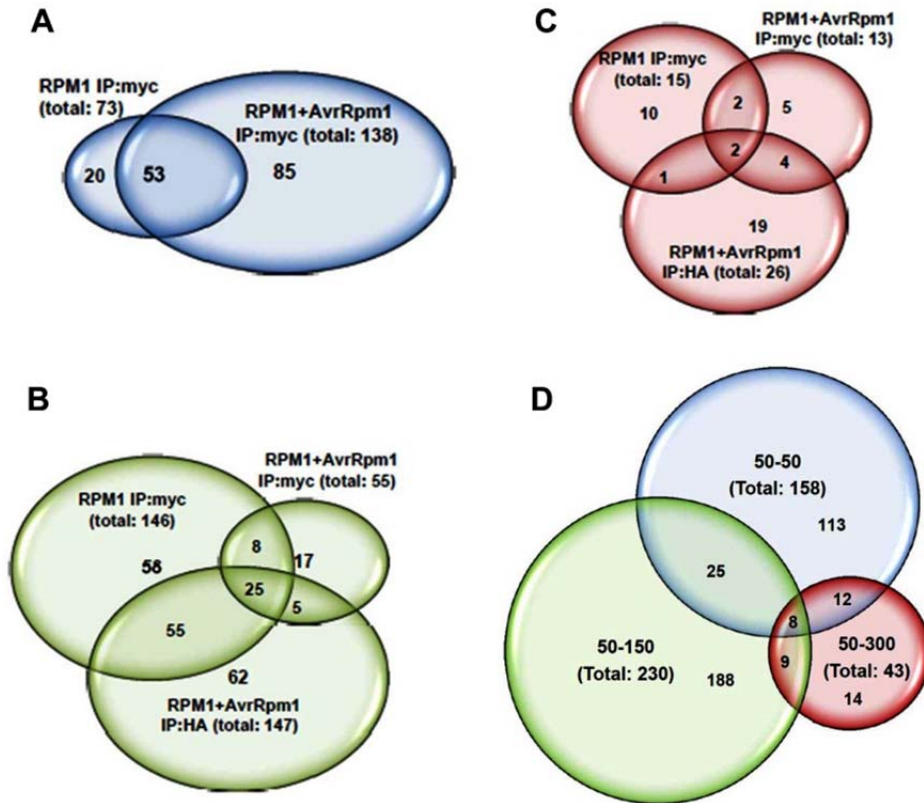


**Figure 2.10. Proteins identified by LC/MS/MS analysis from Co-IPs performed using three different washing conditions.**

- (A) Protein profiles in low stringency washing conditions. 158 proteins were identified from an anti-myc Co-IP using microsomal extracts derived from RPM1:myc and Dex-AvrRpm1-HA RPM1:myc (RPM1+AvrRPM1) plants. Microsomal extracts from *rpm1 rps2 rin4* plants were used as a negative control to subtract false positives. Among 158 proteins, 53 proteins were identified in both genotypes. 20 and 85 proteins were unique to RPM1 and RPM1+AvrRpm1, respectively.
- (B) Protein profiles in medium stringency washing conditions. 230 proteins were identified from Co-IPs with anti-myc and anti-HA. 168 proteins were co-immunoprecipitated with anti-myc antibodies from extracts from RPM1 (146) and RPM1+AvrRpm1 (55). 147 proteins were identified using the anti-HA antibody for co-immunoprecipitation. Microsomal extracts from *rpm1 rps2 rin4* plants were used as a negative control to subtract false positives. Comparison of all protein profiles from all Co-IPs demonstrates that 25 proteins were found under all conditions.
- (C) Protein profiles in high stringency washing conditions. 24 proteins were detected from Co-IPs with anti-myc antibody from microsomal extracts derived from RPM1:myc and Dex-AvrRpm1-HA RPM1:myc plants. 26 proteins were identified from a Co-IP with anti-HA antibodies using extracts derived from RPM1+AvrRpm1 plants.
- (D) Comparative analysis of all three different washing conditions. 33 proteins were identified in both low and medium stringency washing conditions (21% overlap for low- and 17% overlap for medium-stringency washing conditions).

Stringency conditions overlapped with proteins from either low or medium washing conditions (Figure 2.10D). Therefore, Table 2.1 presents a list of proteins detected in at least two of three different conditions. Eight proteins found in all three conditions were ribosomal proteins subunits, 26S proteasome regulatory subunits and chloroplast-derived proteins which were considered as “false positives” (Van Leene et al., 2010). This can be explained by the fact that these proteins are quite abundant in plant cells.

It is not clear whether the identified proteins may have a function in RPM1-mediated resistance because RPM1 peptides were not detected by MS although coimmunoprecipitation with less than 5% of total bound proteins showed both RPM1 and RIN4 (Figure 2.9). Moreover, RPM1 forms known protein complexes with Hsp90, Sgt1, Rar1 (Hubert et al., 2003), and RIN4 (Mackey et al., 2002). However, in the MS profiles, only Hsp90 (At5g52640) was detected in low and medium stringency washing, which is also consistent with interaction capacity of RPM1 and RIN4 (Figure 2.9). The current data set may open the possibility to now identify the real candidates by further repetitions under optimized conditions

**Table 2.1. Proteins identified at least two different conditions.**

Proteins detected in low (50-50), medium (50-150) and high (50-300) stringency washing conditions are listed. Proteins identified in any condition were marked as “v”.

Protein ID	Accession	MW	50-50	50-150	50-300
60S ribosomal protein L3 (RPL3A), (cyto)	At1g43170.1	44541.6	V	V	V
26S proteasome regulatory subunit, putative (RPN7) (nucleus)	At4g24820.1	44266.3	V	V	V
adenosylhomocysteinase, putative	At3g23810.1	53141.7	V	V	V
ATP synthase gamma chain 1, chloroplast (ATPC1),	At4g04640.1	40893.9	V	V	V
Encodes a protein thought to be a part of the translocon at the chloroplast inner envelope	At1g06950.1	112105.6	V	V	V
H <sup>+</sup> -transporting two-sector ATPase, putative (PM)	At3g28710.1	40775	V	V	V
lipoxygenase (LOX2) (ch)	At3g45140.1	102031	V	V	V
protochlorophyllide reductase B, chloroplast	At4g27440.1	43342.5	V	V	V
26S proteasome AAA-ATPase subunit (RPT3) (nucleus)	At5g58290.1	45734.3	V	V	
26S proteasome AAA-ATPase subunit (RPT6a) (nucleus)	At5g19990.1	47230.8	V	V	
3-oxoacyl-(acyl-carrier-protein) synthase I (mt/ch)	At5g46290.1	50396.5	V	V	
allene oxide synthase (AOS) / hydroperoxide dehydrase / cytochrome P450 74A (CYP74A)	At5g42650.1	58181.6	V	V	
ATP-citrate synthase, putative / ATP-citrate (pro-S)-lyase (cyto)	At3g06650.1	65797.2	V	V	
cell elongation protein / DWARF1 / DIMINUTO FAD binding domain (BR-pathway/Ca2+binding)	At3g19820.1	65377.8	V	V	
chaperonin, similar to T-complex protein 1, delta subunit (TCP-1-delta) (Homo sapiens) (?)	At3g18190.1	57758.4	V	V	
chloroplast inner envelope membrane protein, putative (APG1), methyltransferase, UbiE	At3g63410.1	37909.7	V	V	
clathrin heavy chain (Endo)	At3g08530.1	193258.1	V	V	
expressed protein (Ch)	At2g43950.1	38818.5	V	V	
expressed protein (Ch)	At2g44640.1	49814.5	V	V	
fasciclin-like arabinogalactan-protein (FLA8) – GPI-anchor (PM)	At2g45470.1	43058.3	V	V	
fructose-bisphosphate aldolase, putative (ch)	At2g21330.1	42913.5	V	V	
fructose-bisphosphate aldolase, putative (ch/mt)	At4g38970.1	42970.1	V	V	
glutamate:glyoxylate aminotransferase 1 (GGT1) (Peroxisome)	At1g23310.1	53284.6	V	V	
heat shock protein, putative (Arabidopsis thaliana)	At5g52640.1	81648.1	V	V	
heavy-metal-associated domain-containing protein (cyto)	At5g19090.1	59603.4	V	V	
L-ascorbate peroxidase 3 (APX3) (peroximal membrane)	At4g35000.1	31554.8	V	V	
luminal binding protein 1 (BiP-1) (BP1) Hsp70 like (ER)	At5g28540.1	73612.9	V	V	
NADH-ubiquinone dehydrogenase, similar to NADH-ubiquinone oxidoreductase (mt)	At5g37510.1	81164.3	V	V	
prohibitin, putative (mt)	At1g03860.1	31793.5	V	V	
ribulose-phosphate 3-epimerase, chloroplast, putative / pentose-5-phosphate 3-epimerase	At5g61410.1	29990.5	V	V	
RPL10A / Wim's tumor suppressor protein-related, similar to tumor suppressor (cyto)	At1g14320.1	24899.5	V	V	
transketolase, putative, strong similarity to transketolase 1 (Capsicum annuum) (ch)	At3g60750.1	79952.1	V	V	
vacuolar ATP synthase subunit C (VATC) / V-ATPase C subunit (PM)	At1g12840.1	42601.6	V	V	
40S ribosomal protein S5 (RPS5A) (cyto)	At2g37270.1	22973		V	V
60S ribosomal protein L4/L1 (RPL4D), 60S ribosomal protein L4, Arabidopsis thaliana (cyto)	At5g02870.1	44704.4		V	V
ATPase 10, plasma membrane-type, putative / proton pump 10, putative (PM)	At1g17260.1	104802.2		V	V
ATPase F subunit (ch)	ATCG00130	21039.8		V	V
dyskerin, putative / nucleolar protein NAP57, putative (?)	At3g57150.1	63009.3		V	V
expressed protein (PTAC16) (Ch)	At3g46780.1	54340.6		V	V
Gar1 RNA-binding region family protein (ch)	At3g03920.1	20965.4		V	V
geranylgeranyl reductase, identical to geranylgeranyl reductase (ch)	At1g74470.1	51820.8		V	V
peptidase M3 family protein / thimet oligopeptidase protein, metaloendopeptidase activity)	At5g10540.1	79028.3		V	V
acetyl co-enzyme A carboxylase carboxyltransferase alpha subunit family,	At2g38040.1	85291.5	V		V
actin, putative, very strong similarity to SP:P53496 Actin 11 (Arabidopsis thaliana)	At2g42100.1	42100	V		V
chlorophyll A-B binding protein, chloroplast (LHCB6), nearly identical to Lhcb6 protein	At1g15820.1	27505.5	V		V
clathrin heavy chain, putative,	At3g11130.1	193232.2	V		V
elongation factor 1B-gamma, putative / eEF-1B gamma, putative	At1g57720.1	46383.8	V		V
elongation factor Tu family protein, similar to Cryptosporidium parvum elongation factor-2	At1g06220.1	110425	V		V
GTP-binding protein / phragmoplastin, putative, strong similarity to GTP-binding protein	At5g42080.1	68156.7	V		V
plasma membrane intrinsic protein 1B (PIP1B) / aquaporin PIP1.2 (PIP1.2) /	At2g45960.1	30580.5	V		V
pyrophosphate-energized vacuolar membrane proton pump	At1g15690.1	80804.5	V		V
Semialdehyde dehydrogenase family protein,	At1g14810.1	40727.6	V		V
similar to ethylene-responsive late embryogenesis-like protein (Lycopersicon esculentum)	At2g44060.1	36020	V		V
The protein undergoes thiolation following treatment with the oxidant tert-butylhydroperoxide.	At5g17920.1	84340.4	V		V

## **DISCUSSION**

Protein complexes function as biological machines to orchestrate cellular processes. Multi-protein assemblies are not static, and their composition can be modified by exposing the cells to various stimuli (Nourry et al., 2003). Dynamic associations between modular protein domains govern spatial and temporal integration and the transmission of cellular signals (Gavin and Superti-Furga, 2003; Nourry et al., 2003). This work aimed at (1) describing the macromolecular protein complexes associated with plant disease resistance proteins of the NB-LRR class, and (2) studying the behavior of these complexes following pathogen infection. The data suggest that RPM1 forms complexes *in planta* before and after recognizing the bacterial type III effectors AvrRpm1, with no clear dynamics. In the resting state, RPM1 interacts in a homotypic manner. The distribution of RIN4 indicates associations with at least AvrRpm1 *in planta*. By employing Co-IP coupled with Mass Spectrometry, possible interacting proteins with RPM1 were identified, although further investigation is needed. These data suggest that RPM1 can be present as homotypic protein complexes in resting interaction platforms, which can potentially be activated via signaling complexes in the plant immune system. RPM1 disappears after infection (Boyes et al., 1998). The behavior of the RPM1- and/or RIN4-containing complexes following AvrRpm1-driven activation of RPM1 was tested. RIN4 is modified by differential phosphorylation and the most heavily phosphorylated form elutes in an approximately 300kDa complex, possibly with RPM1. A phosphorylated form of RIN4 and AvrRpm1 can be found together in the same protein complexes (Figure

2.5; see Chapter 3). The current data suggest that RPM1 may be present in this protein complex. Interestingly, phosphorylated RIN4, even before bacterial infection, may associate transiently with the RPM1-containing complex of ~300kDa (Fraction 17-19). RPM1 can be degraded after its activation (Figure 2.4A, 10 hpi), thus it might be more complicated to detect 'active complexes' after RPM1-activation. The nature of the apparent HMW complex (fractions 9-10) is still unclear, although it may contain many proteins. The differential detergent extraction results obtained in this chapter are consistent with the idea that apparent HMW fraction might consist of lipid microdomains that could facilitate assembly of signaling complexes (Munro, 2003; Simons and Toomre, 2000).

It has been suggested that NB-LRR protein activity is negatively regulated via intra- or inter-molecular interactions (Belkhadir et al., 2004a; Moffett et al., 2002; Rathjen and Moffett, 2003). RIN4 negatively regulates ectopic activation of both RPS2 and RPM1 before infection (Belkhadir et al., 2004b). Increased fractionation of phosphorylated RIN4 into the ~300 kDa complex following infection might relieve this negative regulatory function on RPM1 and hence facilitate subsequent signaling. Collectively, this suggests that, while there is some RIN4 associated with RPM1 before infection (Mackey et al., 2002), higher levels of phosphorylated RIN4 are recruited following RPM1 activation. This hypothesis is consistent with the general predictions of the Guard Hypothesis, namely that an NB-LRR protein could (1) constitutively associate with its "guardee", RIN4 in this study (2) dynamically recruit more of that guardee following stimulation, and (3) disengage from the complex after

type III effector manipulation of the guard cell. This last step would lead to activation of the NB-LRR protein (Dangl and Jones, 2001; Jones and Dangl, 2006).

RIN4 distribution is independent of either RPM1 or RPS2 (Figure 2.4, Figure 2.6). RIN4 distribution patterns are also unchanged after AvrRpm1 stimulation in *rpm1* plants (Figure 2.4A bottom). This is consistent with our model that RIN4 is required for RPM1 localization on the plasma membrane. RIN4 recruitment to protein complexes is independent of recognition, but might respond to a virulence activity of type III effectors such as AvrRpm1 and AvrB. However, the RIN4 elution profile is not affected by AvrRpm1. No RIN4 re-distribution occurs in the *rpm1 rps2* double mutant following induction of AvrRpm1. The amount of AvrRpm1 delivered via the conditional expression system is apparently much higher than the amount delivered by bacteria (Tornero et al., 2002). The lack of RIN4 distribution dynamics in *rpm1 rps2* is not a function of the amount of type III effector delivered (Figure 2.5A and 2.5C). The distribution of AvrRpm1 does not appear to require RPM1, RPS2 or RIN4 (compare Figure 2.5A and Figure 2.5D), although AvrRpm1 is mainly detected in the same fractions as the majority of RIN4 (Fractions 18-20). Thus, AvrRpm1 forms protein complex with RIN4 and activates RIN4 forming protein complexes to trigger RPM1-mediated HR. Also, it can be speculated that AvrRpm1 targets additional host protein complexes of over 200 kDa because the elution profile of AvrRpm1 is not dependent on RPM1 which is over 100 kDa in size. Based on a protein structure homology search (Cherkis and Dangl, unpublished data), AvrRpm1 seems to possess an ADP-ribosyltransferase-like 3D structure, which supports the idea that AvrRpm1 can target multiple host proteins for its virulence function.

Recently, Liu and colleagues identified RIN4-interacting proteins through Co-IP based LC/MS/MS analysis (Liu et al., 2009). They detected RPS2 and seven other proteins: two plasma membrane (PM) H<sup>+</sup>-ATPase, a MATH domain containing protein, two Jacalin domain proteins, ERD4, and a remorin. They also demonstrated that RIN4 can regulate the PM H<sup>+</sup>ATPase to control basal defense through control of stomata aperture during infection in the same study. One of best known interactors of RIN4, NDR1 (At3g20600) (Coppinger et al., 2004; Day et al., 2006), was not detected in this screening. RPM1 was not identified either, confirming that the transient interaction of RIN4-RPM1 and low expression levels of RPM1 may preclude identification by mass spectrometry. Qi and Katagiri (2009) utilized an improved tandem affinity purification (TAP) tag called HBP tag to enrich for RPS2, and identified RIN4 and 9 other interacting proteins: Aquaporin PIP1.2, Receptor-like kinase (RLK), Phototropin 1 and 2 (PHOT1 / 2), two band 7 proteins, Patellin-1 (PATL1), Epithiospecifier modifier 1 (ESM1), and Heavy metal ATPase 3 (HMA3). From the two reference data (Liu et al., 2009; Qi and Katagiri, 2009), more than 100 proteins as a whole were identified exhibiting approximately 5% overlap in two independent data sets from different groups. In my experiments, the medium stringency washing condition provided the best resolution of protein profiles (Table 2.2). Interestingly, I detected three PM H<sup>+</sup> ATPase (3, 8 and 10), three MATH domain containing protein, the Jacalin domain proteins, Aquaporin, and three band 7 proteins under medium stringency washing condition. Moreover, a Pentatricopeptide

**Table 2.2. Protein IDs identified under medium stringency washing condition.** Each protein profile from Co-IP with anti-myc and anti-HA was shown in different color (see end of table). The “H” and “m” in the last column represents Co-IP with anti-HA and anti-myc. Proteins detected in other study were marked by asterisk (\*).

Protein name	Matches	Accession	MW	R1m	AR1m	r1m	R1H	AR1H	
Symbol: EMB2386   60S ribosomal protein L19 (RPL19A),	1	At1g02780.1	24589.5	0	0	0	0	2	AR1H
Symbol: None   prohibitin, putative, similar to SP:P24142 P	2	At1g03860.1,A	31793.5	0	0	0	0	5	AR1H
Symbol: None   malate dehydrogenase, cytosolic, putative,	1	At1g04410.1	35552.9	0	0	0	0	1	AR1H
Symbol: None   expressed protein   chr1:1289735-1291077	1	At1g04630.1 (r	16107.9	0	0	0	0	4	AR1H
Symbol: None   ATPase 10, plasma membrane-type, putat	1	At1g17260.1 (F	104802	0	0	0	0	1	AR1H
Symbol: None   NADH-ubiquinone oxidoreductase-related,	2	At1g49140.1,A	12512.1	0	0	0	0	2	AR1H
Symbol: None   mitochondrial processing peptidase alpha s	1	At1g51980.1 (r	54385.4	0	0	0	0	12	AR1H
Symbol: None   jacalin lectin family protein, nearly identical	1	At1g52040.1	50149.1	0	0	0	0	1	AR1H
Symbol: None   expressed protein   chr1:20367115-203697	1	At1g54520.1	42827.6	0	0	0	0	1	AR1H
Symbol: None   disease resistance response protein-relate	2	At1g55210.1,A	20600.8	0	0	0	0	1	AR1H
Symbol: None   purine permease-related, low similarity to p	1	At1g57990.1	44165.3	0	0	0	0	1	AR1H
Symbol: None   dynamin-like protein, putative (ADL3), stro	1	At1g59610.1	100213	0	0	0	0	1	AR1H
Symbol: None   haloacid dehalogenase-like hydrolase fami	1	At1g59820.1	137738	0	0	0	0	1	AR1H
Symbol: None   pyruvate dehydrogenase E1 component al	1	At1g59900.1	43042.8	0	0	0	0	1	AR1H
Symbol: None   peptidase U7 family protein, similar to prot	1	At1g73990.1	75080.4	0	0	0	0	1	AR1H
Symbol: None   glycosyl hydrolase family 9 protein, similar	1	At1g75680.1	57852.8	0	0	0	0	2	AR1H
Symbol: None   NADH-ubiquinone oxidoreductase B18 sut	1	At2g02050.1	11722.1	0	0	0	0	1	AR1H
Symbol: FTSH4   encodes an FtsH protease that is localize	1	At2g26140.1	77257.9	0	0	0	0	1	AR1H
Symbol: None   mitochondrial import inner membrane trans	1	At2g28900.1 (r	15464.3	0	0	0	0	7	AR1H
Symbol: None   expressed protein   chr2:14085948-140872	1	At2g33220.1 (r	16104	0	0	0	0	5	AR1H
Symbol: None   60S ribosomal protein L18A (RPL18aB)   c	1	At2g34480.1	21289.9	0	0	0	0	1	AR1H
Symbol: None   fructose-bisphosphate aldolase, putative, s	2	At2g36460.1,A	38369.3	0	0	0	0	1	AR1H
*   Symbol: None   plasma membrane intrinsic protein 2C (PIF	1	At2g37180.1 (F	30411.7	0	0	0	0	2	AR1H
Symbol: None   annexin 4 (ANN4), nearly identical to anne.	1	At2g38750.1 (F	36204.7	0	0	0	0	1	AR1H
Symbol: None   expressed protein   chr2:18207400-182097	1	At2g43950.1 (c	38818.5	0	0	0	0	5	AR1H
Symbol: None   expressed protein   chr2:18424319-184264	1	At2g44640.1 (c	49814.5	0	0	0	0	3	AR1H
Symbol: None   fasciclin-like arabinogalactan-protein (FLA	1	At2g45470.1 (F	43058.3	0	0	0	0	1	AR1H
Symbol: None   importin alpha-1 subunit, putative (IMPA1),	2	At3g06720.1,A	58627.3	0	0	0	0	1	AR1H
Symbol: None   60S ribosomal protein L35 (RPL35A), simil	3	At3g09500.1,A	14268.1	0	0	0	0	1	AR1H
Symbol: MPPALPHA   mitochondrial processing peptidase	1	At3g16480.1 (r	54036.5	0	0	0	0	2	AR1H
Symbol: None   translationally controlled tumor family prote	1	At3g16640.1	18892.8	0	0	0	0	1	AR1H
Symbol: None   meprin and TRAF homology domain-conta	1	At3g20370.1	43433	0	0	0	0	1	AR1H
Symbol: None   AMP-binding protein, putative, similar to At	2	At3g23790.1,A	81131.1	0	0	0	0	1	AR1H
Symbol: None   cytochrome c1, putative, cytochrome c1, h	1	At3g27240.1 (r	33632.9	0	0	0	0	5	AR1H
Symbol: None   prohibitin, putative, strong similarity to proh	2	At3g27280.1,A	30620.7	0	0	0	0	2	AR1H
Symbol: AT14A   Possesses a transmembrane domain anc	2	At3g28290.1,A	42937.4	0	0	0	0	1	AR1H
Symbol: PGP19   Belongs to the family of ATP-binding cas	1	At3g28860.1 (r	136774	0	0	0	0	7	AR1H
Symbol: None   expressed protein   chr3:18450988-184531	1	At3g49720.1	28514.2	0	0	0	0	1	AR1H
Symbol: None   proton-dependent oligopeptide transport (F	1	At3g54140.1	64017.3	0	0	0	0	1	AR1H
Symbol: None   expressed protein, hin1 protein, Nicotiana t	1	At3g54200.1 (e	25767.9	0	0	0	0	1	AR1H
Symbol: None   thylakoid lumenal 20 kDa protein, SP:Q9L	1	At3g56650.1	28612.3	0	0	0	0	1	AR1H
Symbol: None   vacuolar ATPase subunit F family protein, r	1	At4g02620.1	14242	0	0	0	0	1	AR1H
Symbol: None   peptidoglycan-binding domain-containing	1	At4g13670.1 (c	44001.8	0	0	0	0	3	AR1H
Symbol: None   expressed protein   chr4:9280104-928074C	1	At4g16450.1 (r	11396.6	0	0	0	0	3	AR1H
Symbol: DELTA-TIP2   major intrinsic family protein / MIP f	1	At4g17340.1 (F	25062.4	0	0	0	0	2	AR1H
Symbol: None   potassium transporter family protein, simila	1	At4g33530.1 (F	94723.6	0	0	0	0	1	AR1H
Symbol: None   L-ascorbate peroxidase 3 (APX3), identical	1	At4g35000.1 (p	31554.8	0	0	0	0	4	AR1H
Symbol: None   translocate of chloroplast 34 (TOC34) / GT	3	At5g05000.1,A	34690.3	0	0	0	0	1	AR1H
Symbol: None   peptidyl-prolyl cis-trans isomerase cycloph	1	At5g13120.1	28288.4	0	0	0	0	1	AR1H
Symbol: None   translocon-associated protein beta (TRAP	1	At5g14030.1	21087	0	0	0	0	1	AR1H
Symbol: None   40S ribosomal protein S7 (RPS7C), 40S ril	1	At5g16130.1	22043.1	0	0	0	0	1	AR1H
Symbol: None   outer membrane OMP85 family protein, we	1	At5g19620.1	79919.2	0	0	0	0	1	AR1H
Symbol: None   mitochondrial import inner membrane trans	1	At5g24650.1	27755.1	0	0	0	0	1	AR1H
Symbol: None   similar to glycosyl hydrolase family 1 protei	3	At5g25980.1,A	53407	0	0	0	0	1	AR1H
Symbol: None   hexose transporter, putative, strong similar	1	At5g26340.1 (F	57402.9	0	0	0	0	4	AR1H
Symbol: EMB1467   NADH-ubiquinone dehydrogenase, mi	2	At5g37510.1,A	81164.3	0	0	0	0	1	AR1H
Symbol: None   cytochrome c1, putative, cytochrome c1, h	1	At5g40810.1 (r	33672.9	0	0	0	0	5	AR1H
Symbol: None   expressed protein   chr5:21298999-21300f	1	At5g52420.1	26720.3	0	0	0	0	1	AR1H
Symbol: None   porin, putative, similar to 36kDa porin II (Si	1	At5g57490.1 (r	29488.4	0	0	0	0	2	AR1H
Symbol: RPS8   chloroplast 30S ribosomal protein S8   chr	1	ATCG00770.1	15462.5	0	0	0	0	1	AR1H
Symbol: NDHA   NADH dehydrogenase ND1   chrC:11984	1	ATCG01100.1	40006.8	0	0	0	0	1	AR1H
Symbol: ORFB   Encodes the b subunit of the mitochondrie	2	ATMG00480.1.	18194.4	0	0	0	0	2	AR1H

Table 2.2. Continued.

Protein name	Matches	Accession	MW	R1m	AR1m	r1m	R1HAR1H	
Symbol: None   6-phosphogluconate dehydrogenase family	1	At1g64190.1 (€	53360.9	0	1	0	0	AR1m
Symbol: None   ADP-glucose pyrophosphorylase family pro	4	At1g74910.1.A	45546.1	0	1	0	1	AR1mH
Symbol: EMB1956   heat shock protein, putative, strong sir	2	At2g04030.1.A	88648.1	0	1	0	0	AR1m
Symbol: None   phosphoenolpyruvate carboxylase, putativ	2	At2g42600.1.A	90179.5	0	1	0	0	AR1m
Symbol: None   pectinesterase family protein, contains Pfa	1	At3g14310.1 (c	64238.5	0	1	0	0	AR1m
Symbol: None   UDP-glucose 6-dehydrogenase, putative, v	2	At3g29360.1.A	53155.5	0	1	0	0	AR1m
Symbol: None   asparagine synthetase 1 (glutamine-hydrol	3	At3g47340.1.A	65603.9	0	1	0	1	AR1mH
Symbol: None   microfibrillar-associated protein-related, sir	2	At4g08580.1.A	51154.7	0	1	0	0	AR1m
Symbol: None   eukaryotic translation initiation factor 3 sub	1	At4g11420.1	114286	0	1	0	0	AR1m
Symbol: None   RNase L inhibitor protein, putative, similar	1	At4g19210.1	68373.9	0	1	0	0	AR1m
Symbol: None   26S proteasome regulatory subunit, putativ	2	At4g24820.1.A	44266.3	0	1	0	1	AR1mH
Symbol: None   40S ribosomal protein S10 (RPS10A), 40S	3	At4g25740.1.A	19429.9	0	1	0	0	AR1m
Symbol: EMB2726   elongation factor Ts family protein, sir	1	At4g29060.1 (r	103764	0	1	0	0	AR1m
Symbol: None   splicing factor RSZp22 (RSZP22) / 9G8-lik	1	At4g31580.1 (r	22440.2	0	1	0	0	AR1m
Symbol: None   peptidase M3 family protein / thimet oligope	2	At5g10540.1.A	79028.3	0	1	0	0	AR1m
Symbol: None   heavy-metal-associated domain-containing	2	At5g19090.1.A	59603.4	0	1	0	0	AR1m
Symbol: None   malate dehydrogenase (NAD), mitochondri	1	At1g53240.1 (r	35787.2	0	2	0	0	AR1m
Symbol: None   RuBisCO subunit binding-protein alpha sub	1	At2g28000.1 (r	62055.4	0	2	0	1	AR1mH
Symbol: None   splicing factor RSZ33 (RSZ33), nearly iden	2	At2g37340.1.A	32875.7	0	2	0	0	AR1m
Symbol: None   shepherd protein (SHD) / clavata formation	2	At4g24190.1.A	94190.5	0	2	0	0	AR1m
Symbol: SAHH2   adenosylhomocysteinase, putative / S-ac	1	At3g23810.1 (?	53141.7	0	4	0	0	AR1m
Symbol: None   40S ribosomal protein S5 (RPS5A), identic	2	At2g37270.1.A	22973	0	5	0	4	AR1mH
*   Symbol: None   pentatricopeptide (PPR) repeat-containing	1	At1g02150.1 (?	59866.5	1	0	0	0	R1m
Symbol: None   GTP-binding protein (TOC33), identical to :	1	At1g02280.1 (c	32907.9	1	0	0	0	R1m
Symbol: None   multidrug resistance P-glycoprotein, putativ	1	At1g02530.1 (F	136760	1	0	0	3	R1mAR1H
Symbol: None   protochlorophyllide reductase C, chloroplas	2	At1g03630.1.A	43866.2	1	0	0	1	R1mAR1H
Symbol: None   aldo/keto reductase family protein, contain:	1	At1g06690.1 (c	41480.2	1	0	0	0	R1m
Symbol: None   Gene encoding ADP-ribosylation factor anc	8	At1g10630.1.A	20605.5	1	0	0	1	R1mAR1H
Symbol: None   3-oxoacyl-(acyl-carrier protein) reductase, i	1	At1g24360.1 (?	33530.5	1	0	0	0	R1m
Symbol: None   glycyl-tRNA synthetase / glycine-tRNA lig	1	At1g29880.1 (r	81927.6	1	0	0	0	R1m
Symbol: None   carbamoyl-phosphate synthase family prot	1	At1g29900.1 (c	129944	1	0	0	0	R1m
Symbol: None   bifunctional aspartate kinase/homoserine c	1	At1g31230.1 (c	99388	1	0	0	0	R1m
Symbol: None   similar to FF domain-containing protein / W	1	At1g44910.1 (?	109365	1	0	0	0	R1m
Symbol: None   dihydrolipoamide dehydrogenase 1, mitoch	4	At1g48030.1.A	53970.5	1	0	0	0	R1m
Symbol: None   leucine-rich repeat transmembrane protein	2	At1g48480.1.A	71115	1	0	0	1	R1mAR1H
Symbol: None   phosphoethanolamine N-methyltransferase	2	At1g48600.1.A	54001.4	1	0	0	1	R1mAR1H
Symbol: None   40S ribosomal protein S7 (RPS7A), similar	2	At1g48830.1.A	21904.8	1	0	0	0	R1m
Symbol: None   ATP-dependent Clp protease proteolytic su	1	At1g66670.1 (c	33908.7	1	0	0	1	R1mAR1H
Symbol: EMB2184   ribosomal protein L31 family protein, s	1	At1g75350.1 (c	16014.8	1	0	0	1	R1mAR1H
Symbol: None   expressed protein, low similarity to SP:Q9L	1	At2g05080.1 (r	141639	1	0	0	0	R1m
Symbol: None   fructose-bisphosphate aldolase, putative, s	3	At2g21330.1.A	42913.5	1	0	0	0	R1m
Symbol: None   leucine-rich repeat transmembrane protein	1	At2g26730.1 (F	71735	1	0	0	1	R1mAR1H
Symbol: None   vacuolar proton ATPase, putative, similar t	1	At2g28520.1 (€	93401.2	1	0	0	2	R1mAR1H
Symbol: FTSH3   encodes an FtsH protease that is localiz	1	At2g29080.1 (r	89337.2	1	0	0	0	R1m
Symbol: None   ribosomal protein L3 family protein, contair	1	At2g43030.1 (c	29346.3	1	0	0	1	R1mAR1H
Symbol: None   glutathione S-transferase 6 (GST6), identic	1	At2g47730.1 (c	29214.6	1	0	0	0	R1m
Symbol: None   ATP-citrate synthase, putative / ATP-citrate	2	At3g06650.1.A	65797.2	1	0	0	0	R1m
Symbol: None   expressed protein   chr3:2612400-261382€	1	At3g08600.1 (€	34715.6	1	0	0	0	R1m
Symbol: None   40S ribosomal protein S23 (RPS23A), simi	2	At3g09680.1.A	15752.1	1	0	0	0	R1m
Symbol: None   chaperonin, putative, similar to SWISS-PR	1	At3g18190.1 (?	57758.4	1	0	0	0	R1m
Symbol: None   H+-transporting two-sector ATPase, putativ	1	At3g28710.1 (F	40775	1	0	0	1	R1mAR1H
Symbol: None   50S ribosomal protein L9, chloroplast (CL9	1	At3g44890.1 (c	22116.4	1	0	0	3	R1mAR1H
Symbol: PHS2   Encodes a cytosolic alpha-glucan phospho	1	At3g46970.1 (c	95144.3	1	0	0	0	R1m
Symbol: FTSH7   encodes an FtsH protease that is localiz	2	At3g47060.1.A	87785.2	1	0	0	0	R1m
Symbol: None   malate dehydrogenase (NAD), chloroplast	1	At3g47520.1 (c	42388.3	1	0	0	0	R1m
Symbol: None   bacterial transferase hexapeptide repeat-cr	2	At3g48680.1.A	27938.3	1	0	0	1	R1mAR1H
Symbol: None   aspartyl protease family protein, contains F	1	At3g54400.1 (€	45458.1	1	0	0	0	R1m
Symbol: None   ketol-acid reductoisomerase, identical to ke	1	At3g58610.1 (r	63795.9	1	0	0	0	R1m
Symbol: None   mitogen-activated protein kinase, putative /	1	At4g01370.1 (r	42834.9	1	0	0	0	R1m
Symbol: None   protoporphyrinogen oxidase (PPOX), ident	2	At4g01690.1.A	57679.5	1	0	0	0	R1m
Symbol: None   chloroplast outer membrane protein, putati	1	At4g02510.1 (c	160801	1	0	0	2	R1mAR1H
Symbol: None   reticulon family protein (RTNLB2), similar t	2	At4g11220.1.A	30263.6	1	0	0	0	R1m

Table 2.2. Continued.

Protein name	Matches	Accession	MW	R1m	AR1m	r1m	R1HAR1H	
Symbol: None   glycine hydroxymethyltransferase, putative	1	At4g13930.1 (?)	51701.8	1	0	0	0	R1m
Symbol: None   ribosomal protein L19 family protein, simila	1	At4g17560.1 (c)	25501.3	1	0	0	0	R1m
Symbol: None   ABC transporter family protein, similar to rr	1	At4g25450.1 (F)	77911.1	1	0	0	0	R1m
Symbol: None   fibrillarin 2 (FIB2), identical to fibrillarin 2 G	2	At4g25630.1,A	33635.2	1	0	0	0	R1m
Symbol: None   band 7 family protein, similar to stomatin-lii	1	At4g27585.1 (r)	45003.1	1	0	0	0	R1mAR1H
Symbol: ATU2AF65A   U2 snRNP auxiliary factor large sut	3	At4g36690.1,A	63533.6	1	0	0	0	R1m
Symbol: None   xyloglucan:xyloglucosyl transferase, putativ	1	At4g37800.1 (c)	33663.3	1	0	0	0	R1m
Symbol: None   vacuolar ATP synthase subunit B, putative	4	At4g38510.1,A	54288.8	1	0	0	0	R1m
Symbol: None   isocitrate dehydrogenase, putative / NAD+	1	At5g03290.1 (r)	40607.3	1	0	0	0	R1m
Symbol: None   formate dehydrogenase (FDH), identical to	1	At5g14780.1 (c)	42392.5	1	0	0	0	R1m
Symbol: None   plastid-lipid associated protein PAP-relatec	1	At5g19940.1 (c)	26465.1	1	0	0	0	R1mAR1H
Symbol: None   Ras-related GTP-binding nuclear protein (F	3	At5g20010.1,A	25258.1	1	0	0	0	R1m
Symbol: None   chaperonin, putative, similar to SWISS-PR	1	At5g20890.1 (?)	57269.6	1	0	0	0	R1m
Symbol: None   expressed protein   chr5:8749730-8751635	3	At5g25250.1,A	52291.9	1	0	0	0	R1mAR1H
Symbol: None   expressed protein, predicted proteins, Ara	1	At5g28500.1 (c)	48219.2	1	0	0	0	R1mAR1H
Symbol: None   allene oxide synthase (AOS) / hydroperoxi	1	At5g42650.1 (F)	58181.6	1	0	0	0	R1m
Symbol: None   glucose-6-phosphate isomerase, cytosolic	1	At5g42740.1 (?)	61700.4	1	0	0	0	R1m
Symbol: None   NADH-ubiquinone oxidoreductase-related,	1	At5g52840.1 (r)	19161.2	1	0	0	0	R1m
Symbol: None   quinone reductase, putative, similar to 1,4-	1	At5g54500.1 (?)	21778.2	1	0	0	0	R1mAR1H
Symbol: None   calcium-transporting ATPase 8, plasma me	2	At5g57110.1,A	116159	1	0	0	0	R1mAR1H
Symbol: None   ATPase 3, plasma membrane-type / protor	1	At5g57350.1 (F)	104435	1	0	0	0	R1mAR1H
Symbol: None   26S proteasome AAA-ATPase subunit (RF	1	At5g58290.1 (r)	45734.3	1	0	0	0	R1mAR1H
Symbol: None   malate dehydrogenase (NADP), chloroplas	3	At5g58330.1,A	48299.3	1	0	0	0	R1m
Symbol: None   histone H2A, putative, similar to histone H2	1	At5g59870.1 (r)	15948.7	1	0	0	0	R1m
Symbol: None   calmodulin-binding family protein, contains	1	At5g62390.1 (?)	51551.8	1	0	0	0	R1m
Symbol: None   bacterial transferase hexapeptide repeat-c	1	At5g66510.1 (r)	27818.9	1	0	0	0	R1mAR1H
Symbol: ATPF   ATPase F subunit.   chrC:11529-12798 RE	1	ATCG00130.1	21039.8	1	0	0	0	R1m
Symbol: ATPE   ATPase epsilon subunit   chrC:52265-526	1	ATCG00470.1	14481.3	1	0	0	0	R1mAR1H
Symbol: RPL22   encodes a chloroplast ribosomal protein l	1	ATCG00810.1	18569.5	1	0	0	0	R1m
Symbol: None   histone H2B, putative, strong similarity to h	9	At1g07790.1,A	16385	1	1	0	0	all
Symbol: None   26S proteasome AAA-ATPase subunit (RF	1	At1g53750.1 (r)	47786.3	1	1	0	0	all
Symbol: None   phosphoglucomutase, cytoplasmic, putativ	1	At1g70730.1 (c)	63465.5	1	1	0	0	all
Symbol: None   fructose-bisphosphate aldolase, putative, s	2	At4g38970.1,A	42970.1	1	1	0	0	all
Symbol: EMB2728   ribulose-phosphate 3-epimerase, chlo	2	At5g61410.1,A	29990.5	1	1	0	0	R1mAR1m
Symbol: None   60S ribosomal protein L10 (RPL10A) / Wilr	3	At1g14320.1,A	24899.5	1	2	0	0	all
Symbol: None   geranylgeranyl reductase, identical to gera	1	At1g74470.1 (c)	51820.8	1	2	0	0	all
Symbol: None   plastid-lipid associated protein PAP, putativ	1	At2g35490.1 (c)	40488.9	1	2	0	0	R1mAR1m
Symbol: None   dyskerin, putative / nucleolar protein NAP5	1	At3g57150.1 (c)	63009.3	1	2	0	0	R1mAR1m
Symbol: None   tRNA synthetase class II (G, H, P and S) fe	2	At3g62120.1,A	60737.7	1	2	0	0	all
Symbol: None   60S ribosomal protein L24 (RPL24A)   chr2	2	At2g36620.1,A	18833	1	3	0	0	all
Symbol: None   K+ efflux antiporter, putative (KEA1), identi	1	At1g01790.1 (F)	64970.5	2	0	0	0	R1mAR1H
Symbol: TIC110   Encodes a protein thought to be a part of	1	At1g06950.1 (c)	112106	2	0	0	0	R1mAR1H
Symbol: None   ATP-dependent Clp protease proteolytic su	1	At1g11750.1 (c)	29364.7	2	0	0	0	R1mAR1H
Symbol: None   uridylyltransferase-related, similar to (Prote	2	At1g16880.1,A	31277.8	2	0	0	0	R1m
Symbol: None   O-methyltransferase, putative, similar to Gl	2	At1g21130.1,A	40730.4	2	0	0	0	R1mAR1H
Symbol: None   glutamate:glyoxylate aminotransferase 1 (C	6	At1g23310.1,A	53284.6	2	0	0	0	R1m
Symbol: None   disease resistance protein-related / LRR pr	1	At1g33590.1 (e)	51727.7	2	0	0	0	R1m
Symbol: None   serine-glyoxylate aminotransferase-related	1	At1g47260.1 (r)	30047	2	0	0	0	R1mAR1H
Symbol: None   formate--tetrahydrofolate ligase / 10-formyl	1	At1g50480.1 (?)	67785.3	2	0	0	0	R1mAR1H
Symbol: None   monodehydroascorbate reductase, putative	4	At1g63940.1,A	52485.1	2	0	0	0	R1mAR1H
Symbol: None   b-keto acyl reductase, putative (GLOSSY8	1	At1g67730.1 (e)	35745.7	2	0	0	0	R1mAR1H
Symbol: None   serine-glyoxylate aminotransferase-related	2	At2g13360.1,A	44191.1	2	0	0	0	R1m
Symbol: None   vacuolar proton ATPase, putative, similar t	1	At2g21410.1 (r)	93090.4	2	0	0	0	R1mAR1H
Symbol: None   epsin N-terminal homology (ENTH) domair	3	At2g25430.1,A	72067.6	2	0	0	0	R1mAR1H
Symbol: None   glutamate synthase, chloroplast (GLU2) / fr	3	At2g41220.1,A	177737	2	0	0	0	R1m
Symbol: None   40S ribosomal protein S7 (RPS7B), similar	2	At3g02560.1,A	22178.4	2	0	0	0	R1m
Symbol: None   cell elongation protein / DWARF1 / DIMINL	2	At3g19820.1,A	65377.8	2	0	0	0	R1mAR1H
Symbol: None   arginosuccinate synthase family, contains l	1	At4g24830.1 (c)	53828.4	2	0	0	0	R1mAR1H
Symbol: None   coatomer gamma-2 subunit, putative / gam	1	At4g34450.1 (e)	98474.2	2	0	0	0	R1m
Symbol: None   26S proteasome AAA-ATPase subunit (RF	2	At5g19990.1,A	47230.8	2	0	0	0	R1mAR1H
Symbol: None   luminal binding protein 1 (BiP-1) (BP1), SV	1	At5g28540.1 (E)	73612.9	2	0	0	0	R1m
Symbol: None   band 7 family protein, similar to hypersensi	1	At5g51570.1 (F)	32360	2	0	0	0	R1mAR1H

Table 2.2. Continued.

	Protein name	Matches	Accession	MW	R1m	AR1m	r1m	R1HAR1H	
	Symbol: None   phosphoglucosyltransferase, chloroplast (PGM) (l	1	At5g51820.1 (c	67973.7	2	0	0	0	R1m
*	Symbol: None   band 7 family protein, strong similarity to h	1	At5g62740.1 (F	31412.9	2	0	0	3	R1mAR1H
	Symbol: RPS4   Chloroplast encoded ribosomal protein S4	1	ATCG00380.1	23223.2	2	0	0	2	R1mAR1H
	Symbol: ACCD   carboxyltransferase beta subunit   chrC:57	1	ATCG00500.1	55595	2	0	0	0	R1m
	Symbol: RPS18   chloroplast-encoded ribosomal protein S	1	ATCG00650.1	12043.2	2	0	0	0	R1m
	Symbol: NAD2A   encodes subunit of mitochondrial NAD(P	2	ATMG00285.1	54866.2	2	0	0	3	R1mAR1H
	Symbol: NAD1C   Encodes subunit of mitochondrial NAD(F	4	ATMG00516.1	35659.8	2	0	0	5	R1mAR1H
	Symbol: None   Ras-related GTP-binding protein, putative,	12	At1g02130.1,A	22300.8	2	1	0	0	R1mAR1m
	Symbol: None   similar to multidrug resistance P-glycoprote	2	At1g10680.1,A	139897	2	1	0	2	all
	Symbol: None   elongation factor Tu family protein, similar	1	At1g62750.1 (c	86041	2	1	0	0	R1mAR1m
	Symbol: None   vestitone reductase-related, low similarity t	1	At4g35250.1 (c	43705.8	2	1	0	0	R1mAR1m
	Symbol: None   harpin-induced family protein / HIN1 family	1	At5g06320.1 (F	25930.5	2	1	0	3	all
	Symbol: None   dicarboxylate/tricarboxylate carrier (DTC), l	1	At5g19760.1 (r	31895.3	2	1	0	1	all
	Symbol: None   3-oxoacyl-(acyl-carrier-protein) synthase I,	2	At5g46290.1,A	50396.5	2	1	0	1	all
	Symbol: None   lipoxygenase (LOX2), identical to SP:P384	1	At3g45140.1 (c	102031	2	5	0	6	all
	Symbol: None   hydrolase, alpha/beta fold family protein, Ic	2	At1g52510.1,A	41822.8	3	0	0	1	R1mAR1H
	Symbol: None   multidrug resistant (MDR) ABC transporter	2	At2g47000.1,A	139015	3	0	0	10	R1mAR1H
	Symbol: None   cell division cycle protein 48 (CDC48A) (CI	3	At3g09840.1,A	89378	3	0	0	2	R1mAR1H
	Symbol: None   chloroplast inner envelope membrane prot	1	At3g63410.1 (c	37909.7	3	0	0	2	R1mAR1H
	Symbol: None   60S ribosomal protein L4/L1 (RPL4D), 60S	1	At5g02870.1 (c	44704.4	3	0	0	3	R1mAR1H
	Symbol: None   ABC1 family protein, contains Pfam domai	2	At5g64940.1,A	86008	3	0	0	1	R1mAR1H
	Symbol: None   40S ribosomal protein S15 (RPS15A), Stro	4	At1g04270.1,A	17112	3	1	0	3	all
	Symbol: None   aminomethyltransferase, putative, similar t	2	At1g11860.1,A	44427.8	3	2	0	1	all
	Symbol: None   phosphoglucosyltransferase, cytoplasmic, putativ	1	At1g23190.1 (c	63154	3	2	0	1	all
	Symbol: EMB2207   60S ribosomal protein L3 (RPL3A), ide	3	At1g43170.1,A	44541.6	3	2	0	3	all
	Symbol: None   coatomer protein complex, subunit alpha, p	1	At2g21390.1 (E	136452	3	2	0	1	all
	Symbol: None   Gar1 RNA-binding region family protein, cc	2	At3g03920.1,A	20965.4	3	2	0	1	all
	Symbol: None   phosphoglycerate kinase, putative, similar	2	At1g79550.1,A	42114.9	4	0	0	4	R1mAR1H
	Symbol: None   pyruvate kinase, putative, similar to pyruva	2	At2g36580.1,A	57490.9	4	0	0	0	R1m
	Symbol: None   leucine-rich repeat transmembrane protein	1	At3g02880.1 (F	67736.5	4	0	0	3	R1mAR1H
	Symbol: None   26S protease regulatory complex subunit 4	2	At2g20140.1,A	49330.5	4	2	0	1	all
	Symbol: None   26S proteasome regulatory complex subur	2	At1g45000.1,A	44739.7	5	0	0	2	R1mAR1H
	Symbol: None   beta-adaptin, putative, strong similarity to ξ	2	At4g11380.1,A	99357	5	1	0	0	R1mAR1m
	Symbol: None   40S ribosomal protein S5 (RPS5B), similar	2	At3g11940.1,A	22903.9	5	7	0	5	all
	Symbol: None   40S ribosomal protein S3A (RPS3aB)   chr	1	At4g34670.1 (C	29786.1	6	0	0	0	R1m
	Symbol: None   chloroplast nucleoid DNA-binding protein-n	1	At1g09750.1 (ε	47643.8	6	1	0	0	R1mAR1m
	Symbol: None   ATP synthase gamma chain 1, chloroplast	1	At4g04640.1 (C	40893.9	6	1	0	2	all
	Symbol: None   40S ribosomal protein S2 (RPS2A), similar	6	At1g58380.1,A	30723.2	6	4	0	8	all
	Symbol: None   vacuolar ATP synthase subunit C (VATC) /	1	At1g12840.1 (F	42601.6	7	0	0	5	R1mAR1H
*	Symbol: None   band 7 family protein, strong similarity to h	4	At1g69840.1,A	31387.4	7	0	0	11	R1mAR1H
	Symbol: None   H <sup>+</sup> -transporting two-sector ATPase, putativ	1	At3g28715.1 (F	40770.9	7	0	0	7	R1mAR1H
	Symbol: None   protochlorophyllide reductase B, chloroplast	3	At4g27440.1,A	43342.5	8	1	0	3	all
	Symbol: None   transketolase, putative, strong similarity to	1	At3g60750.1 (C	79952.1	10	9	0	5	all
	Symbol: None   clathrin heavy chain, putative, similar to Sw	1	At3g08530.1 (ε	193258	18	0	0	21	R1mAR1H

Color code: 1) light gray: protein IDs in Co-IP with anti-HA in AvrRpm1:HA expressed transgenic plants, 2) dark gray: protein IDs in Co-IP with anti-myc from RPM1:myc plants, 3) purple: protein IDs in Co-IP with anti-myc from AvrRpm1:HA expressed transgenic plants, 4) orange: protein IDs in both Co-IPs with anti-myc from RPM1:myc and anti-HG from AvrRpm1:HA expressed transgenic plants, 5) red: protein IDs in Co-IPs with anti-myc and anti-HA from AvrRpm1:HA expressed transgenic plants, 6) white (no color): protein IDs in Co-IPs with anti-myc from RPM1:myc and AvrRpm1:HA expressed transgenic plants, and 7) blue: protein IDs in Co-IPs with anti-myc from RPM1:myc and AvrRpm1:HA expressed transgenic plants, and anti-HA from AvrRpm1:HA transgenic plants.

(PPR) repeat-containing protein and three FtsH proteases family were commonly identified in all three different studies giving rise to an idea that there may common interacting protein families associating with different NB-LRR proteins, RPM1 and RPS2. These results also indicate that our current data obtained by medium stringency washing might provide a good first step in the identification of RPM1-associated proteins *in planta*, although RPM1 protein was not detected due to its low expression. Thus, we expect that repetitions using the same conditions (medium stringency washing) can be employed to monitor consistency and to validate candidate RPM1 interacting proteins.

Directly related with AvrRpm1-triggered RPM1 activation, proteomic analysis by two-dimensional gel electrophoresis (2DE) identified 52 unique proteins from 73 spots (Jones et al., 2006). Three proteins were increased protein level by AvrRpm1 in the presence of RPM1. The TCTP (The translationally controlled tumor protein) homolog (At3g16640) and 14-3-3-like protein (At5g10450: GF14 $\lambda$ ) were also detected in my MS data, especially Co-IP with anti-HA. TCTP functions in the guanine nucleotide exchange factor for the Ras GTPase as a molecular switch in most eukaryotes (Cans et al., 2003). In Arabidopsis, it involves in vegetative growth and auxin signaling (Berkowitz et al., 2008). However, the role of TCTP in plant immune response is not clear. The 14-3-3 proteins are able to bind various proteins such as kinases, phosphatases and transmembrane receptors (Mhaweck, 2005). A recent study showed that 14-3-3 protein (GF14 $\lambda$ ) interacts with C-terminal of RPW8.2 and confers basal and RPW8-mediated resistance to powdery mildew (Yang et al., 2009). Furthermore, several isoforms of 14-3-3 proteins can interact

with the tobacco N protein and viral replicase as scaffold proteins to control the N protein-mediated defense response (Konagaya et al., 2004). The 14-3-3 protein interacts with MAPKKK alpha, a positive regulator of programmed cell death (PCD) in tomato, and regulates AvrPto or AvrPtoB-triggered immunity through Pto kinase (Oh et al., 2010). Two more isoforms of 14-3-3 were detected in the low stringent washing condition. This brings, therefore, a speculation that 14-3-3 proteins may involve RPM1-mediated immune response in Arabidopsis.

Ribosomal proteins and proteasome regulatory subunits were commonly identified in three different conditions. Both protein families were detected in various proteomic approaches and considered as “false positive” signals (Van Leene J, 2010). Although the 26S proteasome subunit might be considered a “false positive”, it cannot be excluded that RPM1 degradation or disappearance after its activation by effectors might be dependent on the 26S proteasome (Boyes et al., 1998). Aquaporin PIPs have a role in water transport (Kaldenhoff and Fischer, 2006; Maurel, 2007) suggesting that aquaporins may contribute to ABA induced stomata closure (Cui et al., 2008). RPS2 has been shown to positively regulate stomatal closure (Melotto et al., 2006). Furthermore, it is known that RPM1 is involved in basal defense (Belkhdar et al., 2004), although it is unclear whether RPM1 functions in control of stomatal aperture. Thus, it would be interesting to monitor the role of RPM1 in stomatal closure in concert with aquaporin function.

Band 7 proteins (At1g69840, At5g51570 and At5g62740) share the stomatin/prohibitin/flotillin/HflK/C (SPFH) domain (Morrow and Parton, 2005; Rivera-Milla et al., 2006) and are also known as hypersensitive induced reaction (HIR)

proteins. SPFH domain family proteins are found in lipid rafts in sphingolipid and cholesterol enriched PM microdomains (Langhorst et al., 2005; Morrow and Parton, 2005), which are referred to as detergent-resistant membranes (DRMs) in plants. SPFH domain proteins function as scaffolds via oligomerization (Browman et al., 2007; Langhorst et al., 2005). Recently, a rice RPM1 ortholog was detected by mass spectrometry in rice DRM preparations (Minami et al., 2009), implicating that RPM1 in *Arabidopsis* may function on the plasma membrane in DRMs or lipid rafts as well. Thus, it can be speculated that SPFH domain family proteins may function as a scaffold for the RPM1 complex in lipid rafts.

The plasma membrane compartmentalization after eliciting with flg22 peptide was monitored (Keinath et al., 2010). Interestingly, most (seven: At3g28715, At3g28710, At4g39080, At1g78900, At2g21410, At3g42050 and At1g12840) of vacuolar (V) H(+)-ATPases and two PM ATPases (At4g30190 and At57350) detected in this chapter were enriched in DRM after flg22 treatment. V-ATPases localize in all types of endomembranes and plasma membrane as well as vacuole (Jefferies et al., 2008; Schumacher, 2006). This suggests the potential role of V-ATPase with RPM1 via endocytic trafficking (Schumacher, 2006). It has been proposed that proteasome-regulated plasma membrane fusion with the vacuolar membrane after challenging with *Pto* DC3000(*avrRpm1*) (Hatsugai et al., 2009; Hatsugai et al., 2004). A NDR1/HIN1-like 3 (NHL3) was detected in my data which accumulated more during the infection of avirulent *Pseudomonas syringae* such as AvrRpm1 and AvrRpt2 (Varet et al., 2002) and exhibited enhanced disease resistance to virulent *P. syringae* when overexpressed (Varet et al., 2003). This

protein accumulated more in DRM post flg22 treatment (Keinath et al., 2010). It still remains, however, to prove whether lipid raft or DRM can participate in RPM1-mediated defense mechanism as mentioned previously.

The MATH domain-containing proteins are characterized as TNF Receptor Associated Factor (TRAF) family proteins in human immune responses. They act during inflammation as protein adapters (Lee and Lee, 2002). They exist throughout the plant kingdom, but not much is known in defense related functions. The MATH domain proteins are involved in restriction of long distance movement of plant viruses (Cosson et al., 2010), which leads the possibility that the MATH proteins may contribute to immune response in plant. Three FtsH proteases (FtsH 3, 4 and 7) were identified in medium stringent washing condition (Table 2.2). FtsHs located in the cytoplasmic membrane functions in degradation of a short-lived proteins and mis-folded proteins in the membrane (Ingmer and Brondsted, 2009). It functions as metalocasease dependent on ATP. One of major role of FtsH protein is proven as quality control of cytoplasmic membrane proteins by sensing abnormalities of target proteins in bacteria (Akiyama, 2009). In Arabidopsis, it has been know that FtsHs localize in mitochondria and chloroplast, and are critical for proper organelle formation (Sakamoto, 2006). However, it is still unclear whether these proteases are involved in plant defense.

The main questions to be addressed in this chapter are (1) what is the status of immune complex-containing NB-LRR proteins in both inactive and active state, and (2) what proteins can function in plant defense responses with NB-LRR proteins Although the results described are not sufficient to elucidate answers for all

questions, they are a stepping stone for an in-depth study including genetic, biochemical and cell biological analyses to further understanding of the molecular mechanism of NB-LRR-mediated plant disease resistance, its interaction with the machinery of basal defense, and their manipulation by pathogen encoded virulence factors.

## **MATERIALS AND METHODS**

**Plants and mutants.** The following mutant alleles and plant genotypes were used in this work: *rpm1-3* has a stop codon following amino acid 87 (Grant et al., 1995). *RPM1-myc* plants are *rpm1-3* plants expressing a c-myc epitope tagged version of *RPM1* under its native promoter (Boyes et al., 1998). The *rps2-101C* has a stop codon following amino acid 235 (Bent et al., 1994). The *rin4* null allele is a T-DNA insertion in the coding region (Mackey et al., 2003). Plants that conditionally express *AvrRpm1* in *rpm1* (*Dex:avrRpm1-HA rpm1*) were previously described (Mackey et al., 2003). These were crossed to *RPM1-myc* plants to generate *Dex:avrRpm1-HA RPM1-myc* (this study).

### ***Pseudomonas syringae* infections and conditional type III effector expression.**

*Pto* DC3000 carrying either pVSP61 (empty vector, EV), or derivatives of this plasmid expressing *avrRpm1* or *avrB* (Ritter and Dangl, 1996) were used in this study. Bacteria were inoculated at  $5 \times 10^7$  cfu/ml into 5-week-old plants on the abaxial surface of leaves. To induce effector proteins in transgenic plants, 5-week-old plants were sprayed with 20  $\mu$ M dexamethasone (Sigma) and 0.0075% Silwet L-77 (CKWitco Corporation).

**Microsomal membrane protein preparation.** 5 grams of leaves were ground in liquid nitrogen with a mortar and pestle. The extract was homogenized by two rounds of 30 seconds using a Polytron (Kinematica) in 20 ml of Buffer 1 (50 mM Tris pH 8.0, 100 mM NaCl, 1X plant protease cocktail (Sigma), 20 mM dithiothreitol (DTT) and 0.33 M sucrose). The plant debris was filtered out using two layers of Miracloth (Calbiochem) and the remaining solution cleared via centrifugation at 3000 x g for 20 min at 4°C. The supernatant was then centrifuged at 100,000 x g in an SW 41.1 rotor (Beckman) for 1 hour at 4°C. The proteins from the microsomal pellet were extracted in 700 µl of Buffer 2 (50 mM Tris pH 9.6, 100 mM NaCl, 1X plant protease cocktail (Sigma), 20 mM DTT, 1% DDM (D-dodecyl maltoside)(Calbiochem)) and incubated for 30 min on an orbital shaker at 25°C or, alternatively, stored overnight at 4°C. The insoluble debris remaining after this re-suspension was removed from the microsomal extracts by centrifugation at 20,000 x g for 15min at 4°C. The pH was then adjusted to 8.0 by adding 1 µl of Tris-HCl pH 6.8. Protein concentration was quantified using the Bio-Rad protein assay (Bio-Rad).

**Size Exclusion chromatography, Immunoprecipitation and Immunoblot Analysis.** For FPLC analysis, 1 mg of microsomal membrane protein was fractionated using a Superose 6 column (Amersham) at a flow rate of 0.8 ml/min equilibrated with Buffer 4 (50 mM Tris pH 8.0, 150 mM NaCl and 0.05% DDM). 400 µl fractions were precipitated overnight at -20°C in four volumes of acetone. The precipitated proteins were collected via centrifugation at 20,000 g for 20 min at 4°C,

re-suspended in 40  $\mu$ L of SDS-sample buffer, and separated on 8% (for RPM1 detection) or 12% (for RIN and AvrRpm1-HA) SDS-PAGE gels.

For co-immunoprecipitations, 600  $\mu$ g of total protein in Buffer 5 (50 mM Hepes pH 7.5, 50 mM NaCl, 10mM EDTA pH 8.0, 1X plant protease cocktail (Sigma) containing 0.5% Triton X-100 and 5 mM DTT) was combined with either 40  $\mu$ l of  $\mu$ MACS-myc or 40  $\mu$ l of HA epitope magnetic beads (Miltenyi Biotec). All reactions were then rolled for 3 hr at 4°C. The beads were washed three times with buffer 5, containing 0.2% Triton X-100 instead of 0.5% Triton X-100, and eluted with sample buffer as instructed by the manufacturer. For total protein extractions, samples were prepared by directly grinding in Buffer 6 (50 mM Tris (8.0), 100 mM NaCl, 1% SDS, plant protease cocktail (Sigma) 20 mM DTT). Protein blots were probed to visualize RPM1 with anti-myc antibodies (Boyes et al., 1998), RIN4 with anti-RIN4 antibodies), AvrRpm1 with anti-HA antibodies (Mackey et al., 2002).

**Mass Spectrometry and Protein Identification.** Proteins were submitted to the Genome Center Proteomics Core at the University of California, Davis, for mass spectrometry (LC/MS/MS)-based protein identification. LC/MS/MS with Nano LC 2D-system (Eksigent) coupled with an LTQ ion trap mass spectrometer (Thermo-Fisher) and Picoview Nano-spray source was employed to identify proteins. All MS/MS samples were analyzed using Mascot (Matrix Science, version 2.1.03) and X! Tandem ([www.thegpm.org](http://www.thegpm.org); version 2006.04.01.2). Ion mass tolerance of 0.60 Da and a parent ion tolerance of 2.0 Da were adapted in Mascot and X! Scaffold (version Scaffold\_2\_01\_02, Proteome Software Inc.). MS/MS-based peptide and protein identifications were validated through Scaffold (ver. 1.01,

Proteome Software Inc.). Peptide identifications which exhibited over 95.0% probability were selected.

## **REFERENCES**

- Abramovitch, R.B., Kim, Y.J., Chen, S., Dickman, M.B., and Martin, G.B. (2003). *Pseudomonas* type III effector AvrPtoB induces plant disease susceptibility by inhibition of host programmed cell death. *Embo J* 22, 60-69.
- Ade, J., DeYoung, B.J., Golstein, C., and Innes, R.W. (2007). Indirect activation of a plant nucleotide binding site-leucine-rich repeat protein by a bacterial protease. *Proc Natl Acad Sci U S A* 104, 2531-2536.
- Alfano, J.R., and Collmer, A. (1997). The type III (Hrp) secretion pathway of plant pathogenic bacteria: trafficking harpins, Avr proteins, and death. *J Bacteriol* 179, 5655-5662.
- Axtell, M.J., and Staskawicz, B.J. (2003). Initiation of *RPS2*-specified disease resistance in *Arabidopsis* is coupled to the AvrRpt2-directed elimination of RIN4. *Cell* 112, 369-377.
- Belkhadir, Y., Nimchuk, Z., Hubert, D.A., Mackey, D., and Dangl, J.L. (2004a). *Arabidopsis* RIN4 negatively regulates disease resistance mediated by *RPS2* and *RPM1* downstream or independent of the *NDR1* signal modulator, and is not required for the virulence functions of bacterial type III effectors AvrRpt2 or AvrRpm1. *Plant Cell* 16, 2822-2835.
- Belkhadir, Y., Subramaniam, R., and Dangl, J.L. (2004b). Plant disease resistance protein signaling: NBS-LRR proteins and their partners. *Curr Opin Plant Biol* 7, 391-399.
- Berkowitz, O., Jost, R., Pollmann, S., and Masle, J. (2008). Characterization of TCTP, the translationally controlled tumor protein, from *Arabidopsis thaliana*. *The Plant Cell* 20, 3430-3447.
- Boyes, D.C., Nam, J., and Dangl, J.L. (1998). The *Arabidopsis thaliana* *RPM1* disease resistance gene product is a peripheral plasma membrane protein that is degraded coincident with the hypersensitive response. *Proc Natl Acad Sci U S A* 95, 15849-15854.
- Browman, D.T., Hoegg, M.B., and Robbins, S.M. (2007). The SPFH domain-containing proteins: more than lipid raft markers. *Trends in cell biology* 17, 394-402.
- Burckstummer, T., Bennett, K.L., Preradovic, A., Schutze, G., Hantschel, O., Superti-Furga, G., and Bauch, A. (2006). An efficient tandem affinity purification procedure for interaction proteomics in mammalian cells. *Nat Methods* 3, 1013-1019.
- Cans, C., Passer, B.J., Shalak, V., Nancy-Portebois, V., Crible, V., Amzallag, N., Allanic, D., Tufino, R., Argentini, M., Moras, D., *et al.* (2003). Translationally controlled tumor protein acts as a guanine nucleotide dissociation inhibitor on the translation elongation factor eEF1A. *Proceedings of the National Academy of Sciences of the United States of America* 100, 13892-13897.
- Chisholm, S.T., Dahlbeck, D., Krishnamurthy, N., Day, B., Sjolander, K., and Staskawicz, B.J. (2005). Molecular characterization of proteolytic cleavage sites of the *Pseudomonas syringae* effector AvrRpt2. *PNAS* 102, 2087-2092.

Chung, E.H., da Cunha, L., Wu, A.J., Gao, Z., Cherkis, K., Afzal, A.J., Mackey, D., and Dangl, J.L. (2011). Specific Threonine Phosphorylation of a Host Target by Two Unrelated Type III Effectors Activates a Host Innate Immune Receptor in Plants. *Cell Host & Microbe* 9, 125-136.

Collier, S.M., and Moffett, P. (2009). NB-LRRs work a "bait and switch" on pathogens. *Trends in Plant Science* 14, 521-529.

Coppinger, P., Repetti, P.P., Day, B., Dahlbeck, D., Mehlert, A., and Staskawicz, B.J. (2004). Overexpression of the plasma membrane-localized NDR1 protein results in enhanced bacterial disease resistance in *Arabidopsis thaliana*. *Plant J* 40, 225-237.

Cui, X.H., Hao, F.S., Chen, H., Chen, J., and Wang, X.C. (2008). Expression of the *Vicia faba* VfPIP1 gene in *Arabidopsis thaliana* plants improves their drought resistance. *J Plant Res* 121, 207-214.

da Cunha, L., Sreerekha, M.V., and Mackey, D. (2007). Defense suppression by virulence effectors of bacterial phytopathogens. *Current Opinion in Plant Biology* 10, 349-357.

Dangl, J.L., and Jones, J.D.G. (2001). Plant pathogens and integrated defence responses to infection. *Nature* 411, 826-833.

Day, B., Dahlbeck, D., and Staskawicz, B.J. (2006). NDR1 interaction with RIN4 Mediates the Differential Activation of Multiple Disease Resistance Pathways. *Plant Cell in press*.

Gavin, A.C., and Superti-Furga, G. (2003). Protein complexes and proteome organization from yeast to man. *Curr Opin Chem Biol* 7, 21-27.

Gomez-Gomez, L., and Boller, T. (2002). Flagellin perception: a paradigm for innate immunity. *Trends Plant Sci* 7, 251-256.

Grant, M.R., Godiard, L., Straube, E., Ashfield, T., Lewald, J., Sattler, A., Innes, R.W., and Dangl, J.L. (1995). Structure of the *Arabidopsis* RPM1 gene enabling dual specificity disease resistance. *Science* 269, 843-846.

Gregan, J., Riedel, C.G., Petronczki, M., Cipak, L., Rumpf, C., Poser, I., Buchholz, F., Mechtler, K., and Nasmyth, K. (2007). Tandem affinity purification of functional TAP-tagged proteins from human cells. *Nat Protoc* 2, 1145-1151.

Gutierrez, J.R., Balmuth, A.L., Ntoukakis, V., Mucyn, T.S., Gimenez-Ibanez, S., Jones, A.M., and Rathjen, J.P. (2010). Prf immune complexes of tomato are oligomeric and contain multiple Pto-like kinases that diversify effector recognition. *The Plant journal : for cell and molecular biology* 61, 507-518.

Hatsugai, N., Iwasaki, S., Tamura, K., Kondo, M., Fujii, K., Ogasawara, K., Nishimura, M., and Hara-Nishimura, I. (2009). A novel membrane fusion-mediated plant immunity against bacterial pathogens. *Genes & development* 23, 2496-2506.

Hatsugai, N., Kuroyanagi, M., Yamada, K., Meshi, T., Tsuda, S., Kondo, M., Nishimura, M., and Hara-Nishimura, I. (2004). A plant vacuolar protease, VPE, mediates virus-induced hypersensitive cell death. *Science* 305, 855-858.

Hauck, P., Thilmony, R., and He, S.Y. (2003). A *Pseudomonas syringae* type III effector suppresses cell wall-based extracellular defense in susceptible *Arabidopsis* plants. *Proc Natl Acad Sci U S A* *100*, 8577-8582.

Jamir, Y., Guo, M., Oh, H.S., Petnicki-Ocwieja, T., Chen, S., Tang, X., Dickman, M.B., Collmer, A., and Alfano, J.R. (2004). Identification of *Pseudomonas syringae* type III effectors that can suppress programmed cell death in plants and yeast. *Plant J* *37*, 554-565.

Jefferies, K.C., Cipriano, D.J., and Forgac, M. (2008). Function, structure and regulation of the vacuolar (H<sup>+</sup>)-ATPases. *Archives of Biochemistry and Biophysics* *476*, 33-42.

Jones, A.M., Thomas, V., Bennett, M.H., Mansfield, J., and Grant, M. (2006). Modifications to the *Arabidopsis* defense proteome occur prior to significant transcriptional change in response to inoculation with *Pseudomonas syringae*. *Plant Physiology* *142*, 1603-1620.

Jones, J.D., and Dangl, J.L. (2006). The plant immune system. *Nature* *444*, 323-329.

Kaldenhoff, R., and Fischer, M. (2006). Functional aquaporin diversity in plants. *Biochimica et biophysica acta* *1758*, 1134-1141.

Keinath, N.F., Kierszniowska, S., Lorek, J., Bourdais, G., Kessler, S.A., Shimosato-Asano, H., Grossniklaus, U., Schulze, W.X., Robatzek, S., and Panstruga, R. (2010). PAMP (pathogen-associated molecular pattern)-induced changes in plasma membrane compartmentalization reveal novel components of plant immunity. *The Journal of Biological Chemistry* *285*, 39140-39149.

Kim, H.S., Desveaux, D., Singer, A.U., Patel, P., Sondek, J., and Dangl, J.L. (2005). The *Pseudomonas syringae* effector AvrRpt2 cleaves its C-terminally acylated target, RIN4, from *Arabidopsis* membranes to block RPM1 activation. *Proc Natl Acad Sci U S A* *102*, 6496-6501.

Knol, J., Sjollem, K., and Poolman, B. (1998). Detergent-mediated reconstitution of membrane proteins. *Biochemistry* *37*, 16410-16415.

Langhorst, M.F., Reuter, A., and Stuermer, C.A. (2005). Scaffolding microdomains and beyond: the function of reggie/flotillin proteins. *Cellular and molecular life sciences : CMLS* *62*, 2228-2240.

Le Maire, M., Champeil, P., and Moller, J.V. (2000). Interaction of membrane proteins and lipids with solubilizing detergents. *Biochem Biophys Acta* *1508*, 86-111.

Liu, J., Elmore, J.M., Fuglsang, A.T., Palmgren, M.G., Staskawicz, B.J., and Coaker, G. (2009). RIN4 Functions with Plasma Membrane H-ATPases to Regulate Stomatal Apertures during Pathogen Attack. *PLoS biology* *7*, e1000139.

Lu, D., He, P., and Shan, L. (2010). Bacterial effectors target BAK1-associated receptor complexes: One stone two birds. *Commun Integr Biol* *3*, 80-83.

Mackey, D., Belkhadir, Y., Alonso, J.M., Ecker, J.R., and Dangl, J.L. (2003). *Arabidopsis* RIN4 is a target of the type III virulence effector AvrRpt2 and modulates RPS2-mediated resistance. *Cell* *112*, 379-389.

- Mackey, D., Holt III, B.F., Wiig, A., and Dangl, J.L. (2002). RIN4 interacts with *Pseudomonas syringae* Type III effector molecules and is required for RPM1-mediated disease resistance in *Arabidopsis*. *Cell* 108, 743-754.
- Maurel, C. (2007). Plant aquaporins: novel functions and regulation properties. *FEBS Letters* 581, 2227-2236.
- Melotto, M., Underwood, W., Koczan, J., Nomura, K., and He, S.Y. (2006). Plant Stomata Function in Innate Immunity against Bacterial Invasion. *Cell* 126, 969-980.
- Mestre, P., and Baulcombe, D.C. (2006). Elicitor-mediated oligomerization of the tobacco N disease resistance protein. *Plant Cell* 18, 491-501.
- Mhaweche, P. (2005). 14-3-3 proteins--an update. *Cell Res* 15, 228-236.
- Minami, A., Fujiwara, M., Furuto, A., Fukao, Y., Yamashita, T., Kamo, M., Kawamura, Y., and Uemura, M. (2009). Alterations in detergent-resistant plasma membrane microdomains in *Arabidopsis thaliana* during cold acclimation. *Plant Cell Physiol* 50, 341-359.
- Moffett, P., Farnham, G., Peart, J., and Baulcombe, D.C. (2002). Interaction between domains of a plant NBS-LRR protein in disease resistance-related cell death. *Embo J* 21, 4511-4519.
- Morrow, I.C., and Parton, R.G. (2005). Flotillins and the PHB domain protein family: rafts, worms and anaesthetics. *Traffic* 6, 725-740.
- Munro, S. (2003). Lipid rafts: elusive or illusive? *Cell* 115, 377-388.
- Nguyen, H.P., Yeam, I., Angot, A., and Martin, G.B. (2010). Two virulence determinants of type III effector AvrPto are functionally conserved in diverse *Pseudomonas syringae* pathovars. *The New phytologist* 187, 969-982.
- Nimchuk, Z., Eulgem, T., Holt, B.F., 3rd, and Dangl, J.L. (2003). Recognition and response in the plant immune system. *Annual review of genetics* 37, 579-609.
- Nimchuk, Z., Marois, E., Kjemtrup, S., Leister, R.T., Katagiri, F., and Dangl, J.L. (2000). Eukaryotic fatty acylation drives plasma membrane targeting and enhances function of several Type III effector proteins from *Pseudomonas syringae*. *Cell* 101, 353-363.
- Nishimura, M.T., and Dangl, J.L. (2010). *Arabidopsis* and the plant immune system. *The Plant Journal* 61, 1053-1066.
- Nourry, C., Grant, S.G., and Borg, J.P. (2003). PDZ domain proteins: plug and play! *Sci STKE* 2003, RE7.
- Oh, C.S., Pedley, K.F., and Martin, G.B. (2010). Tomato 14-3-3 protein 7 positively regulates immunity-associated programmed cell death by enhancing protein abundance and signaling ability of MAPKKK {alpha}. *The Plant Cell* 22, 260-272.

Puig, O., Caspary, F., Rigaut, G., Rutz, B., Bouveret, E., Bragado-Nilsson, E., Wilm, M., and Seraphin, B. (2001). The tandem affinity purification (TAP) method: a general procedure of protein complex purification. *Methods* 24, 218-229.

Qi, Y., and Katagiri, F. (2009). Purification of low-abundance Arabidopsis plasma-membrane protein complexes and identification of candidate components. *Plant J* 57, 932-944.

Rathjen, J.P., and Moffett, P. (2003). Early signal transduction events in specific plant disease resistance. *Curr Opin Plant Biol* 6, 300-306.

Rivera-Milla, E., Stuermer, C.A., and Malaga-Trillo, E. (2006). Ancient origin of reggie (flotillin), reggie-like, and other lipid-raft proteins: convergent evolution of the SPFH domain. *Cellular and molecular life sciences : CMLS* 63, 343-357.

Rohila, J.S., Chen, M., Cerny, R., and Fromm, M.E. (2004). Improved tandem affinity purification tag and methods for isolation of protein heterocomplexes from plants. *The Plant journal : for cell and molecular biology* 38, 172-181.

Rohila, J.S., Chen, M., Chen, S., Chen, J., Cerny, R.L., Dardick, C., Canlas, P., Fujii, H., Gribskov, M., Kanrar, S., *et al.* (2009). Protein-protein interactions of tandem affinity purified protein kinases from rice. *PLoS One* 4, e6685.

Schumacher, K. (2006). Endomembrane proton pumps: connecting membrane and vesicle transport. *Current Opinion in Plant Biology* 9, 595-600.

Shao, F., Golstein, C., Ade, J., Stoutemyer, M., Dixon, J.E., and Innes, R.W. (2003). Cleavage of Arabidopsis PBS1 by a bacterial type III effector. *Science* 301, 1230-1233.

Simonich, M.T., and Innes, R.W. (1995). A disease resistance gene in Arabidopsis with specificity for the *avrPph3* gene of *Pseudomonas syringae* pv. *phaseolicola*. *Mol Plant Microbe Interact* 8, 637-640.

Simons, K., and Toomre, D. (2000). Lipid rafts and signal transduction. *Nat Rev Mol Cell Biol* 1, 31-39.

Tornero, P., Chao, R.A., Luthin, W.N., Goff, S.A., and Dangl, J.L. (2002). Large-scale structure-function analysis of the Arabidopsis RPM1 disease resistance protein. *The Plant Cell* 14, 435-450.

Van Leene J, H.J., Eeckhout D, Persiau G, Van De Slijke E, Stals H, Van Isterdael G, Verkest A, Neiryneck S, Buffel Y, De Bodt S, Maere S, Laukens K, Pharazyn A, Ferreira PC, Eloy N, Renne C, Meyer C, Faure JD, Steinbrenner J, Beynon J, Larkin JC, Van de Peer Y, Hilson P, Kuiper M, De Veylder L, Van Onckelen H, Inzé D, Witters E, De Jaeger G (2010). Targeted interactomics reveals a complex core cell cycle machinery in Arabidopsis thaliana. *Molecular Systems Biology* 6, 12.

Varet, A., Hause, B., Hause, G., Scheel, D., and Lee, J. (2003). The Arabidopsis NHL3 gene encodes a plasma membrane protein and its overexpression correlates with increased resistance to *Pseudomonas syringae* pv. *tomato* DC3000. *Plant Physiology* 132, 2023-2033.

Varet, A., Parker, J., Tornero, P., Nass, N., Nürnberger, T., Dangl, J.L., Scheel, D., and Lee, J. (2002). *NHL25* and *NHL3*, two *NDR1/HIN1*-like genes in *Arabidopsis thaliana* with potential role(s) in plant defense. *Molec Plant-Microbe Interact* 15, 608-616.

Yang, X., Wang, W., Coleman, M., Orgil, U., Feng, J., Ma, X., Ferl, R., Turner, J.G., and Xiao, S. (2009). *Arabidopsis* 14-3-3 lambda is a positive regulator of RPW8-mediated disease resistance. *The Plant journal : for cell and molecular biology* 60, 539-550.

## CHAPTER 3

**Specific threonine phosphorylation of a host target mediated by two unrelated type III effector proteins results in activation of a host innate immune receptor in plants**

### **PREFACE**

The following chapter was published in *Cell Host & Microbe* (2011). I am the first author for this paper. I contributed for the paper all figures and tables except Figure 3.1, where I collaborated with members of Dr. David Mackey's lab at OSU, and Figure 3.2 (Y2H and modeling) where I collaborated with Dr. A.-J. Wu and Karen Cherkis, respectively) I created and edited figures in the manuscript. Figures and tables were re-numbered for chapter.

### **ABSTRACT**

RPM1 is an Arabidopsis NB-LRR immune receptor mediating disease resistance in response to *Pseudomonas syringae* type III effector proteins AvrB and AvrRpm1. Arabidopsis RIN4 regulates host defenses, is targeted by both effectors, and

associates with RPM1 at the plasma membrane. AvrRpm1 and AvrB drive post-translational phosphorylation of RIN4, though neither are obvious kinases. We hypothesized that this modification on RIN4 activates RPM1. We provide compelling evidence supporting this model. RIN4<sub>142-176</sub>, previously co-crystallized with AvrB, is necessary and, when present with appropriate localization sequences, sufficient to support effector-triggered RPM1 activation. Threonine 166 is necessary for AvrB-triggered RPM1 activation. Phosphomimic substitutions at T166 cause effector-independent RPM1 activation that requires the RPM1 P-loop. RIN4 T166 is phosphorylated *in vivo* in the presence of AvrB or AvrRpm1. RIN4 mutants that lose interaction with AvrB cannot be co-immunoprecipitated with RPM1. This defines a common interaction platform required for activation by phosphorylated RIN4. We conclude that AvrB and AvrRpm1 activate RPM1 by mediating the phosphorylation of RIN4 T166. Wide conservation of an analogous threonine across a small family of RIN4-like proteins indicates a key function for this residue beyond the regulation of RPM1.

## **INTRODUCTION**

Plants use an active immune system to fend off most microbes, but the induction of a successful response to a pathogen relies on specific recognition of pathogen-encoded molecules. Effector proteins produced by pathogens and translocated into plant cells, where they function as virulence factors, can be specifically recognized by intracellular immune receptors in plants (Dodds and Rathjen, 2010; Jones and Dangl, 2006). Type III effectors (T3Es) are produced by Gram-negative phytopathogenic bacteria and injected into host cells through the hypodermic needle-like type III secretion apparatus (He et al., 1994; Jones and Dangl, 2006).

Although they can trigger immune receptor function, pathogen-encoded effector proteins, including bacterial T3Es, have evolved to promote virulence (Jakobek et al., 1993). Once delivered, effector proteins are trafficked to a variety of sub-cellular locations (Nomura et al., 2005). Host-derived modifications, such as acylation, often influence sub-cellular targeting of effectors (Nimchuk et al., 2000). Despite their varied sites of action, many effectors share the ability to suppress host defenses via targeting and modification of host proteins that can function to regulate host defense output processes (Gimenez-Ibanez et al., 2009; Hauck et al., 2003; Rosebrock et al., 2007; Shan et al., 2008; Wilton et al., 2010). One example is Arabidopsis RIN4, which is a negative regulator of basal plant defense and is targeted by multiple T3Es, including two investigated in this study, AvrRpm1 and AvrB from *Pseudomonas syringae* (Kim et al., 2005b; Mackey et al., 2002).

The virulence functions of effectors within host cells make them vulnerable to detection by immune receptors. Plants encode disease resistance (R) proteins that recognize the presence of effectors (Dangl and Jones, 2001; Dodds and Rathjen, 2010; Jones and Dangl, 2006). The majority of intracellular plant disease resistance proteins share a common a central nucleotide binding domain and C-terminal leucine-rich repeats (NB-LRR). The N-terminus of RPM1 is composed of a coiled-coil domain (CC-NB-LRR), while a second class of NB-LRR proteins has Toll/interleukin-1 motifs at their N-termini (TIR-NB-LRR). These proteins are analogous to animal innate immune receptors of the NLR class (Ting et al., 2010; Ting et al., 2008).

*Arabidopsis* encodes ~150 NB-LRR proteins, a number that might seem insufficient to offer direct recognition of the diversity of pathogen-encoded effector proteins. However, if pathogen effectors repeatedly target a finite number of host molecules, then NB-LRR proteins indirectly recognizing perturbation of these molecules could provide a robust protective function (Dangl and Jones, 2001; Jones and Dangl, 2006). RIN4 and associated proteins provide key evidence for this hypothesis. RIN4 is a negative regulator of immune responses elicited by microbe associated molecular patterns (MAMPs) (Kim et al., 2005b). Multiple T3Es with the ability to suppress MAMP-triggered immunity (MTI) target RIN4, including AvrRpm1, AvrB, AvrRpt2, HopF2 (Axtell and Staskawicz, 2003; Mackey et al., 2003; Mackey et al., 2002; Wang et al.; Wilton et al., 2010), and potentially others (Luo et al., 2009). Paralleling the independent evolution of T3Es targeting RIN4, *Arabidopsis* deploys two distinct CC-NB-LRR proteins, RPM1 and RPS2, to monitor RIN4 integrity (Axtell

and Staskawicz, 2003; Mackey et al., 2003; Mackey et al., 2002; Wang et al.; Wilton et al., 2010). Soybean and lettuce deploy additional NB-LRR-proteins that likely monitor RIN4 orthologues (Ashfield et al., 2004; Jeuken et al., 2009). RPM1 and RPS2 each interact with RIN4 at the plasma membrane in un-challenged Arabidopsis (Axtell and Staskawicz, 2003; Mackey et al., 2003; Mackey et al., 2002). AvrRpm1, AvrB and AvrRpt2 are acylated subsequent to delivery and thus localized to the host membrane where they encounter their targets, including RIN4 (Nimchuk et al., 2000). RPM1 responds to AvrRpm1 and AvrB, both of which interact with and induce phosphorylation of RIN4. RPS2 responds to AvrRpt2, a cysteine protease effector that cleaves RIN4 at two sites (Chisholm et al., 2005; Coaker et al., 2005; Kim et al., 2005a). A strong Effector Triggered Immunity (ETI) is induced upon NB-LRR activation. This response is sufficient to bypass blocks in the MTI output caused by other co-delivered effectors, and leads to an efficient plant immune response.

Our current model holds that RPM1 indirectly recognizes AvrRpm1 and AvrB via RIN4 phosphorylation (Mackey et al., 2002). To test this hypothesis, we sought to identify phosphorylation sites and other RIN4 residues that regulate function of RPM1. RIN4 has two NOI domains (plant specific nitrate-induced domain; Pfam: PF05627). The C-terminal NOI (NOI2) includes amino acids 142-176, which were co-crystalized with AvrB and contain the AvrB binding site (BBS; (Desveaux et al., 2007)). We show here that NOI2 is necessary and, together with the C-terminus of RIN4 that includes an acylation site required for proper membrane targeting (Kim et al., 2005a), sufficient for effector-triggered RPM1 function. Point mutation of RIN4

residues in this domain revealed that Threonine 166 is necessary for AvrB-triggered RPM1 activation. Phosphomimic substitutions at T166 caused effector-independent RPM1 activation which is, like effector-triggered RPM1 activation, dependent on the RPM1 P-loop. RIN4 T166 is phosphorylated *in vivo* in the presence of AvrB or AvrRpm1. A RIN4 T166A mutant that cannot be phosphorylated fully disrupts AvrB activation of RPM1, and partially disrupts AvrRpm1 activation of RPM1, indicating that AvrRpm1 and AvrB have overlapping but distinguishable mechanisms of activating RPM1. Additional mutations in residues around T166 compromise the ability of RIN4 to interact with both AvrB and RPM1, indicative of a common interaction platform. We conclude that effector-dependent phosphorylation of RIN4 T166 activates RPM1.

## **RESULTS**

### **The C-terminal NOI2 domain of RIN4 is sufficient to trigger RPM1-mediated HR.**

RIN4 residues from 142-176 (the AvrB-binding site, or BBS) mediate AvrB interaction (Desveaux et al., 2007). This short region, which includes one of the two AvrRpt2 cleavage sites in RIN4 (RCS2, between position 152 and 153), is part of the NOI2 domain conserved in RIN4 homologs from mosses to all flowering plants analyzed to date. We constructed two RIN4 deletion mutants (Figure 3.1A). The first is an N-terminal deletion from residue 1-141 (1 $\Delta$ 141). This construct expresses the NOI2 and the C-terminal palmitoylation/prenylation sequence required for RIN4 localization (Kim et al., 2005a). We also generated a RIN4 derivative that disrupts the BBS and the NOI2 (149 $\Delta$ 176). The former construct tests for sufficiency of this domain in RIN4 function, while the latter tests for necessity. We expressed these derivatives, and a wild type RIN4 control, from the native *RIN4* promoter with N-terminal T7 epitope tags as cDNA transgenes in *RPM1-myc rpm1 rps2 rin4* (shortened to *RPM1-myc r1 r2 r4* in some figures; see Experimental Procedures). Homozygous T3 lines expressed RIN4 protein of the appropriate apparent molecular weight (Figure 3.1B). As expected, *RPM1-myc r1 r2 r4* is effectively *rpm1* since RIN4 is required for RPM1 accumulation, and hence, function (Figure 3.1C, 3.1D; Mackey et al., 2002). RIN4 1 $\Delta$ 141 complemented AvrB- and AvrRpm1-triggered RPM1 function as well as the full-length *RIN4* cDNA transgene (FL:RIN4). By contrast, RIN4 149 $\Delta$ 176 did not. These results were confirmed using conductivity measurements (Figure 3.1D). In both assays, we noted that the complementation of

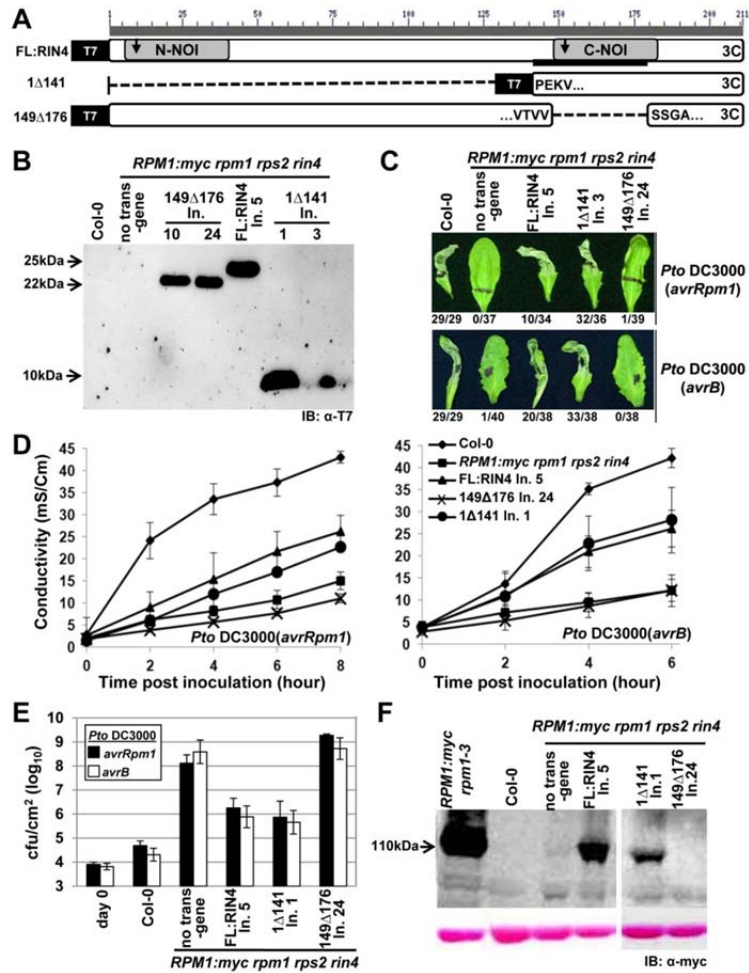


**Figure 3.1. The C-terminal NOI of RIN4 is required for RPM1 function.**

- (A) Schematic diagram of RIN4 derivatives. Gray boxes are N- and C-terminal NOI domains, the black bar is the AvrB binding site (BBS), the arrows indicate the two AvrRpt2 cleavage sites, and the “3C” represents the C-terminal palmitoylation/prenylation site (Kim et al., 2005). Within the derivatives, the amino acids flanking the breakpoints are indicated. Each derivative has an N-terminal T7 epitope-tag.
- (B)  $\alpha$ -T7 immunoblot of microsomal membrane protein fractions from transgenic lines expressing the indicated RIN4 derivatives from (A) under control of the native *RIN4* promoter in *RPM1-myc rpm1 rps2 rin4* plants. The background pattern differs in the right hand panel because this is a higher percentage gel used to resolve 1 $\Delta$ 141 (9 kDa). Line numbers designate plant families homozygous for a single insertion locus that were derived from independent T-DNA insertion events.
- (C) HR phenotypes of the indicated plants after infiltration with 5x10<sup>7</sup> cfu/mL of *Pto* DC3000 expressing AvrRpm1 or AvrB, as noted at right. Representative leaves were photographed 20 hours after infiltration and the numbers below indicate the occurrence of macroscopic HR per number of tested leaves.
- (D) Conductivity measurements after infiltration of the indicated plants with 5x10<sup>7</sup> cfu/mL of *Pto* DC3000 expressing AvrRpm1 (left) or AvrB (right). Eight leaf discs that received the same infiltration were floated in a single tube and the conductivity of the solution was measured over time. Standard errors are from data combined from three separate experiments.
- (E) Growth analysis 3 days after infiltration of 10<sup>5</sup> cfu/mL of *Pto* DC3000 expressing AvrRpm1 or AvrB into the indicated plants. The day 0 measurements show the number of bacteria in Col-0 plants immediately following infiltration. The results are from one of four representative experiments. Standard errors are from three separate experiments.
- (F) RPM1 expression in microsomal fractions from the indicated lines. The strong signal in the line *RPM1:myc rpm1-3* shows the high level of RPM1:myc accumulation in the presence of native RIN4.

AvrRpm1-driven HR with wild type RIN4 was weak. In pathogen growth restriction assays (Figure 3.1E), RPM1 function was restored in transgenic lines expressing FL:RIN4 or RIN4 1 $\Delta$ 141, but not in those expressing RIN4 149 $\Delta$ 176. All functional data was consistent with RPM1-myc accumulation levels observed in the respective lines (Figure 3.1F). These data show that RIN4 residues 149-176 are necessary and, in the presence of required localization sequences, the NOI2 is sufficient to mediate RPM1-myc accumulation and effector-triggered function.

#### **RIN4 residues contacting AvrB are required for interaction.**

We generated missense mutants in the BBS based on contact residues in the co-crystal structure between RIN4 peptide and AvrB (Figure 3.2A). Our yeast two-hybrid data confirmed that RIN4 142 $\Delta$ 176 failed to interact with AvrB (Figure 3.2B). Further, mutation of I168A and F169A (Desveaux et al., 2007) in the RIN4 BBS disrupted the interaction with AvrB, indicating that RIN4 ring-stacking interactions with AvrB Q208 and R209 are required for interaction (Figure 3.2C). Interestingly, a RIN4 T166A mutant retained interaction with AvrB, whereas RIN4 T166D, a phosphomimic mutant, lost this interaction. Expression of all RIN4 mutants was confirmed by immunoblot in total yeast protein extracts after mating (Figure 3.2D), hence loss of interaction with AvrB is due to RIN4 mutation.

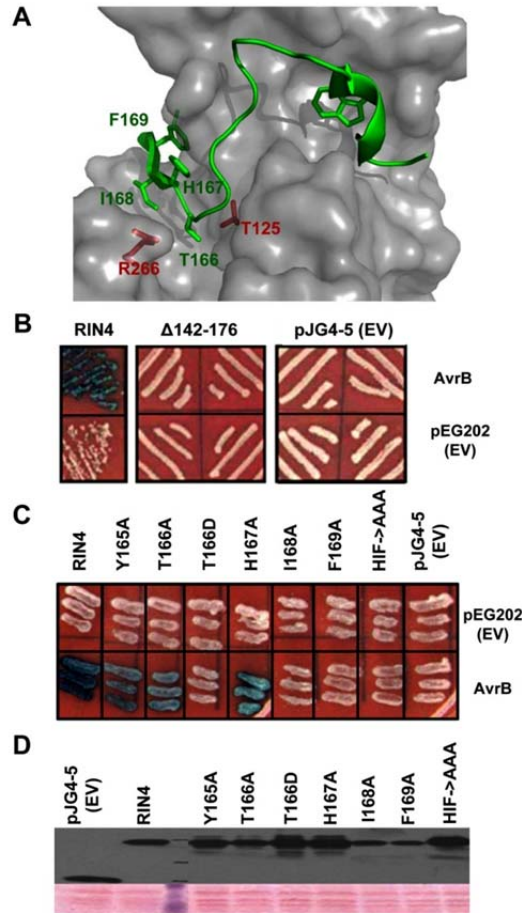


**Figure 3.2. Point mutations in RIN4 BBS residues that contact AvrB alter interaction with AvrB in Yeast two-hybrid system.**

- (A) Co-crystal structure between AvrB and RIN4 peptide (142-176). The AvrB crystal structure is displayed with semitransparent grey color. Key residues of AvrB contacting with RIN4 peptide are marked in red (T125 and R266). RIN4 residues required for the interaction with AvrB are shown in green (T166, H167, I168 and F169).
- (B) Loss of interaction of RIN4 142 $\Delta$ 176 with AvrB. Yeast two hybrid assay was performed as described in experimental procedures. Empty pEG202 and pJG4-5 vector were used as negative controls for interaction.
- (C) Contact AvrB-binding site (BBS) residues of RIN4 are required for interaction. T166D, I168A, F169A and HIF-AAA RIN4 mutants lose the ability to interact with AvrB. Y165A, T166A and H167A retain the interaction with AvrB. Picture was taken two days after streaking mated yeast cells on the X-gal-selective media (-U -H -W).
- (D) All AvrB-binding site (BBS) mutants and wild type RIN4 are expressed in yeast. Immunoblot analysis was performed with  $\alpha$ -HA which is fused with wild type or each RIN4 BBS mutants in the pJG4-5 prey vector for yeast two hybrid assay.

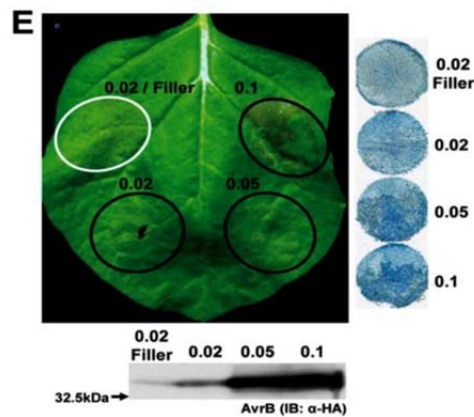
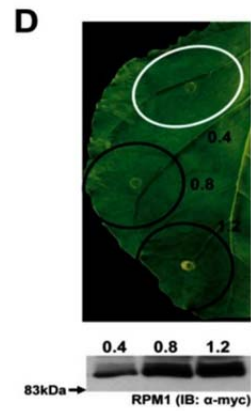
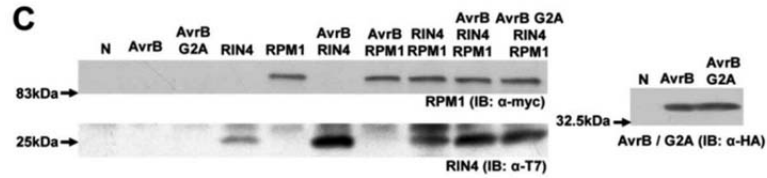
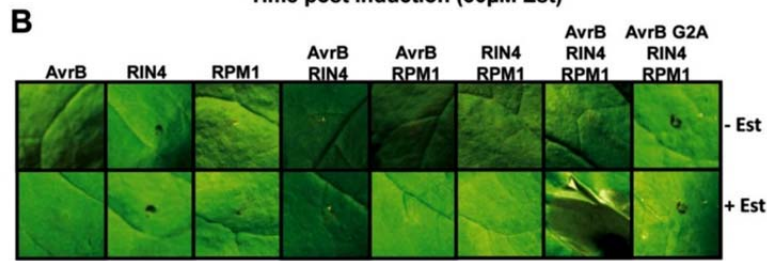
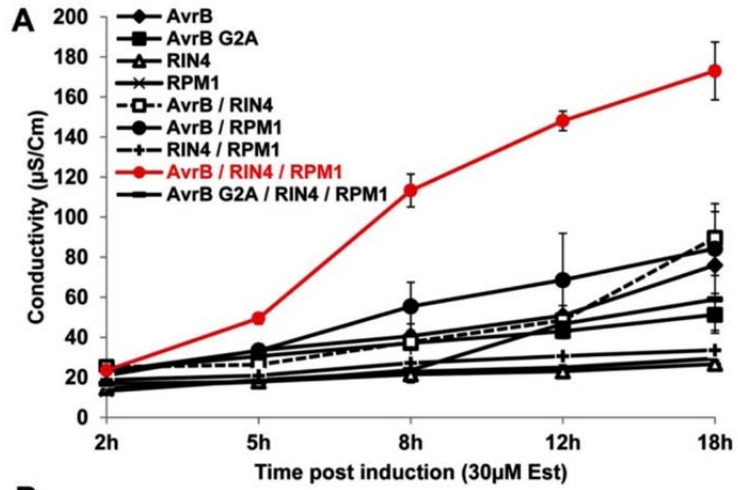


**Figure 3.3. RPM1-dependent HR triggered by AvrB and mediated by RIN4 can be reconstructed in *Nicotiana benthamiana* using Agrobacterium-mediated transient gene expression.**

- (A) Conductivity measurements after agro-infiltration with strains expressing the indicated proteins. *N. benthamiana* leaves were hand-infiltrated with Agrobacterium C58C1 strains expressing Est:AvrB:HA or Est:AvrB G2A:HA ( $OD_{600}=0.02$ ), pRIN4:T7:RIN4 ( $OD_{600}=0.4$ ) and pRPM1:RPM1:myc ( $OD_{600}=0.4$ ). For single and double infiltration of each construct, C58C1 cells carrying the empty vector were used as filler to adjust the total amount of cells ( $OD_{600}=0.82$ ). Two days after infiltration, 30 $\mu$ M Estradiol was applied to induce AvrB and AvrB G2A expression twice with a 1 hour interval before collection of tissue. Measurement started 2 hours post-induction. Error bar represents 2x SE in each case.
- (B) Reconstruction of RPM1-dependent HR following co-infiltration of AvrB, RIN4 and RPM1 on *N. benthamiana* leaves. Photo was taken 12h post Est-treatment.
- (C) Immunoblot with  $\alpha$ -HA,  $\alpha$ -T7 and  $\alpha$ -myc for AvrB, AvrB G2A, RIN4 and RPM1, respectively, demonstrating that all constructs were expressed following Agrobacterium-mediated transient expression assay. Protein samples were extracted 6 hours post Estradiol treatment.
- (D) No ectopic HR following over-expression of RPM1 was observed at three different ODs ( $OD_{600}=0.4$ , 0.8, and 1.2). The leaf was photographed 2.5 days post infiltration, which corresponds to 12 hours post Est-treatment in the co-infiltration assay in (A). Protein samples for immunoblot were harvested simultaneously. The OD noted with a white circle was used for all subsequent *N. benthamiana* experiments in this study.
- (E) AvrB alone can trigger cell death at high doses. Three different ODs ( $OD_{600}=0.02$ , 0.05 and 0.1) were infiltrated on *N. benthamiana* leaves. The lowest dose ( $OD_{600}=0.02$ ) was prepared with two sets, with and without filler (C58C1) to a total  $OD_{600}=0.8$  to monitor the difference in expression level in two cases. Leaf picture was obtained 12 hours post Est-induction. For trypan blue staining to detect HR at each dose, leaf discs were cored at the border of each infiltrated area covering a half of the infiltrated zone 8 hours post Est-treatment. The OD noted with a white circle was used for all *N. benthamiana* experiments in this study.

**An RPM1- and RIN4-dependent, AvrB-triggered hypersensitive response (HR) reconstituted in *Nicotiana benthamiana*.**

We optimized a heterologous *Agrobacterium*-mediated transient assay system in *N. benthamiana* to test whether the RIN4 BBS mutants affect the AvrB-elicited RPM1-mediated hypersensitive response (HR). HR in *N. benthamiana* was observed visually and by trypan blue staining, and was quantified by a standard conductivity assay. Importantly, at the optimized concentrations of each strain used, no single or two-partner co-infiltrations of AvrB, RIN4 or RPM1 resulted in cell death (Figure 3.3A). An AvrB G2A mutant, which is mis-localized due to the lack of a required myristoylation site, did not induce HR, consistent with previous data from *Arabidopsis* (Nimchuk et al., 2000). Leaves infiltrated with AvrB, RIN4 and RPM1 showed onset of ion leakage 5-8 hours and macroscopic HR 12 hours post Estradiol treatment; no observable phenotype was detected in the other infiltrations (Figure 3.3A and 3.3B). Over-expression of NB-LRR proteins can result in ectopic cell death in *N. benthamiana*. We investigated possible dose-dependent effects of RPM1 expression using inocula of  $OD_{600}=0.4$ , 0.8 and 1.2 during the optimization process, but we did not observe any cell death (Figure 3.3D). Over-expressed AvrB resulted in ectopic cell death at  $OD_{600}=0.05$  and above, implying that it can be recognized in *N. benthamiana* when grossly over-expressed (Kang et al., 2010; Schechter et al., 2004). We avoided this background by lowering the amount of infiltrated *Agrobacterium* cells. At  $OD_{600}=0.02$ , no visible phenotype was observed, though there was detectable expression of AvrB protein (Figure 3.3E). Thus, we infiltrated *agrobacteria* at  $OD_{600}=0.02$  for AvrB, 0.4 for RIN4 and 0.4 for RPM1 for all further

experiments, including the final data displayed in figure 3.3A demonstrating specific reconstitution of RPM1- and RIN4-dependent, AvrB-triggered HR.

We analyzed the function of our RIN4 BBS mutants in this *N. benthamiana* system. Constructs which expressed RIN4 H167A supported AvrB-triggered, RPM1-dependent HR, but RIN4 derivatives I168A, F169A, an HIF-AAA triple mutant, and a mis-localized non-functional AvrB G2A did not (Figures 3.4A, 3.4C). These results mirrored those from yeast two-hybrid experiments (Figure 3.2). RIN4 T166A, which retained interaction with AvrB (Figure 3.2), lost the ability to support AvrB-triggered, RPM1-dependent HR (Figure 3.4B). On the other hand, RIN4 T166D, which cannot interact with AvrB (Figure 3.2) supported RPM1-dependent HR, even in the absence of AvrB, or in the presence of AvrB G2A (Figure 3.4B). Thus, a RIN4 T166D phosphomimic mutant renders RPM1 activation AvrB-independent, indicating that this residue might be phosphorylated as part of the normal AvrB-triggered activation of RPM1. Equal protein expression was confirmed by immunoblotting with  $\alpha$ -HA,  $\alpha$ -T7 and  $\alpha$ -myc to detect expressed AvrB, RIN4 and RPM1, respectively (Figure 3.4D).

**AvrB-independent activation of RPM1 on membranes can be driven by RIN4 phosphomimics and requires a conserved RPM1 P-loop residue.**

Only RIN4 T166D, activated RPM1 in the absence of AvrB (Figure 3.5A, 3.5B). Neither RIN4 T166D, nor any other RIN4 BBS mutant, caused HR in the absence of RPM1 (Figure 3.6). We extended our finding that RIN4 T166D drives effector-independent RPM1 activation using RIN4 T166E, with glutamic acid as a phosphomimic residue (Figure 3.5B). We demonstrated that RIN4 T166K does not

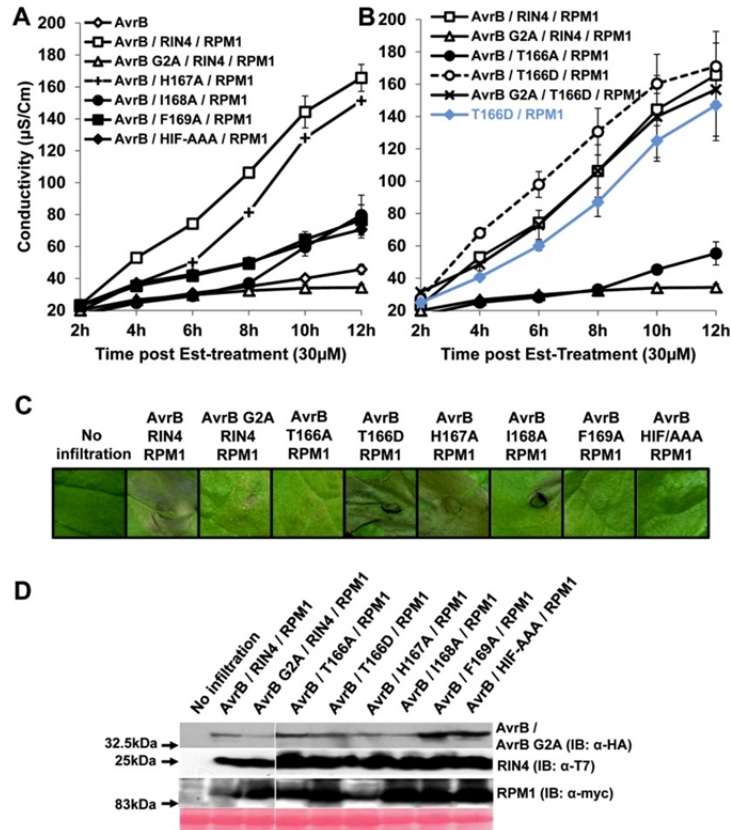


**Figure 3.4. RIN4 T166 is required for AvrB-mediated RPM1-dependent HR in *Nicotiana benthamiana* and a phosphomimic of this residue confers effector independent RPM1 activation.**

- (A) Conductivity measurements after agro-infiltration with strains expressing the indicated proteins. *N. benthamiana* leaves were hand-infiltrated with *Agrobacterium* C58C1 strains expressing AvrB / AvrB G2A, RIN4, H167A, I168A, F169A, HIF-AAA mutant and RPM1 as described in Figure S2A. 30µM of Est was applied two days after co-infiltration. Some error bars are smaller than the symbols.
- (B) Co-infiltration of AvrB and RPM1 with RIN4 T166A and T166D mutants. This result was obtained from the same experiments in (A). Error bars in (A) and (B) represent 2x SE. These results were confirmed four times.
- (C) Visible phenotypes of infiltrated *N. benthamiana* leaves. Two independent leaves were infiltrated with the indicated constructs. One leaf was used to take the picture for phenotypes and the second leaf was used to extract proteins for immunoblot in (D). Pictures were taken 12 hours post Est-treatment. The result is one of four replicates.
- (D) Immunobots with α-HA, α-T7 and α-myc for AvrB / AvrB G2A, RIN4 / BBS mutants and RPM1, respectively, following *Agrobacterium*-mediated transient expression. Protein samples were harvested 6 hours post Est-treatment.

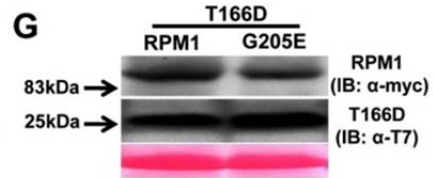
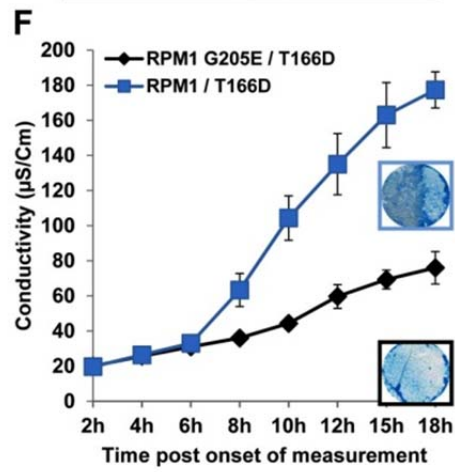
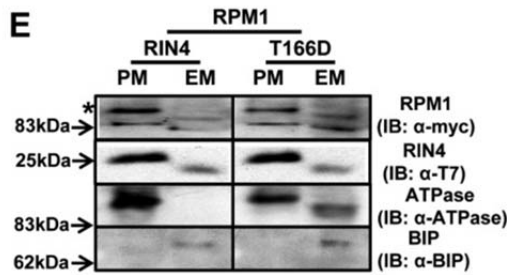
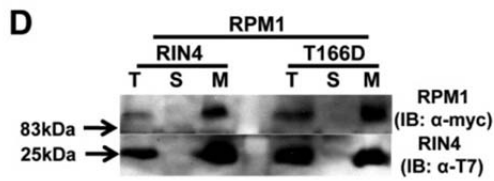
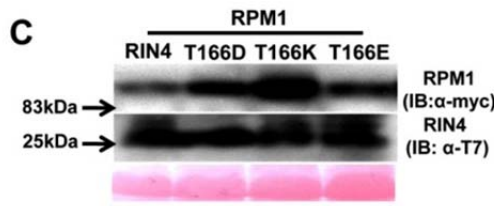
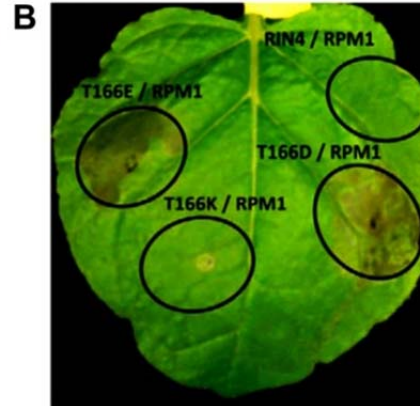
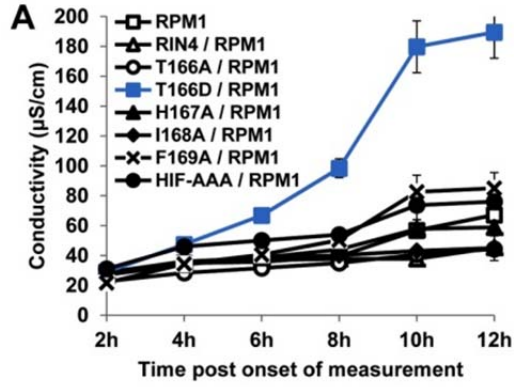


**Figure 3.5. RIN4 T166D activity is dependent on RPM1 P-loop function in *Nicotiana benthamiana***

- (A) The phosphomimic RIN4 T166D mutant drives effector-independent RPM1-mediated HR. Conductivity measurements were performed with *N. benthamiana* leaves infiltrated with *Agrobacterium* C58C1 strains expressing RIN4 BBS mutants (OD<sub>600</sub>=0.4) and RPM1:myc (OD<sub>600</sub>=0.4). The measurements began two days post infiltration. Repeated three times with similar result. The error bars represent 2x SE.
- (B) Phenotypes of RIN4 T166 derivatives. RIN4 T166D, RIN4 T166E and RIN4 T166K driven by the *RIN4* native promoter were co-infiltrated as in (A). Photo was taken 3 days after co-infiltration.
- (C) Expression of RPM1 and RIN4 T166 derivatives. RPM1 and RIN4 T166 derivatives were expressed, and variation does not account for the observed phenotypes. Immunoblots with  $\alpha$ -myc and  $\alpha$ -T7 were performed with 2 day-old-samples post infiltration.
- (D) The RIN4 phosphomimic T166D is localized to a microsomal fraction. *N. benthamiana* leaves were co-infiltrated as in (A). Proteins were extracted from leaf tissues at the onset of HR from T166D/RPM1 co-infiltration, which corresponded to 8 hours in the conductivity experiment in (A). Repeated twice. Total (T), soluble (S) and microsomal (M) fractions were loaded at a 1:1:5 ratio, followed by immunoblotting with  $\alpha$ -T7 and  $\alpha$ -myc to detect RIN4 and RPM1, respectively.
- (E) Two-phase partitioning of RIN4 and RPM1. RIN4 and RIN4 T166D mutant were co-infiltrated with RPM1 as described in (D). The microsomal extraction was used as input for two-phase partitioning. The upper fraction, for plasma membrane (PM), and the lower fraction for endomembranes (EM) were loaded at equal yield, followed by immunoblotting with  $\alpha$ -myc and  $\alpha$ -T7 to detect RPM1(\*) and RIN4, respectively. Plasma membrane-localized (PM) ATPase and ER-localized BIP proteins represented the efficiency of fractioning for PM and EM.
- (F) Conductivity measurements and HR phenotype after co-infiltration of RIN4 T166D with either RPM1 or an RPM1 G205E. *N. benthamiana* leaves were hand-infiltrated with *Agrobacterium* C58C1 strains expressing T166D mutant (OD<sub>600</sub>=0.4) and either *pRPM1:RPM1:myc* (OD<sub>600</sub>=0.4) or RPM1:myc G205E (OD<sub>600</sub>=0.8). C58C1 was used as filler to make up the difference in OD between RPM1:myc and RPM1:myc G205E with OD<sub>600</sub>=0.4. The measurements started two days post infiltration. This result was one of two repeats. Trypan Blue staining with leaf discs covering half of the infiltrated zone was performed 2.5 days after infiltration indicated 12 hr in conductivity measurement.
- (G) Expression of RPM1:myc and RPM1:myc G205E. Protein samples from (F) were prepared 2 days post infiltration. The immunoblot was performed with  $\alpha$ -myc.

cause HR, demonstrating specificity for phosphomimic mutants, as opposed to charge change (Figure 3.5B). RPM1-myc and all RIN4 T166 derivatives were expressed in the agrobacteria-mediated transient assay (Figure 3.5C). These data, together with the loss of HR observed following co-expression of AvrB / RIN4 T166A / RPM1 (Figure 3.4) strongly indicates that RIN4 T166 is phosphorylated in response to AvrB, and that this modification is necessary for subsequent RPM1 activation.

RPM1 and RIN4 are both associated with the plasma membrane (Boyes et al., 1998; Kim et al., 2005a). We addressed whether the localization of RIN4 T166D is altered, compared to wild type RIN4, during RPM1 activation. Both RIN4 T166D and RPM1 were detected in microsomes from transiently expressing *N. benthamiana* leaves. Hence, the RIN4 phosphomimic does not dissociate RIN4 or RPM1 from microsomes (Figure 3.5D). RPM1, RIN4 and RIN4 T166D were all enriched in plasma membrane fractions following two-phase partitioning (Boyes et al., 1998) (Figure 3.5E), indicating that RPM1 activation via RIN4 T166D occurs there. Further, both RIN4 and RIN4 T166D can co-immunoprecipitate with RPM1 *in vivo* from microsomes (see below). Thus, RIN4 T166D, like RIN4, associates with and modulates the activity of RPM1 on the plasma membrane.

Nearly all NB-LRR proteins share highly conserved residues in the kinase 1a (P-loop) motif of their respective nucleotide binding domains. ATP binding and its hydrolysis / exchange with ADP in the NB is thought to alter intra- and inter-molecular folding as part of the NB-LRR activation mechanism (Takken et al., 2006). The RPM1 G205E mutation in the P-loop exhibited a loss-of-function phenotype

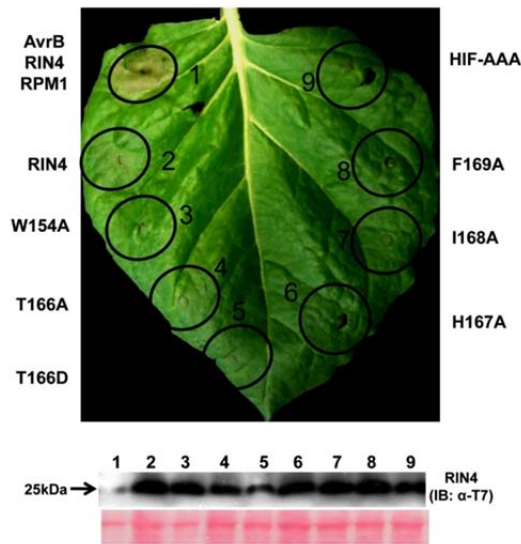


**Figure 3.6. RIN4 T166D does not confer RPM1-independent HR.**

Each RIN4 BBS mutant was hand-infiltrated into two independent *N. benthamiana* leaves at  $OD_{600}=0.4$ . Co-infiltration with AvrB, RIN4 and RPM1 was included as a positive control as in Figure 3.3. The picture was taken 12 hours after  $30\mu\text{M}$  Est-treatment (2.5 days after infiltration). All RIN4 and BBS mutants were expressed; protein samples were prepared 6 hours after Est-treatment.

(Tornero et al., 2002). We used this allele to address whether RIN4 T166D driven RPM1-dependent HR requires wild type P-loop function. Notably, the RIN4 T166D-mediated activation of RPM1 is significantly impaired in combination with RPM1 G205E (Figure 3.5F). Thus, activation of RPM1 by RIN4 T166D is regulated by canonical P-loop function, similar to the requirements for activation of RPM1 by AvrB and AvrRpm1 during infection of Arabidopsis (Tornero et al., 2002).

**The RIN4 T166D phosphomimic retains the ability to be cleaved by AvrRpt2 in *N. benthamiana*.**

RIN4 is a target for a third *P. syringae* type III effector protein, the cysteine protease AvrRpt2. Cleavage of RIN4 at the second of two specific sites activates RPS2-mediated defense resistance (Mackey et al., 2003, Kim et al., 2005a). Co-expression of RIN4 and AvrRpt2 in Agrobacterium-mediated *N. benthamiana* transient assays results in RIN4 cleavage (Day et al., 2005). Both RIN4 and RIN4 T166D were cleaved by AvrRpt2 but not by an AvrRpt2 catalytic mutant (C122A) in this assay (Figure 3.7). Thus, a phosphomimic of RIN4 on T166 cannot block cleavage by AvrRpt2.

**RIN4 T166 contributes to AvrRpm1-dependent RPM1-mediated HR in *N. benthamiana*.**

AvrRpm1 is a *P. syringae* type III effector unrelated to AvrB that can also activate RPM1-mediated HR and be co-immunoprecipitated with RIN4 (Mackey et al., 2002). AvrRpm1 does not interact with RIN4 in Y2H, and it is unstable and unstructured *in*

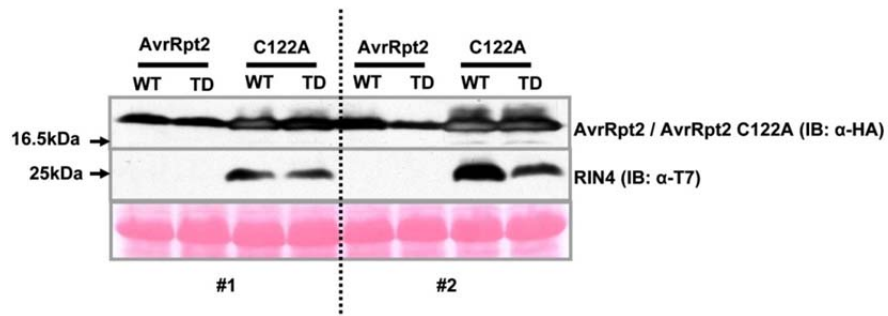


**Figure 3.7. RIN4 T166D retains cleavage by AvrRpt2 in *N. benthamiana*.**

RIN4 constructs ( $OD_{600}=0.4$ ) were co-infiltrated with AvrRpt2:HA ( $OD_{600}=0.1$ ) or AvrRpt2 C122A:HA, a catalytic dead mutant ( $OD_{600}=0.1$ ), into *N. benthamiana* leaves. Total protein was extracted 2 days after infiltration followed by immunoblotting with  $\alpha$ -HA and  $\alpha$ -T7 to detect AvrRpt2 and RIN4, respectively. The same result was observed in two independent *N. benthamiana* leaves.

*in vitro* following purification (K. Cherkis and JLD, unpublished). Therefore, the nature of its direct interaction with RIN4, if any, remains elusive. Hence, we sought to cross reference the RIN4 residues required for AvrB-triggered RPM1 activation to AvrRpm1.

We reconstituted a functional AvrRpm1-triggered RPM1 activation assay in *N. benthamiana* (using *Agrobacterium* carrying an Estradiol-inducible AvrRpm1 T-DNA at OD<sub>600</sub>=0.1; see Experimental Procedures). We observed that RIN4 I168A and F169A mutants could not trigger AvrRm1-triggered RPM1-dependent HR (Figure 3.8), consistent with their phenotypes in AvrB-triggered RPM1-dependent HR (Figure 3.4). Wild type RIN4 and, to a slightly lesser extent, RIN4 T166A supported RPM1-dependent, effector-induced ion leakage (Figure 3.8A) and HR (Figure 3.8B). Protein expression for AvrRpm1, RIN4 and RPM1 was confirmed with immunoblotting (Figure 3.8C). These data, combined with data presented in Figure 2, indicate that RIN4 T166 is required for AvrB-triggered RPM1-dependent HR, but not essential for AvrRpm1-triggered RPM1-dependent HR in *N. benthamiana*.

### **Native expression level RIN4 T166D transgenic lines exhibit ectopic basal defense phenotypes.**

We recapitulated the key results from our transient expression system in transgenic *Arabidopsis* plants. All native promoter *RIN4* constructs used for *Agrobacterium*-mediated transient assay on *N. benthamiana* were stably transformed into *RPM1:myc rpm1 rps2 rin4*. We obtained at least two independent homozygous T3 transgenic lines expressing each RIN4 BBS mutant.

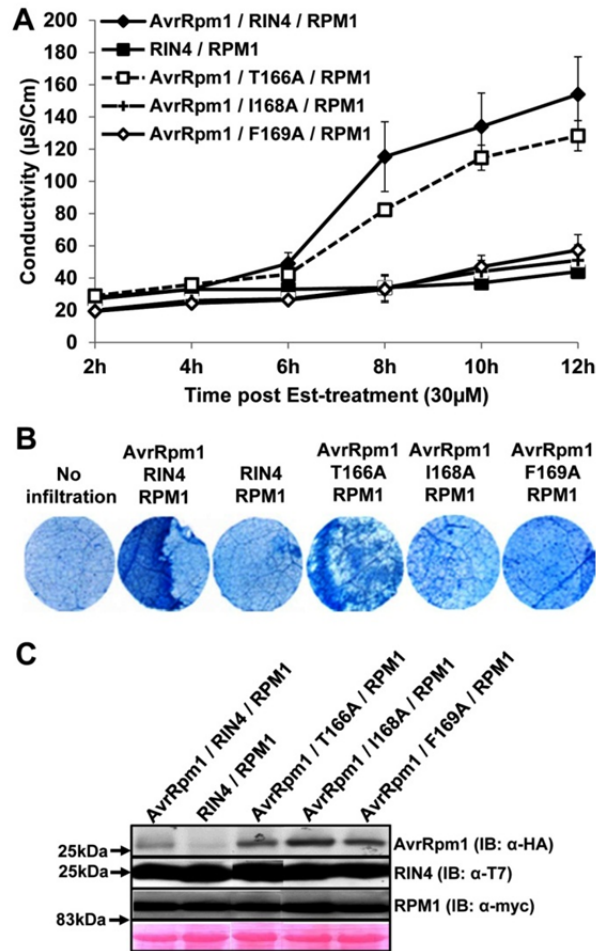


**Figure 3.8. RIN4 T166 contributes to AvrRpm1-dependent RPM1-mediated HR in *N. benthamiana*.**

- (A) Conductivity measurements after agro-infiltration with strains expressing the indicated proteins. *N. benthamiana* leaves were hand-infiltrated with *Agrobacterium* C58C1 strains as in Figure 2A except *Est:AvrRpm1-HA* ( $OD_{600}=0.1$ ) instead of *Est:AvrB:HA*. Co-infiltration of RIN4 and RPM1:myc was used as a negative control with C58C1 cells ( $OD_{600}=0.1$ ). The result was repeated three times. Measurement started 2 hours post induction with 30µM Estradiol. Error bars represent 2x SE.
- (B) HR Phenotypes of infiltrated *N. benthamiana* leaves. Trypan blue staining was performed with leaf discs which covered half of an infiltrated zone at 8 hours after Est-treatment. Data represent one of three independent experiments with consistent result.
- (C) Immunoblots with α-HA, α-T7 and α-myc to detect AvrRpm1, RIN4 and RPM1, respectively. Protein samples were extracted from leaf tissues harvested 6 hours post Est-treatment.

We observed dwarfism and chlorosis in both independent T166D lines, especially under long day conditions, and no obvious phenotype in lines expressing the other BBS mutants (Figure 3.9A). Each RIN4 BBS mutant protein was expressed at levels approximating that of wild type RIN4 in Col-0 and *rpm1-3* (Figure 3.9B). We noted a mild ectopic cell death in lines expressing RIN4 T166D (Figure 3.9C). Furthermore, we observed ectopic PR1 protein expression in RIN4 T166D mutants, consistent with the lesion and morphology phenotypes of constitutive defense mutants (Figure 3.9D). The mild constitutive defense activation phenotype expressed by RIN4 T166D transgenics was sufficient to limit growth of the virulent bacterial pathogen *Pto* DC3000 (Figure 3.9E). These phenotypes were RPM1-dependent (Figure 3.9F).

#### **RIN4 T166 is essential for AvrB-triggered RPM1 function in Arabidopsis.**

We tested RPM1-function following infiltration of *Pto* DC3000 expressing either *avrB* or *avrRpm1* into leaves of the various RIN4 BBS expressing transgenic lines and appropriate controls (Figure 3.10). RIN4 derivatives I168A, F169A and HIF-AAA did not support AvrB- or AvrRpm1-triggered HR, while the RIN4 H167A did (Figure 3.10A, 3.10B). Importantly, RIN4 T166A did not support either HR or increased conductivity following inoculation with *Pto* DC3000(*avrB*) (Figure 3.10A, 3.10B). RIN4 T166A supported an intermediate level of RPM1-dependent HR triggered by *Pto* DC3000(*avrRpm1*) compared to Col-0 or RIN4 wild type transgenic plants (gRIN4) and negative control plants (*rpm1-3* and *RPM1:myc rpm1 rps2 rin4*) (Figure 3.10A). We confirmed and quantified this intermediate phenotype in leaves from two independent homozygous transgenic lines, following inoculation with *Pto*

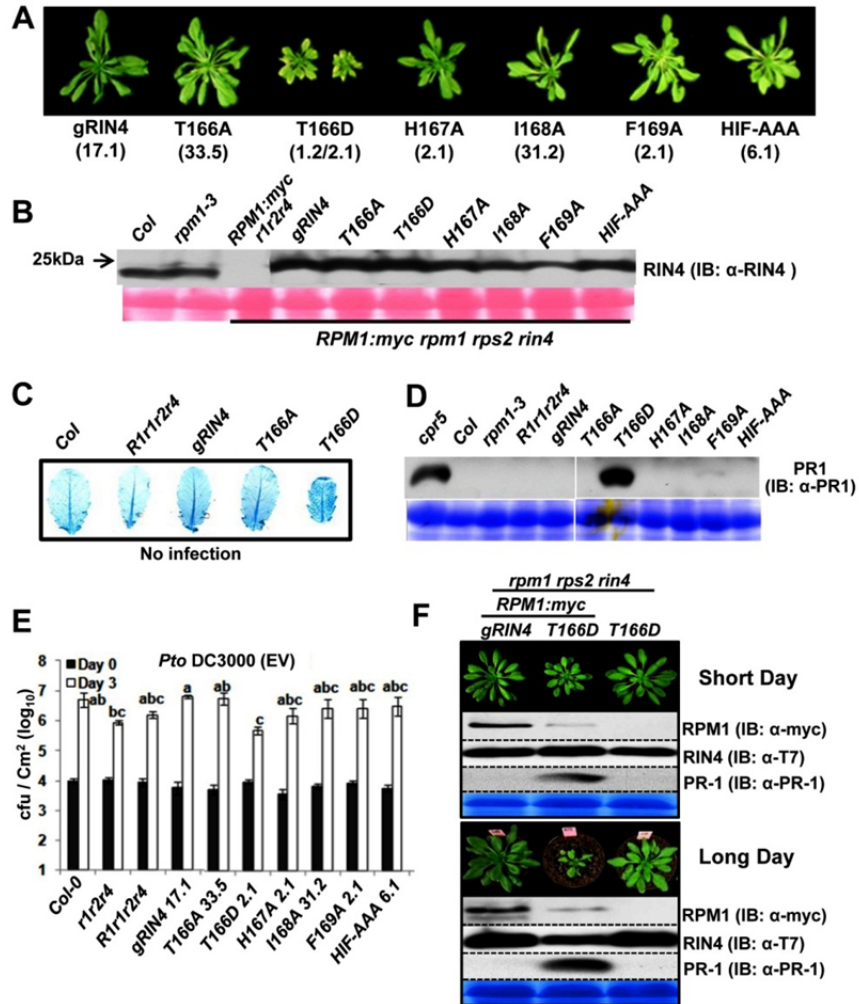


**Figure 3.9. RIN4 T166D drives ectopic cell death and elevated PR-1 expression in the presence of RPM1.**

- (A) Transgenic *Arabidopsis* lines expressing RIN4 T166D exhibit dwarfism, ectopic lesions and chlorosis in two independent T3 homozygous. Each RIN4 BBS mutant was transformed into *RPM1:myc rpm1rps2rin4*. T3 homozygous lines were photographed as 5 week-old plants grown under long day conditions, which enhanced the severe phenotype of the RIN4 T166D mutant.
- (B) Protein expression of RIN4 BBS mutant transgenic *Arabidopsis* plants. 60 µg of total protein from the same lines used in (A) was extracted from homozygous transgenic T3 plants. Immunoblot was performed with α-RIN4 to detect both RIN4 BBS mutants and wild type RIN4.
- (C) Microscopic cell death in RIN4 T166D mutant. Trypan Blue staining without bacterial infection in the noted genotypes from plants grown under long day light period to maximize the induced phenotype in the RIN4 T166D mutant. The result was observed in two independent experiments.
- (D) Induced PR-1 expression in RIN4 T166D expressing transgenic plants. 4 week-old plants were used to extract protein to monitor PR1 expression. These plants were grown under short days to minimize the T166D lesion mimic phenotype. *cpr5* was used as a positive control for PR1 expression. The result was repeated twice independently.
- (E) Bacterial growth analysis of *Pto* DC3000(EV). Bacteria recovered from infiltrated leaves of each transgenic line indicated were counted after hand-inoculation with 10<sup>5</sup> cfu/mL for Day 0 and Day 3. The result was repeated with two independent T3 homozygous lines. Error bars represent 2X SE. Pair-wise comparisons for all means for bacterial growth on day 3 were performed with One-Way ANOVA test followed by Tukey-Kramer HSD at 95% confidence limits.
- (F) The dwarf phenotype of RIN4 T166D transgenic plants is RPM1-dependent. Siblings from a cross of Homozygote T166D transgenic *Arabidopsis* in *RIN4 T166D RPM1:myc rpm1rps2rin4* was crossed with *rpm1rps2rin4*. Plants were grown under both short day (8hr light and 16hr dark) and long day (16hr light and 8hr dark) conditions. Pictures represent one of four plants from two independently derived F2 lines. Immunoblots confirm genotypes and ectopic PR-1 expression in plants expressing RIN4 T166D and RPM1.

DC3000(*avrRpm1*) (Figure 3.10B, T166A lines 32.6 and 33.5). These results are consistent with those from the *N. benthamiana* reconstruction system. Finally, we tested RPM1-mediated bacterial growth restriction in the RIN4 BBS mutant lines following low dose inoculation with *Pto* DC3000(*avrB*) or (*avrRpm1*). Concordant with HR assay results, RIN4 T166A exhibited a loss of RPM1 function phenotype in response to *Pto* DC3000(*avrB*) and slightly reduced function, relative to gRIN4, in response to *Pto* DC3000(*avrRpm1*) (asterisks in Figure 3.10C). These results indicate that RIN4 T166 is required for AvrB-triggered RPM1 function, and contributes to, but is not essential for, AvrRpm1-triggered RPM1 function (summarized in Table 3.1).

Oddly, the RIN4 T166D transgenic lines exhibited RPM1-dependent HR triggered by AvrB (weak) and AvrRpm1 (intermediate) (Figure 3.10A) and, in fact, by *Pto* DC3000 (weak) (Figure 3.11A). These results, coupled with PR1 expression data in Figure 3.10D, indicate that ectopic RPM1 signaling in RIN4 T166D expressing lines results in a lowered threshold for activation of the low level of RPM1 that accumulates in these lines (see below).

### **RIN4 T166 is phosphorylated in response to AvrB and AvrRpm1.**

We addressed whether T7-epitope tagged RIN4 T166 could be phosphorylated by immunoprecipitation of RIN4 with  $\alpha$ -T7 conjugated agarose beads, followed by immunoblotting with a phosphopeptide-specific antibody raised against a 13 amino acid RIN4 peptide containing phosphothreonine ( $\alpha$ -pRIN4; see Experimental Procedures). To enrich for phosphorylated RIN4 in our transient assay, AvrB or

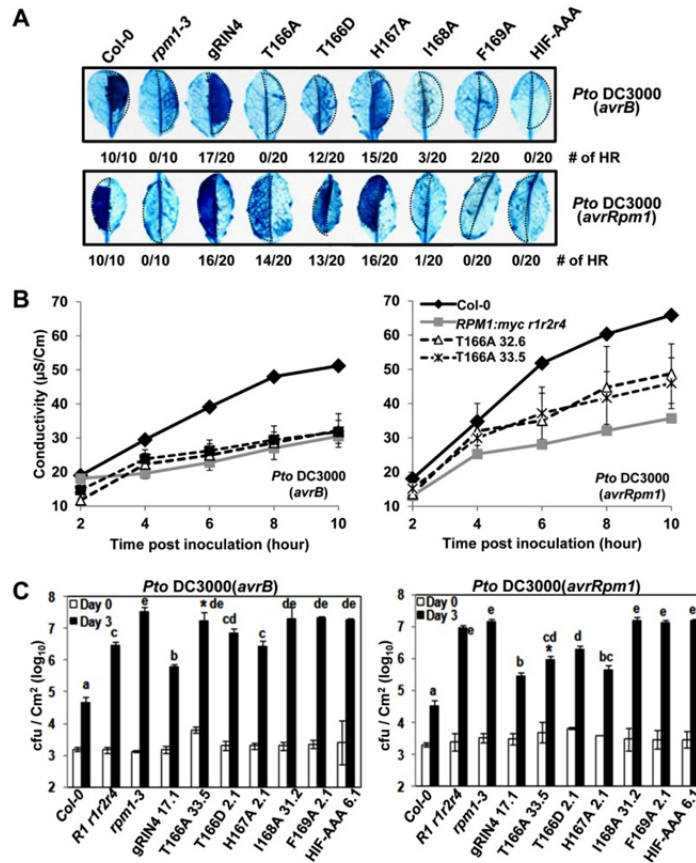


**Figure 3.10. RIN4 T166 is required for AvrB-, and contributes to AvrRpm1-dependent, RPM1-mediated HR in Arabidopsis.**

- (A) HR determined by Trypan Blue staining. 20 independent leaves from transgenic lines expressing each RIN4 BBS mutant were inoculated with  $5 \times 10^7$  cfu/ml ( $OD_{600}=0.1$ ) of *Pto DC3000(avrB)* or (*avrRpm1*) in half of each leaf (dotted area). Leaves were harvested 6 hours after inoculation. The numbers are leaves which displayed the HR phenotype shown over the total. The result was repeated with two independent homozygous transgenic lines for each BBS mutant with similar results.
- (B) Conductivity measurements. Two independent homozygous T166A mutant lines and controls shown at right were used to monitor the loss-of-function phenotype with  $5 \times 10^7$  cfu/mL of *Pto DC3000 (avrB)* or (*avrRpm1*). Error bar represents 2X SE for RIN4 T166A mutant. Four leaf discs were used to measure the conductivity of Col-0 and *RPM1:myc rpm1rps2rin4*.
- (C) Bacteria growth analysis of *Pto DC3000 (avrB)* or (*avrRpm1*). Bacteria recovered from infiltrated leaves of each transgenic line indicated or controls at bottom were counted after hand-inoculation with  $10^5$  cfu/mL for each strain on day 0 and day 3. The result was repeated twice with two independent T3 homozygous transgenic Arabidopsis lines from each RIN4 mutant. Error bars represent 2X SE. Pair-wise comparisons for all means from the day 3 data were performed with One-Way ANOVA test followed by Tukey-Kramer HSD at 95% confidence limits.

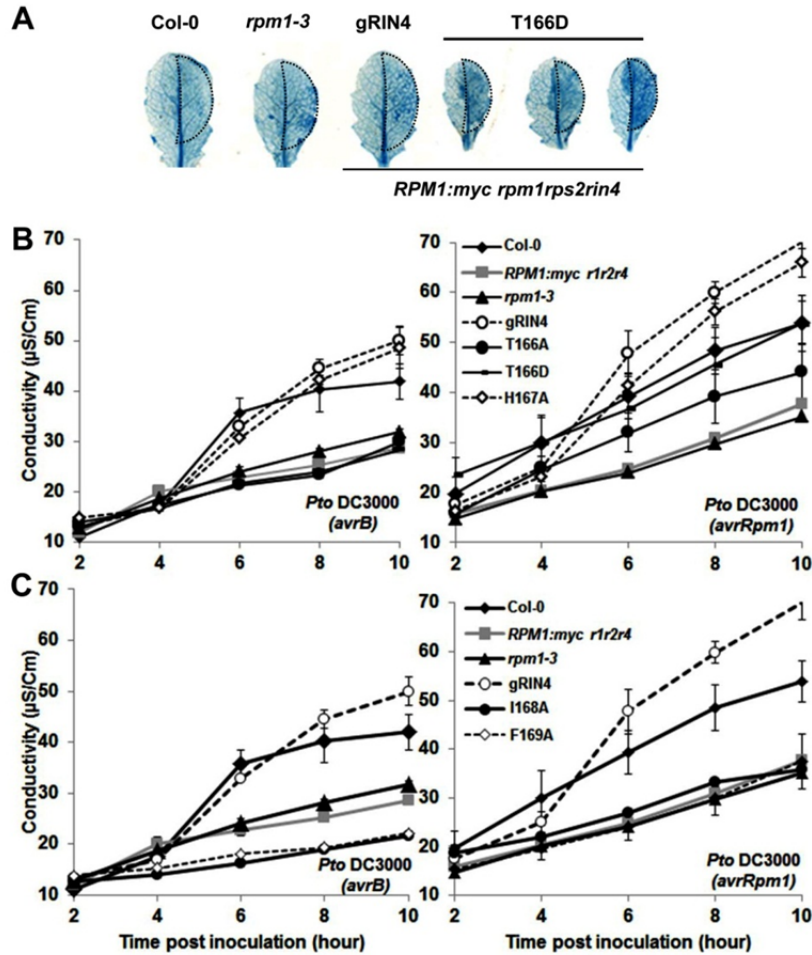


**Figure 3.11. RIN4 BBS residues contribute to effector activation of RPM1 HR.**

- (A) Transgenic lines expressing RIN4 T166D in the presence of RPM1 are hyper-responsive to *Pto DC3000*(EV). Leaves from lines of genotypes shown were hand infiltrated at  $5 \times 10^7$  cfu/mL. Trypan blue staining was performed at 6h post-infiltration. Photos from three different RIN4 T166D plants.
- (B) Conductivity measurement of transgenic *Arabidopsis* lines expressing RIN4 BBS mutants (T166A, T166D and H167A). The method described in Figure 3.10B was used for infiltration and subsequent measure of conductivity following infiltration of full leaves. The result was repeated two times with two independent T3 homozygous *Arabidopsis* transgenic lines for each RIN4 mutant. Error bars represent 2X SE.
- (C) Conductivity measurement of other RIN4 BBS mutants which are not included in (A). Same method described in (A) was employed to measure conductivity with infiltration of *Pto DC3000*(*avrB*) or (*avrRpm1*) of the full leaf. The result was repeated two times with two independent T3 homozygous *Arabidopsis* transgenic lines of each mutant. Error bars represent 2X SE.

AvrRpm1 and RIN4 or RIN4 T166A mutant were co-expressed without RPM1 (Mackey et al., 2002). As displayed in Figure 3.12A, signal detected with  $\alpha$ -pRIN4 was enriched in  $\alpha$ -T7 immunoprecipitates from samples co-expressing wild type RIN4 with either AvrB or AvrRpm1, compared to samples from extracts co-expressing RIN4 T166A and either effector.

We analyzed RIN4 T166 phosphorylation in transgenic *Arabidopsis* expressing native levels of either wild type RIN4 or RIN4 T166A, complementing a *rin4* null allele in the presence RPM1:myc. Transgenic plants were infiltrated with *Pto* DC3000 expressing AvrB:HA or AvrRpm1:HA.  $\alpha$ -HA and  $\alpha$ -T7 immunoblots detected AvrB:HA and AvrRpm1:HA, or the RIN4 derivatives, respectively, in the input for the immunoprecipitations (Figure 3.12B, top).  $\alpha$ -T7 immunoprecipitates were immunoblotted with  $\alpha$ -pRIN4 (figure 3.12B, bottom). We noted T166-dependent enhancement of  $\alpha$ -pRIN4 signal compared to uninfected control in the presence of either effector.

We also demonstrated that the effector-dependent increase in the RIN4 detected with  $\alpha$ -pRIN4 is phosphorylation by treating  $\alpha$ -T7 immunoprecipitates with calf intestinal phosphatase (CIP) followed by blotting with either  $\alpha$ -pRIN4 or  $\alpha$ -T7 (Figure 3.12C). While there is some residual recognition of RIN4 T166A protein by the  $\alpha$ -pRIN4 sera, the increased signals it detects is RIN4-pT166. In sum, the results presented in Figure 3.12 indicate that the presence of either AvrB or AvrRpm1 leads to increased phosphorylation of RIN4 T166 in both *N. benthamiana* and *Arabidopsis* systems.

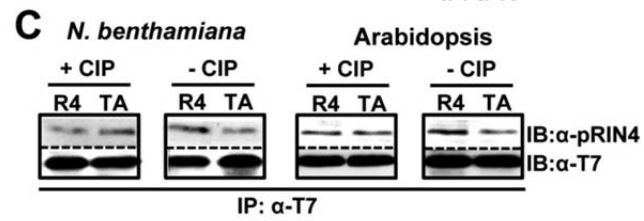
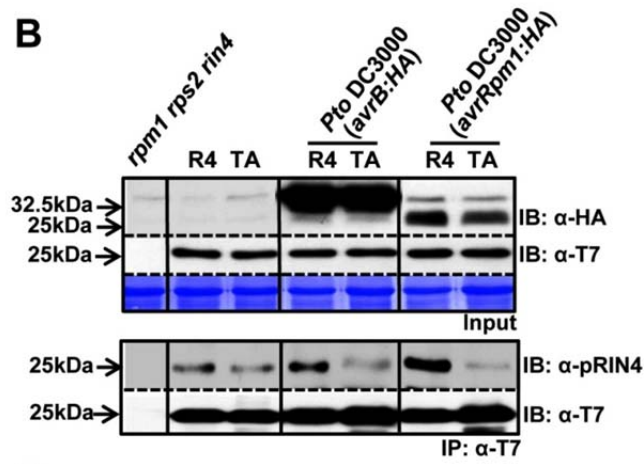
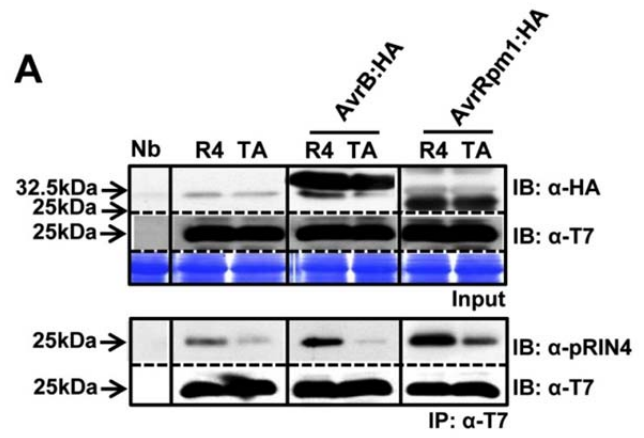


**Figure 3.12. RIN4 T166 residue is phosphorylated by AvrB and AvrRpm1 *in planta***

- (A) T166-dependent RIN4 phosphorylation in *N. benthamiana*. Immunoprecipitation with  $\alpha$ -T7 conjugated agarose beads was used to enrich RIN4 or RIN4 T166A from leaves co-infiltrated with Est:AvrB:HA or AvrRpm1:HA and T7:RIN4 or T7-RIN4 T166A, followed by immunoblotting with  $\alpha$ -pRIN4 (phosphopeptide-specific polyclonal antibody) and  $\alpha$ -T7. Samples 18 hours post 30 $\mu$ M Est-induction were prepared and input levels established by immunoblot with appropriate antibodies (top).  $\alpha$ -T7 immunoprecipitates (bottom) were used for immunoblots with  $\alpha$ -pRIN4. An immunoblot with  $\alpha$ -T7 demonstrated equal expression levels of RIN4 and RIN4 T166A in these immunoprecipitates. The experiment was repeated three times.
- (B) RIN4 T166 is phosphorylated in Arabidopsis following AvrB or AvrRpm1 delivery from *P. syringae*. Transgenic Arabidopsis RIN4 or T166A mutant were inoculated with *Pto* DC3000(*avrB:HA*) or (*avrRpm1:HA*) as described in figure 3.10B. Samples were collected 18 hours after infection. Immunoblots and immunoprecipitations were performed as in (A). Asterisk indicates an Arabidopsis background band mobility similar to that of AvrB. The data represent one of three experiments with similar results.
- (C) The  $\alpha$ -pRIN4 antiserum detects phosphorylated RIN4-pT166 in *N. benthamiana* and transgenic Arabidopsis.  $\alpha$ -T7 immunoprecipitates from either *N. benthamiana* transiently expressing RIN4 and RIN4 with AvrB or AvrRpm1 (left), and transgenic Arabidopsis uninfected or infected with *Pto* DC3000 (*avrB:HA*) or (*avrRpm1:HA*) (right) were divided a half to treat calf intestinal phosphatase (CIP). Tissue samples were prepared as in (A) for *N. benthamiana* and (B) for Arabidopsis.

## **RIN4 BBS residues are required for steady-state microsomal accumulation of RPM1.**

RIN4 can be co-immunoprecipitated with, and is required for accumulation of, RPM1 in unstimulated cells (Belkhadir et al., 2004; Mackey et al., 2002). We therefore performed co-immunoprecipitations with microsomal fractions from the RIN4 BBS mutant transgenic lines (Figure 3.13). While the RIN4 BBS mutant proteins accumulated equally on microsomes, they supported variable levels of RPM1 accumulation in the input extracts (Figure 3.13A). Immunoprecipitation of all of the available RPM1 from microsomes led to differentially co-immunoprecipitated RIN4 BBS mutant proteins (Figure 3.13A). Wild type RIN4 and RIN4 T166A retained the ability to associate with RPM1, and supported nearly wild type RPM1 accumulation levels. RIN4 BBS alleles that lost both the ability to interact with AvrB (Figure 3.2C) and the ability to support AvrB-triggered RPM1 functions (Figure 3.10) also lost the ability to associate with, and/or support accumulation of, RPM1 (RIN4 I168A, F169A and HIF-AAA; see Table 3.1).

The inability of these RIN4 derivatives to support RPM1 accumulation is likely due to a disruption of the interaction between RIN4 and RPM1 at the membrane. This is striking for RIN4 F169A, which fails to co-immunoprecipitate with RPM1. RIN4 T166D drives activation and consequent disappearance of RPM1 at steady state in the transgenics. Nevertheless, a very low level of RPM1 is detected and it can co-immunoprecipitate RIN4 T166D (Figure 3.13A). We therefore constructed a RIN4 T166D F169A double mutant. This RIN4 derivative accumulates normally on microsomes, but cannot be co-immunoprecipitated with RPM1 (Figure 3.13B) or

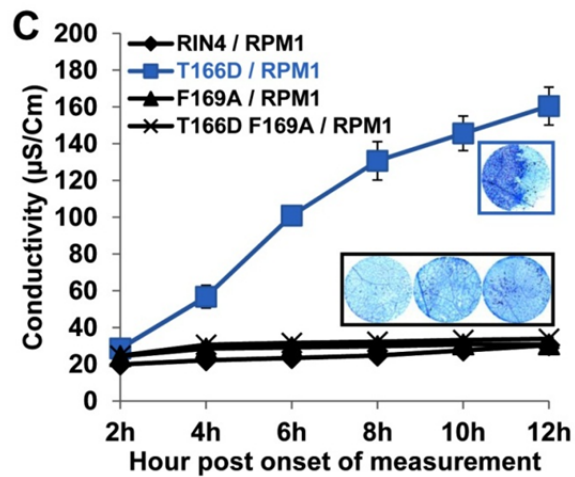
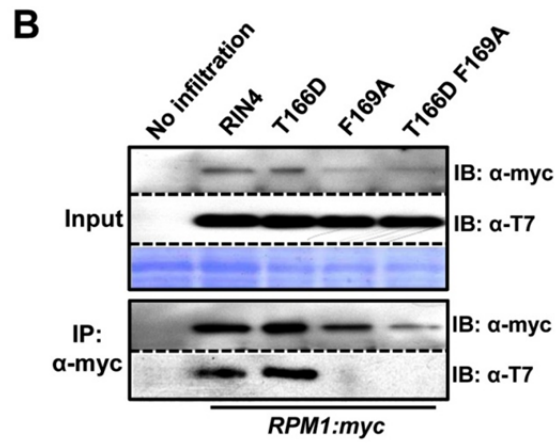
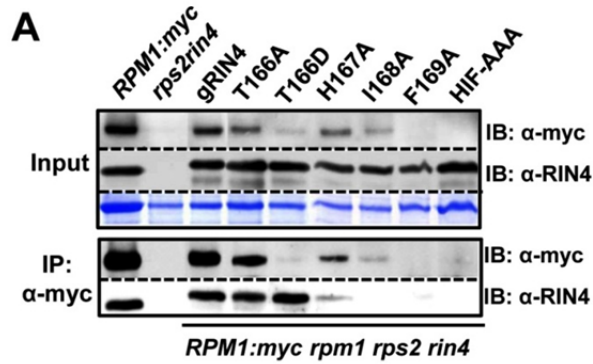


**Figure 3.13. Differential coimmunoprecipitation of RPM1 with RIN4 BBS mutants identifies residues required for interaction and RPM1 accumulation.**

- (A) Co-immunoprecipitation of RIN4 BBS mutants with RPM1. The microsomal fraction was enriched in extracts from each RIN4 BBS mutant transgenic Arabidopsis, followed by immunoprecipitation with  $\alpha$ -myc. The overall level of RPM1 is displayed in the input (left top). RIN4 expression in each mutant was confirmed by immunoblotting with  $\alpha$ -RIN4. Immunoprecipitated RPM1 was shown by immunoblotting with  $\alpha$ -myc. Co-immunoprecipitated RIN4 with RPM1 was confirmed with  $\alpha$ -RIN4 immunoblot. Two week-old seedlings from each line were used to collect the microsomal fraction.
- (B) Loss of co-immunoprecipitation of RIN4 T166D F169A with RPM1. Agrobacterium transient assays were performed as in Figure 3.5. Loading controls, immunoprecipitation with  $\alpha$ -myc and subsequent immunoblots were performed as in Figure 3.13A, with the use of  $\alpha$ -T7 to detect RIN4 and RIN4 BBS mutants.
- (C) Loss of effector-independent RPM1 activation in RIN4 T166D F169A. Agrobacterium transient assays, conductivity measurements and trypan blue staining were performed as in Figure 3.5.

support effector-independent activation of RPM1 HR in the *N. benthamiana* transient assay system (Figure 3.13C). In this transient expression assay, a high level of RIN4 T166D maintains interaction with the relatively low levels of RPM1, even as the latter is being activated. Hence, RIN4 F169 is required for the interaction of RIN4 with AvrB (Figure 3.2) and also controls interaction with, and thus stability of, RPM1. Further, this interaction is required for activation of RPM1 by RIN4 T166D.

**Table 3.1. Summary of RIN4 BBS for interaction and function with effector proteins and RPM1**

Genotype	Interaction		RPM1 activation			
	with AvrB	with RPM1	<i>Nicotiana benthamiana</i>		Arabidopsis	
	by Y2H	by Co-IP	by AvrB	by AvrRpm1	by AvrB	by AvrRpm1
RIN4	Yes	Yes	Yes	Yes	Yes	Yes
T166A	Yes	Yes	No	intermediate	No	intermediate
T166D	No	Yes	ND*	ND*	ND*	ND*
H167A	Yes	Yes	Yes	Yes	Yes	Yes
I168A	No	No	No	No	No	No
F169A	No	No	No	No	No	No

\* ND: not determined because RIN4 T166D exhibited effector-independent HR with RPM1

## **DISCUSSION**

We present a mechanism for effector-dependent activation of a typical NB-LRR plant intracellular immune receptor. Arabidopsis RPM1 is activated in response to two unrelated bacterial type III effector proteins, AvrB and AvrRpm1. We initially proposed that a host target of both effectors, RIN4, is 'guarded' by RPM1. We suggested that modification of RIN4 by AvrB or AvrRpm1 activates RPM1, resulting in suppression of bacterial growth and a hypersensitive response (HR) (Mackey et al., 2002). We noted that the presence of either AvrB or AvrRpm1 resulted in phosphorylation of RIN4, though neither effector has kinase activity *in vitro*; and we noted that this modification was more pronounced in the absence of RPM1 (Mackey et al., 2002). RIN4 negatively regulates MAMP-triggered immunity (MTI) and both AvrB and AvrRpm1 suppress MTI in plants lacking RPM1 (Kim et al., 2005b). Based on the data presented above, a reasonable speculation is that phosphorylation of RIN4 T166 potentiates the negative regulation of MTI by RIN4. In the absence of RPM1, AvrB or AvrRpm1 'lock' RIN4 as a negative regulator of MTI. RPM1 responds to the effector-induced phosphorylation of RIN4.

The specific RIN4 residues phosphorylated in the presence of AvrB or AvrRpm1 were previously unknown, and a requirement for RIN4 modification in RPM1 activation had not been demonstrated. Here, we provide evidence that phosphorylation of RIN4 T166 is required for AvrB-dependent activation of RPM1 and contributes to AvrRpm1-dependent RPM1 activation. Further, a phosphomimic at this residue (T166D) causes effector-independent activation of RPM1. These

data, together with previous publications, provide a mechanism whereby AvrB enters the cell, is targeted by acylation to the host plasma membrane (Nimchuk et al., 2000), is activated (Desveaux, et al., 2007) perhaps by a host MAPK (Cui et al., 2010) or other kinases, and enhances the phosphorylation of RIN4 on T166 and potentially other residues. Because AvrB and RPM1 require the same binding site on RIN4, RIN4 phosphorylation is unlikely to occur while it associates with RPM1. AvrB likely dissociates once RIN4 is phosphorylated since the T166D derivative of RIN4 no longer interacts with AvrB. Dissociation of phosphorylated RIN4 from AvrB appears key to RPM1 activation.

RIN4 is phosphorylated in the absence of effectors (Mackey et al., 2002) and on residues other than T166 after perception of the flagellin MAMP peptide, flg22 (Nuhse et al., 2007). Given the sensitivity of NB-LRR activation, it may be that a threshold level of RIN4 T166 phosphorylation must be attained for RPM1 activation. Additional effector-induced modifications of RIN4, perhaps other phosphorylation events or conformational changes, may increase the propensity of modified RIN4 to activate RPM1. This appears to be the case for AvrRpm1; RIN4 T166A only partially compromises activation of RPM1. Additional phosphorylation of RIN4 by AvrRpm1 is consistent with AvrRpm1 inducing a significantly greater mobility shift in RIN4 than does AvrB (Mackey et al., 2002). Other possible target residues for phosphorylation within the genetically defined region of RIN4 required for AvrRpm1-dependent RPM1 activation include S160 and S161. However, phosphomimics of either of these residues did not result in effector-independent RPM1 activation and mutations to alanine did not compromise either AvrRpm1- or AvrB-dependent RPM1 activation.

AvrRpm1 may direct functionally relevant phosphorylation or additional modifications of RIN4 residues outside of the NOI2 domain.

Effector-independent activation of RPM1 mediated by RIN4 T166D requires the P-loop within the RPM1 NB domain. Hence, pRIN4 T166 is a physiological elicitor of RPM1. Current models of NB-LRR activation envisage an ADP-bound resting state conformation involving intra- and possibly inter-molecular interactions that result in the LRR domain inhibiting activation at the NB. Activation is proposed to be driven, or accompanied, by nucleotide exchange and/or hydrolysis, which are thought to activate downstream processes (Takken and Tameling, 2009; van Ooijen et al., 2007). It has been thus far difficult to establish an order of events for this activation with respect to nucleotide binding and/or turnover. Our results are consistent with a model wherein RPM1 recognition of RIN4pT166 precedes, or is coincident with, ADP/ATP exchange/hydrolysis, since a loss of function RPM1 P-loop mutation also blocks both effector- and RIN4 T166D-mediated RPM1 activation. Our data support a model in which effector-dependent modification of RIN4 activates RPM1. This model differs from the model of activation of RPS2 via elimination of RIN4 that we and others proposed (Axtell and Staskawicz, 2003; Mackey et al., 2003). RIN4 is, genetically, a negative regulator of both RPM1 and RPS2 (Belkhadir et al., 2004). However, in the absence of RIN4, ectopic activation of RPS2 occurs and the result is seedling lethality. In contrast, the lack of RIN4 contributes only weakly to ectopic RPM1 activation (Belkhadir et al., 2004). The inability of RIN4 T166D F169A to activate RPM1 indicates that RIN4 must interact with RPM1 to

activate it, and that merely disrupting the association of RPM1 with RIN4 is insufficient to fully activate RPM1.

It is instructive to compare the regulation of RPM1 and RPS2 activation via RIN4 to other well studied examples of recognition of modified self by plant NB-LRR proteins. The Arabidopsis RPS5 NB-LRR protein is activated by cleavage of the host kinase PBS1 by the type III effector cysteine protease AvrPphB (Ade et al., 2007; Shao et al., 2003). There is no ectopic RPS5 activation in *pbs1* null plants, indicating that PBS1 is not formally a negative regulator of RPS5. However, AvrPphB suppresses MTI by cleaving PBS1 and related host kinases that may function redundantly to inhibit RPS5 activation (Zhang et al., 2010). Similarly, the Pto kinase family in tomato is targeted by multiple type III effectors and post-translational modification of these kinases activates the Prf NB-LRR protein in ETI (Ntoukakis et al., 2009). Thus, cleaved PBS1 and modified Pto are likely to activate RPS5 and Prf, respectively, similar to the activation of RPM1 by phosphorylated RIN4. The activation of plant NB-LRR proteins by modified self may be similar to the activation of animal NLR proteins of similar structure in response to the presence of MAMPs and / or non-self (Vance et al., 2009).

RIN4 is targeted by four different bacterial type III effectors that perturb it in four different ways: proteolysis by AvrRpt2 (Axtell et al., 2003; Axtell and Staskawicz, 2003; Coaker et al., 2005; Mackey et al., 2003), possible ADP-ribosylation by HopF2 (Wang et al.; Wilton et al., 2010), and differential phosphorylation in the presence of AvrB and AvrRpm1 (this study). The proteolysis and phosphorylation events target an overlapping short domain on RIN4, the C-terminal NOI2 domain, which is part of

a family of proteins cleaved by AvrRpt2 (Chisholm et al., 2005). Arabidopsis encodes ~15 paralogous NOI-domain containing proteins. Positions analogous to RIN4 T166 and F169 are nearly invariant within the NOI2 domains of 58 RIN4 orthologues (phytozome.org; Cluster #23252144), and across 91 additional proteins orthologous to the remaining Arabidopsis NOI2-containing paralogues across the plant kingdom (phytozome.org; Clusters #23252690, #23250407 and #23251786). Both AvrB and AvrRpm1 can promote virulence in plants lacking RIN4, indicating the existence of additional targets that may include other NOI containing proteins (Belkhadir et al., 2004). Thus, we hypothesize that AvrB and AvrRpm1 suppress MTI by targeting RIN4 and additional NOI2 containing proteins, and that T166 and F169, or equivalent residues, are central to these interactions. By extension, NOI2-domain containing Arabidopsis proteins other than RIN4 also are likely to have roles in regulating plant defense. Our findings focus future experiments on this domain in RIN4 and its paralogues, the kinase(s) that phosphorylate RIN4 and, possibly, other NOI2 domain-containing proteins, the precise mechanism by which AvrB and AvrRpm1 modulate this phosphorylation event, and the definition of functions for the other NOI2 domain family members.

## **MATERIALS AND METHODS**

**Vectors.** All cloning was performed using the Gateway system (Invitrogen, Carlsbad, CA). AvrB / AvrB G2A and AvrRpm1 / AvrRpm1 ORFs were cloned with direct fusions of influenza haemagglutinin (HA) epitope tag at the C-terminus into pDONR207 vector (Invitrogen, Carlsbad, CA). To generate estradiol-inducible constructs, each effector was cloned into the pMDC7 vector via an LR reaction. A T7-epitope tag (MASMTGGQQMG) (Day et al., 2005) was added between the *RIN4* promoter (1.6kb) and a genomic *RIN4* fragment (1.2kb). The *RIN4* promoter was amplified with 5'- and 3'-primers which contain the T7-epitope tag as an overhang sequence. Gene-specific primers for genomic *RIN4* were generated to incorporate a T7-epitope sequence directly at the N-terminus of genomic *RIN4* using the native stop codon in the 3'-primer. These full length genomic *RIN4* constructs with the native promoter and T7-epitope tag were subcloned into pDONR207 vector. All AvrB-binding site (BBS) mutants of *RIN4* were generated by site-directed mutagenesis using wild type genomic *RIN4* as a template. To clone the genomic *RIN4* construct into the binary vector, we generated a pBAR1-GW destination vector (this study) by inserting a Gateway cassette (Invitrogen, Carlsbad, CA) into the multi-cloning site of pBAR1 (McDowell et al., 1998), followed by restriction and ligation with *HindIII* and *SacI* fragments of pBAR1. Genomic *RPM1* driven by the native promoter in the pGPTV-HPT binary vector was used.

**Plants.** *Nicotiana benthamiana* for Agrobacterium-mediated transient assays were sown in soil (Day et al., 2005; Day et al., 2006) and germinated in the greenhouse at 24°C with a long day photoperiod (16h-light/8h-dark). Two week-old seedlings were transplanted to 4-inch square pots (one seedling per one pot) and grown for 5-6 weeks before infiltration with Agrobacteria. For all transient assays, fully expanded leaves which are the 3rd to the 5th from the first leaf at the bottom were utilized.

*Arabidopsis* Col-0 wild type and isogenic mutants were sown and grown as described (Boyes et al., 1998). To generate transgenic plants transformed with RIN4 BBS mutants, a *RPM1myc rpm1 rps2 rin4* line was generated by crossing the *RPM1-myc rpm1-3* (line AT5; Boyce et al., 1998) with *rpm1 rps2 rin4* (Belkhadir et al., 2004). All expression constructs contained the *RIN4* native promoter with a T7-epitope tag at the N-terminus of genomic *RIN4* wild type or *RIN4* BBS mutants. Plant transformation was performed using the floral dip method (Clough and Bent, 1998). For each *RIN4* BBS mutant, 18 independent T1 transformants were selected by spraying Basta on two-week old seedlings. The segregation of T2 progeny from 18 independent T1 transgenic lines was monitored on 0.5X Murashige & Skoog Media (Murashige and Skoog, 1962) with 30 µM Basta and 100 µg/mL of Cefotaxime. In the T3 generation, at least two independent homozygous transgenic lines per *RIN4* wild type and *RIN4* BBS mutant were confirmed by protein blot and chosen for the experiments in the text.

**Yeast two-hybrid in the LexA system.** LexA-based yeast two-hybrid was performed with AvrB, RIN4 and RIN4 BBS mutants cloned into the gateway-compatible LexA binding domain (BD) fusion for AvrB in pEG202 and B42 activation domain (AD) fusion for RIN4 derivatives in pJG4-5 after performing an LR reaction (Invitrogen). The MATCHMAKER LexA system (Clontech, <http://www.clontech.com>) was employed to perform yeast two-hybrid analysis based on the manufacturer's instructions. Two yeast strains, RFY206 (MAT $\alpha$ ) carrying pSH18-34 (the lacZ reporter plasmid) and EGY48 (MAT $\alpha$ :Clontech) were transformed with AvrB and RIN4 derivatives, respectively. Yeast transformation was performed using the Frozen-EZ Yeast Transformation II kit (Zymo Research) for the preparation of highly competent yeast cells and small-scale lithium acetate transformation. Interactions between AvrB and RIN4 derivatives were monitored by pairwise matings according to the manufacturer's protocol (Clontech Yeast Protocols Handbook).

**Agrobacterium-mediated transient assay in *Nicotiana benthamiana*.** To reconstruct AvrB- or AvrRpm1-mediated, RPM1-dependent HR with RIN4 and RPM1 in *Nicotiana benthamiana*, a three way *A. tumefaciens* infiltration was used. Strains of C58C1 (pCH32) transformed with AvrB or AvrRpm1 and their derivatives expressed in pMDC7 vector, the same strain carrying RIN4 and its derivatives in pBAR1GW binary vector, and RPM1 in pGPTV-HPT binary vector were infiltrated into the abaxial side of 5-6 week-old *N. benthamiana* leaves by hand infiltration with a 1 mL needless syringe. Agrobacterium strains were grown overnight at 28°C in 5mL of 2 x YT media containing 100 µg/mL of rifampicin, 5 µg/ml of tetracycline with

the addition of 100 µg/mL of Spectinomycin for AvrB and AvrRpm1 derivatives or 100 µg/mL of kanamycin for RIN4 derivatives and RPM1. Cells were resuspended in induction media (10mM MES, pH5.6, 10mM MgCl<sub>2</sub>, and 150µM actosyringone) and incubated at room temperature for 2 hours before infiltration. AvrB or AvrB G2A transformed Agrobacterium were infiltrated at a final OD<sub>600</sub> of 0.02. Agrobacterium cells containing AvrRpm1 were infiltrated at a final OD<sub>600</sub> of 0.1. Agrobacterium cells carrying RPM1, RIN4 and RIN4 BBS mutant constructs were infiltrated at a final OD<sub>600</sub> of 0.4. The RPM1 P-loop dead mutant, G205E, was infiltrated at a final OD<sub>600</sub> of 0.8 due to its low expression compared to wild type RPM1. To adjust the final concentration of *A. tumefaciens* infiltrated into leaves, *A. tumefaciens* strain C58C1 was utilized as a 'filler' to achieve a final cell density of OD<sub>600</sub> of 0.8. To induce AvrB, AvrB G2A or AvrRpm1 expression after infiltration, 30µM of β-estradiol with 0.005% Silwet was applied twice with a one hour interval.

We noted that RPM1 G205E accumulates to lower levels than wild type RPM1 when inoculating Agrobacterium at OD<sub>600</sub>=0.4. To compensate for this, we infiltrated agrobacteria carrying the RPM1 G205E mutant at OD<sub>600</sub>=0.8. The data displayed in Figure 3F and 3G are from experiments using this modification.

**Immunoprecipitation, and immunoblot analyses.** Immunoprecipitation was performed as described (Mackey et al., 2002) with slight modifications. 1g of leaf tissue was collected and ground in a mortar and pestle with liquid nitrogen. The fine powder was resuspended in 2ml of extraction buffer (50 mM HEPES-KOH pH 7.5, 50

mM NaCl, 10 mM EDTA pH 8.0, 0.2 % Triton X-100, 5 mM DTT and 1x plant protease inhibitor cocktail (Sigma-Aldrich), followed by homogenizing with a polytron (Kinematica). Soluble supernatants were collected by centrifugation at 10,000 x g for 10 min at 4°C, and passed through two-layers of Miracloth (Calbiochem). The clean supernatants were combined with 50 µL of α-myc conjugated magnetic beads for RPM1-myc precipitation, or with 50 µL of α-T7 agarose beads (Novagen) for T7:RIN4 precipitation after equilibrating beads in extraction buffer. After incubation at 4°C for 6 hrs, the mixture of α-myc immunoprecipitation were passed through MACS Separation column (Miltenyi Biotec), followed by washing three times with washing buffer (same as extraction buffer except 0.1% Triton X-100 instead of 0.2%). Bound proteins were collected by adding pre-heated elution buffer (50 mM Tris-HCl pH 6.8, 50 mM DTT, 1% SDS, 1 mM EDTA pH 8.0, 0.005% bromphenol blue and 10% glycerol) three times with 20, 50 and 50 µL, respectively. In the case of T7:RIN4, the agarose beads were collected by centrifugation at 1,000 x g for 5min at 4°C and rinsed three times with washing buffer (as above). The bound proteins were collected with 100 µL of elution buffer (50mM glycine pH2.5, 50mM NaCl and 0.1% Triton X-100) followed by neutralizing with 10 uL of 2M Tris-base without disturbing beads. The immunoprecipitates from α-myc and α-T7 were loaded on 8 % and 12 % SDS-PAGE to detect RPM1 and RIN4, respectively.

Phosphorylated RIN4 was detected by immunoblot with polyclonal rabbit α-pRIN4 (GenScript) raised using RIN4<sub>155-168</sub>(DENNPSSADGYpTHI). The antisera were affinity purified and absorbed against phosphorylated and unphosphorylated peptide. Both wild type and RIN4 T166A protein from *N. benthamiana* transiently

transformed with Arabidopsis to co-express AvrB or AvrRpm1 in or from Arabidopsis transgenic plants infected with *Pto* DC3000 (*avrB:HA*) or (*avrRpm1:HA*) were enriched first by immunoprecipitation with  $\alpha$ -T7-agarose beads. The bound proteins were eluted as mentioned above, followed by immunoblot with  $\alpha$ -pRIN4. Immunoblot with  $\alpha$ -T7 from input was performed to demonstrate equal loading.

Phosphorylation of RIN4 by effector proteins were test by treatment with calf alkaline intestinal phosphatase (CIP) (Mackey et al., 2002). Plant extracts were immunoprecipitated with  $\alpha$ -T7-agarose beads, and divided in half for CIP treatment (10 units). Both immunoprecipitates with or without CIP were incubated at 37°C for 1hr.

**Microsomal fractionation and two-phase partitioning.** The microsomal fraction was extracted based on (Boyes et al., 1998). For aqueous two-phase partitioning, the microsomal fraction was used to separate plasma membrane and endomembrane fraction as described previously (Kawasaki et al., 2005). Aqueous two-phase partitioning was done with a polymer concentration of 6.6% (wt/vol).  $\alpha$ -ATPase (Agrisera) and  $\alpha$ -BIP (Santa Cruz Biotechnology) antibodies were used as controls for plasma membrane and endomembrane fraction, respectively.

**Bacterial growth assay *in planta*.** *Pto* DC3000 (*avrB*) and (*avrRpm1*) were grown on KB media (10 g glycerin, 10 g peptone, 10 g tryptone, 10 mL 10% K<sub>2</sub>HOP<sub>4</sub> and 10 mL 10% MgSO<sub>4</sub> and 15 g agar per 1 L) with appropriate antibiotics (100  $\mu$ g / mL

of rifampicin and 25 µg / mL of kanamycin) for two days. To measure the growth of *Pto* DC3000(*EV*), the same method was employed except the amount of initial inoculum was 10<sup>4</sup> CFU / mL. Statistical difference in bacterial growth at Day 3 was analyzed by Pair-wise comparisons for all means using One-Way ANOVA test followed by Tukey-Kramer HSD with JMP 7.0 software (SAS Institute Inc.).

**Staining and quantification of hypersensitive response (HR) *in planta*.** HR triggered by *Pto* DC3000 (*avrB*) and *Pto* DC3000 (*avrRpm1*) was visualized by trypan blue staining and quantified by conductivity measurement. Bacteria suspension from *Pto* DC3000 either possessing *AvrB* or *AvrRpm1* were prepared as for the growth assay except the final concentration for infiltration was 5 x 10<sup>7</sup> CFU/mL. The bacteria were infiltrated on the abaxial side of leaf. For staining with trypan blue, half of each leaf was inoculated to compare the infiltrated and non-infiltrated zone for HR. To better visualize HR, approximately 20 leaves were stained by trypan blue staining. To measure the conductivity from infiltrated leaves, four leaf discs were collected and submerged into 6 mL of double distilled water with three replicates per sample (n=12), and then measured by conductivity meter (Orion, model 130) with indicated time points.

## **REFERENCES**

Ade, J., DeYoung, B.J., Golstein, C., and Innes, R.W. (2007). Indirect activation of a plant nucleotide binding site-leucine-rich repeat protein by a bacterial protease. *Proc Natl Acad Sci U S A* *104*, 2531-2536.

Ashfield, T., Ong, L.E., Nobuta, K., Schneider, C.M., and Innes, R.W. (2004). Convergent evolution of disease resistance gene specificity in two flowering plant families. *Plant Cell* *16*, 309-318.

Axtell, M.J., and Staskawicz, B.J. (2003). Initiation of *RPS2*-specified disease resistance in *Arabidopsis* is coupled to the *AvrRpt2*-directed elimination of *RIN4*. *Cell* *112*, 369-377.

Belkhadir, Y., Nimchuk, Z., Hubert, D.A., Mackey, D., and Dangl, J.L. (2004). *Arabidopsis* *RIN4* negatively regulates disease resistance mediated by *RPS2* and *RPM1* downstream or independent of the *NDR1* signal modulator, and is not required for the virulence functions of bacterial type III effectors *AvrRpt2* or *AvrRpm1*. *Plant Cell* *16*, 2822-2835.

Boyes, D.C., Nam, J., and Dangl, J.L. (1998). The *Arabidopsis thaliana* *RPM1* disease resistance gene product is a peripheral plasma membrane protein that is degraded coincident with the hypersensitive response. *Proc Natl Acad Sci, USA* *95*, 15849-15854.

Chisholm, S.T., Dahlbeck, D., Krishnamurthy, N., Day, B., Sjolander, K., and Staskawicz, B.J. (2005). Molecular characterization of proteolytic cleavage sites of the *Pseudomonas syringae* effector *AvrRpt2*. *PNAS* *102*, 2087-2092.

Clough, S.J., and Bent, A.F. (1998). Floral dip: A simplified method for *Agrobacterium*-mediated transformation of *Arabidopsis thaliana*. *Plant J* *16*, 735-743.

Coaker, G., Falick, A., and Staskawicz, B. (2005). Activation of a Phytopathogenic Bacterial Effector Protein by a Eukaryotic Cyclophilin. *Science* *308*, 548-550.

Cui, H., Wang, Y., Xue, L., Chu, J., Yan, C., Fu, J., Chen, M., Innes, R.W., and Zhou, J.M. (2010). *Pseudomonas syringae* effector protein *AvrB* perturbs *Arabidopsis* hormone signaling by activating MAP kinase 4. *Cell Host Microbe* *7*, 164-175.

Dangl, J.L., and Jones, J.D.G. (2001). Plant pathogens and integrated defence responses to infection. *Nature* *411*, 826-833.

Day, B., Dahlbeck, D., Huang, J., Chisholm, S.T., Li, D., and Staskawicz, B.J. (2005). Molecular Basis for the *RIN4* Negative Regulation of *RPS2* Disease Resistance. *Plant Cell* *17*, 1292-1305.

Day, B., Dahlbeck, D., and Staskawicz, B.J. (2006). NDR1 interaction with RIN4 Mediates the Differential Activation of Multiple Disease Resistance Pathways. *Plant Cell in press*.

Desveaux, D., Singer, A.U., Wu, A.J., McNulty, B.C., Musselwhite, L., Nimchuk, Z., Sondek, J., and Dangl, J.L. (2007). Type III effector activation via nucleotide binding, phosphorylation, and host target interaction. *PLoS Pathog* 3, e48.

Dodds, P.N., and Rathjen, J.P. (2010). Plant immunity: towards an integrated view of plant-pathogen interactions. *Nat Rev Genet* 11, 539-548.

Gimenez-Ibanez, S., Hann, D.R., Ntoukakis, V., Petutschnig, E., Lipka, V., and Rathjen, J.P. (2009). AvrPtoB targets the LysM receptor kinase CERK1 to promote bacterial virulence on plants. *Curr Biol* 19, 423-429.

Hauck, P., Thilmony, R., and He, S.Y. (2003). A *Pseudomonas syringae* type III effector suppresses cell wall-based extracellular defense in susceptible *Arabidopsis* plants. *Proc Natl Acad Sci U S A* 100, 8577-8582.

He, S.Y., Bauer, D.W., Collmer, A., and Beer, S.V. (1994). Hypersensitive response elicited by *Erwinia amylovora* harpin requires active plant metabolism. *Mol- Plant-Microbe Interact* 7, 289-292.

Jakobek, J.L., Smith, J.A., and Lindgren, P.B. (1993). Suppression of bean defense responses by *Pseudomonas syringae*. *Plant Cell* 5, 57-63.

Jeuken, M.J., Zhang, N.W., McHale, L.K., Pelgrom, K., den Boer, E., Lindhout, P., Michelmore, R.W., Visser, R.G., and Niks, R.E. (2009). Rin4 causes hybrid necrosis and race-specific resistance in an interspecific lettuce hybrid. *Plant Cell* 21, 3368-3378.

Jones, J.D., and Dangl, J.L. (2006). The plant immune system. *Nature* 444, 323-329.  
Kang, H.G., Oh, C.S., Sato, M., Katagiri, F., Glazebrook, J., Takahashi, H., Kachroo, P., Martin, G.B., and Klessig, D.F. (2010). Endosome-Associated CRT1 Functions Early in Resistance Gene-Mediated Defense Signaling in *Arabidopsis* and Tobacco. *Plant Cell*.

Kim, H.S., Desveaux, D., Singer, A.U., Patel, P., Sondek, J., and Dangl, J.L. (2005a). The *Pseudomonas syringae* effector AvrRpt2 cleaves its C-terminally acylated target, RIN4, from *Arabidopsis* membranes to block RPM1 activation. *Proc Natl Acad Sci U S A* 102, 6496-6501.

Kim, M.-G., da Cunha, L., Belkadir, Y., DebRoy, S., Dangl, J.L., and Mackey, D. (2005b). Two *Pseudomonas syringae* type III effectors inhibit RIN4-regulated basal defense in *Arabidopsis*. *Cell* 121, 749-759.

Luo, Y., Caldwell, K.S., Wroblewski, T., Wright, M.E., and Michelmore, R.W. (2009). Proteolysis of a negative regulator of innate immunity is dependent on resistance genes in tomato and *Nicotiana benthamiana* and induced by multiple bacterial effectors. *Plant Cell* 21, 2458-2472.

Mackey, D., Belkhadir, Y., Alonso, J.M., Ecker, J.R., and Dangl, J.L. (2003). *Arabidopsis* RIN4 is a target of the type III virulence effector AvrRpt2 and modulates RPS2-mediated resistance. *Cell* 112, 379-389.

Mackey, D., Holt III, B.F., Wiig, A., and Dangl, J.L. (2002). RIN4 interacts with *Pseudomonas syringae* Type III effector molecules and is required for RPM1-mediated disease resistance in *Arabidopsis*. *Cell* 108, 743-754.

Murashige, T., and Skoog, F. (1962). A revised medium for rapid growth and bioassays with tobacco tissue cultures. *Physiol Plant* 15, 473-497.

Nimchuk, Z., Marois, E., Kjemtrup, S., Leister, R.T., Katagiri, F., and Dangl, J.L. (2000). Eukaryotic fatty acylation drives plasma membrane targeting and enhances function of several Type III effector proteins from *Pseudomonas syringae*. *Cell* 101, 353-363.

Nomura, K., Melotto, M., and He, S.Y. (2005). Suppression of host defense in compatible plant-*Pseudomonas syringae* interactions. *Curr Opin Plant Biol* 8, 361-368.

Ntoukakis, V., Mucyn, T.S., Gimenez-Ibanez, S., Chapman, H.C., Gutierrez, J.R., Balmuth, A.L., Jones, A.M., and Rathjen, J.P. (2009). Host inhibition of a bacterial virulence effector triggers immunity to infection. *Science* 324, 784-787.

Nuhse, T.S., Bottrill, A.R., Jones, A.M., and Peck, S.C. (2007). Quantitative phosphoproteomic analysis of plasma membrane proteins reveals regulatory mechanisms of plant innate immune responses. *Plant J* 51, 931-940.

Rosebrock, T.R., Zeng, L., Brady, J.J., Abramovitch, R.B., Xiao, F., and Martin, G.B. (2007). A bacterial E3 ubiquitin ligase targets a host protein kinase to disrupt plant immunity. *Nature* 448, 370-374.

Schechter, L.M., Roberts, K.A., Jamir, Y., Alfano, J.R., and Collmer, A. (2004). *Pseudomonas syringae* type III secretion system targeting signals and novel effectors studied with a Cya translocation reporter. *J Bacteriol* 186, 543-555.

Shan, L., He, P., Li, J., Heese, A., Peck, S.C., Nurnberger, T., Martin, G.B., and Sheen, J. (2008). Bacterial effectors target the common signaling partner BAK1 to disrupt multiple MAMP receptor-signaling complexes and impede plant immunity. *Cell Host Microbe* 4, 17-27.

- Shao, F., Golstein, C., Ade, J., Stoutemyer, M., Dixon, J.E., and Innes, R.W. (2003). Cleavage of Arabidopsis PBS1 by a bacterial type III effector. *Science* 301, 1230-1233.
- Takken, F.L., and Tameling, W.I. (2009). To nibble at plant resistance proteins. *Science* 324, 744-746.
- Takken, F.L.W., Albrecht, M., and Tameling, W.I.L. (2006). Resistance proteins: molecular switches of plant defence. *Current Opinion in Plant Biology* 9, 383-390.
- Ting, J.P., Duncan, J.A., and Lei, Y. (2010). How the noninflammasome NLRs function in the innate immune system. *Science* 327, 286-290.
- Ting, J.P., Willingham, S.B., and Bergstralh, D.T. (2008). NLRs at the intersection of cell death and immunity. *Nat Rev Immunol* 8, 372-379.
- Tornero, P., Chao, R., Luthin, W., Goff, S., and Dangl, J.L. (2002). Large scale structure-function analysis of the Arabidopsis *RPM1* disease resistance protein. *Plant Cell* 14, 435-450.
- van Ooijen, G., van den Burg, H.A., Cornelissen, B.J., and Takken, F.L. (2007). Structure and function of resistance proteins in solanaceous plants. *Annu Rev Phytopathol* 45, 43-72.
- Wang, Y., Li, J., Hou, S., Wang, X., Li, Y., Ren, D., Chen, S., Tang, X., and Zhou, J.M. (2010). A *Pseudomonas syringae* ADP-ribosyltransferase inhibits Arabidopsis mitogen-activated protein kinase kinases. *Plant Cell* 22, 2033-2044.
- Wilton, M., Subramaniam, R., Elmore, J., Felsensteiner, C., Coaker, G., and Desveaux, D. (2010). The type III effector HopF2Pto targets Arabidopsis RIN4 protein to promote *Pseudomonas syringae* virulence. *Proc Natl Acad Sci U S A* 107, 2349-2354.
- Zhang, J., Li, W., Xiang, T., Liu, Z., Laluk, K., Ding, X., Zou, Y., Gao, M., Zhang, X., Chen, S., *et al.* Receptor-like cytoplasmic kinases integrate signaling from multiple plant immune receptors and are targeted by a *Pseudomonas syringae* effector. *Cell Host Microbe* 7, 290-301.

## CHAPTER 4

### CONCLUSIONS and FUTURE DIRECTIONS

#### **BACKGROUND AND SIGNIFICANCE**

RPM1 is an NB-LRR protein composed of Nucleotide-Binding site (NB) and Leucine Rich Repeat (LRR) domains, as are most other plant disease resistance (R) proteins (Moffett, 2009; Takken et al., 2006). For immune responses, RPM1 associates with RIN4, a common host target of the bacterial type III effectors AvrB and AvrRpm1. Modification of RIN4 by phosphorylation by these effectors is recognized by RPM1 and initiates an RPM1-mediated immune response. RIN4 interacts with AvrB and AvrRpm1 (Mackey et al., 2002). In Chapter 2, size exclusion chromatography (SEC), a common method to identify proteins complexes, demonstrated protein complexes with RPM1 or RIN4 *in vivo*. RPM1-containing protein complexes ranged from 500 kDa to an apparently high molecular weight of 1 MDa. RIN4-associated protein complexes were mainly detected from 200 kDa to 300 kDa, where AvrRpm1 and AvrB were also detected. Notably, effector phosphorylated RIN4 was identified in protein complexes around 300 kDa. I did not observe a significant alteration of RPM1 and RIN4 protein complexes after delivery or expression of effector proteins indicating that a transient mechanism underlies the activation of RPM1 through RIN4

in our experimental conditions. By Co-IP coupled mass spectrometry analysis from microsomal extracts of RPM1:myc and AvrRpm1-expressing RPM1:myc transgenic plants, some candidate interactors, possibly associated with RPM1, were identified. Several of these had also been identified by independent MS-based approaches in other labs. However, more experimental repeats to confirm the functional significance of the interaction candidates are still required.

Detailed evidence demonstrating the mechanistic features of RPM1 and its interacting protein, RIN4, has been presented in Chapter 3 (Chung et al., 2011). The region of RIN4 sufficient for RPM1-mediated immune responses triggered by AvrRpm1 and AvrB is the C-terminal RIN4<sub>142-211</sub> region, which contains the AvrB-binding site (BBS) (Desveaux et al., 2007). This region, previously co-crystallized with AvrB, is necessary for RPM1 activation by both effectors. A series of missense point mutations in RIN4<sub>142-176</sub> identifies two important residues for activation and interaction of RIN4 with RPM1: threonine 166 in RIN4 is required for full activation of AvrB-dependent HR by RPM1. Phosphomimic (T166D and T166E) mutants support effector-independent activation of RPM1 via P-loop function, a critical region of NB-LRR proteins for activation in response to effectors. Substitution of threonine166 to alanine abolishes the host immune response triggered by AvrB completely and by AvrRpm1 partially. T166 is phosphorylated *in vivo* in the presence of AvrB or AvrRpm1. A RIN4 phenylalanine 169 mutant (F169A) loses interaction with AvrB and cannot be co-immunoprecipitated with RPM1, defining a common interaction platform required for activation. Hence, AvrB and AvrRpm1 activate RPM1 by the

phosphorylation of RIN4 T166. The current working model of RPM1 after phosphorylation by AvrB is presented in Figure 4.1.

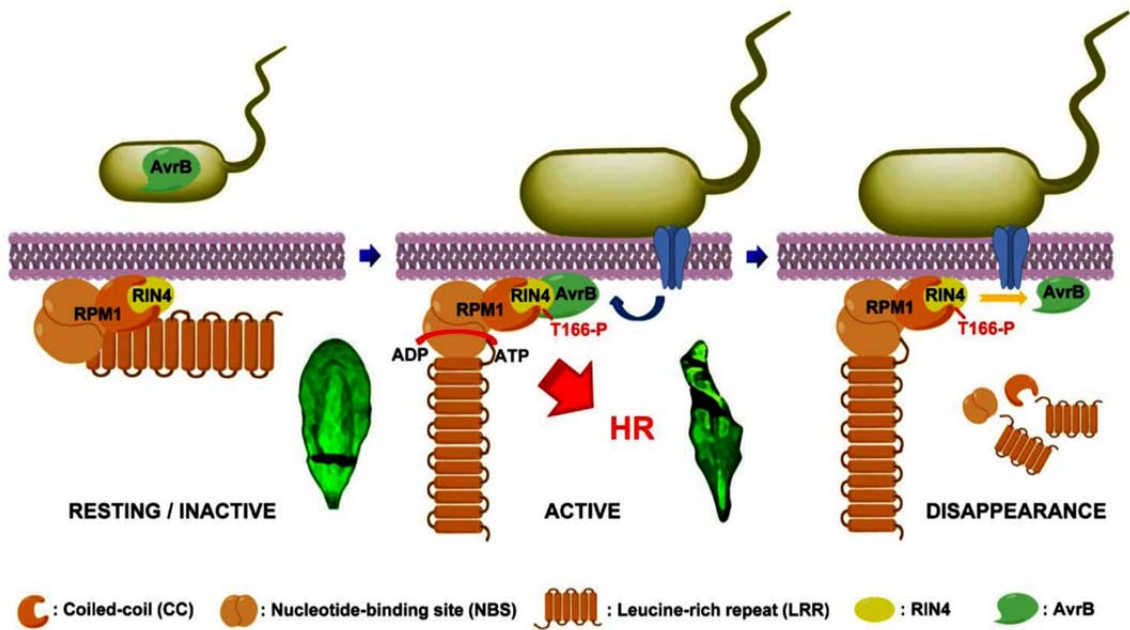


**Figure 4.1. Working model of RPM1-mediated HR with RIN4 phosphorylation on T166**

Inactive RPM1 is folded via intra-molecular interaction and associates with RIN4 (left). AvrB triggers phosphorylation of the RIN4 T166 residue resulting in recognition of RIN4 by RPM1 and subsequent hypersensitive response (HR) (middle). AvrB dissociates from phosphorylated RIN4 (right).

## **FUTURE DIRECTIONS**

Much work remains to be done, especially for the work presented in Chapter 2 to provide clear evidence for RPM1-associated immune complexes. The distribution of RIN4 by SEC was monitored through immunoblot with anti-RIN4 which showed cross-reactivity in the apparent high molecular weight (HMW) complexes. In this work, I considered RIN4 detected in the HMW as a background signal based on its presence in the *rin4* mutant. However, redistribution of RIN4 to HMW after delivery of effector proteins for RPM1 activation cannot be excluded because RIN4 in the HMW protein complexes simply may be masked by the non-specific signal. I generated native expression level *RPM1:myc T7:RIN4* transgenic Arabidopsis (Chapter 3). Interaction and function of both epitope tagged proteins was confirmed. Thus, it will be possible use the respective epitope tags to characterize the RPM1 and RIN4-associated protein complexes. Combined with SEC experiments, the Blue Native Polyacrylamide Gel Electrophoresis (BN-PAGE) can be adapted to monitor multi-protein complexes for RPM1 and RIN4 because BN-PAGE can distinguish both constitutive/abundant and signal-induced transient/low abundant complexes with higher resolution than gel filtration or sucrose density ultracentrifugation in range from 10 kDa to 10 mDa (Camacho-Carvajal et al., 2004). A preliminary result has been obtained with RIN4 wild type or RIN4 T166D in *RPM1:myc rpm1 rps2 rin4* as an “inactive” and “active” states of RPM1 (Figure 4.2).

One dimensional BN-PAGE followed by immunoblotting with  $\alpha$ -myc and  $\alpha$ -T7 showed that RPM1 is widely distributed from 150 kDa over 720 kDa in RIN4 wild type (“inactive”), consistent with the SEC data presented (blue asterisk), while a

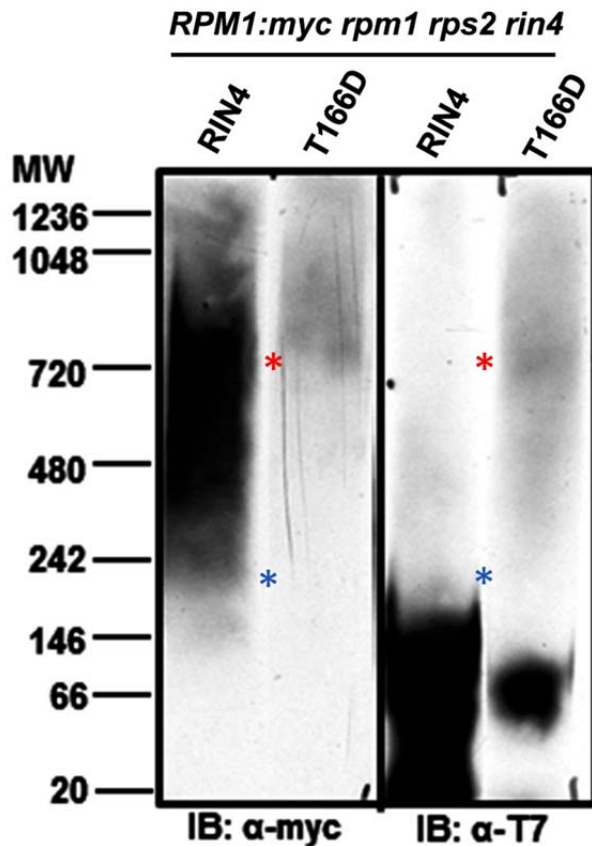


**Figure 4.2. RPM1 complexes in an “inactive” and “active” state in Arabidopsis**

Multiprotein complexes of RPM1 and RIN4 were determined by Blue Native Polyacrylamide Gel Electrophoresis (BN-PAGE). Triton X-100 (0.5%) was used to extract protein complexes. RIN4 and T166D (pRIN4:T7:RIN4/T166D; Chapter 3) in *RPM1:myc rpm1 rps2 rin4* represent the “inactive” and “active” state of RPM1-mediated immune response, respectively. Microsomal fractions from each genotype were used to determine protein complexes. Immunoblot with anti-myc and anti-T7 detects protein complexes which contain both or either RPM1 or RIN4. Once RPM1 is activated by RIN4 T166D, RPM1 associated with the phosphomimic RIN4 in the high molecular weight (~750 kDa) and the low molecular weight (~66 kDa), while the expression level of RPM1 was decreased much.

weak RPM1 band was detected in protein complexes of approx. 700 kDa in the “active” state (red asterisk) consistent with the disappearance of RPM1 post activation (Chung et al., 2011; Mackey et al., 2002). “Inactive” RIN4 distributed between 20 kDa and 200 kDa (Blue asterisk). Notably, “active”, phosphomimic RIN4 (T166D) migrated also at 720 kDa, where RPM1 existed in the “active” state (red asterisk) as well. Therefore, BN-PAGE would be a very useful tool to monitor RPM1 and RIN4-related protein complexes before and after the effector dependent elicitation of RPM1-mediated immune responses. Broadening BN-PAGE from 1D to 2D analysis would also be beneficial to identify other components in RPM1 and RIN4 protein complexes. Moreover, potential interaction candidates from Co-IP coupled MS analysis using medium stringency washing can provide comprehensive information for RPM1 and RIN4-associated immune complexes in Arabidopsis.

As shown in chapter 3, the T166 residue of RIN4 can be phosphorylated and is important for ETI mediated by RPM1. RIN4 has a dual role as a negative regulator of PTI and ETI (Chung et al., 2011; Kim et al., 2005; Mackey et al., 2002). Increased phosphorylation of RIN4 by AvrRpm1 and AvrB occurs in the absence of RPM1 (Mackey et al., 2002). This gives rise to the question of whether the RIN4 T166 residue contributes to the negative function of RIN4 in PTI. To confirm the PTI-related phenotype by phosphorylation of RIN4 T166 residue, I generated RIN4 wild type, T166A and T166D mutant in the *rpm1* mutant background (*rpm1 rps2 rin4*) by crossing. These plants can be utilized immediately to investigate the role of phosphorylation of the T166 residue with regard to the virulence function of AvrRpm1, possibly AvrB, and PTI against virulent bacteria. Recently, other potential

phosphorylation sites in RIN4, T21, S47, S141 and S160 were detected (Benschop et al., 2007; Liu et al., 2011; Nuhse et al., 2007; Nuhse et al., 2004), although the biological and pathological relevance was not clearly addressed. A PAMP-peptide, flg22, induces RIN4 phosphorylation by the action of MPK4 *in vitro*. AvrB phosphorylates MPK4 with physical interaction (Cui et al., 2010). RIPK (a receptor-like protein kinase) phosphorylates both AvrB and RIN4 (Liu et al., 2011). However, it is not obvious what phosphorylation sites are required for both or either AvrB-/PAMP-triggered RIN4 phosphorylation. As a part of my researches which is not included in this dissertation, I generated Arabidopsis transgenic plants which contain RIN4 S47 and S141 residues substituted with alanine (A) or glutamic acid (E) in the presence / absence of RPM1 (in *rps2 rin4* or *rpm1 rps2 rin4*) to investigate the role of both residues for phosphorylation in ETI (*RPM1*) and PTI (*rpm1*) responses. Preliminary data indicates slightly enhanced callose deposition (Figure 4.3A), a PTI phenotype, in S141E and S47E S141E mutants without flg22 treatment, while S141A and S47A S141A mutants lose the ability to accumulate callose in response to flg22 (Figure 4.3B). Interestingly, the S141 residue of RIN4 is adjacent to the proline residue (P142) where MPK4 phosphorylates its substrate MKS1 (MPK4 substrate 1) *in vitro* (Caspersen et al., 2007). Thus, I will further investigate whether the known phosphorylation sites in RIN4 are phosphorylated by putative kinases such as RIPK and MPK4 during PTI response. The phosphorylation of RIN4 at T166 is required for AvrB-triggered HR via RPM1 activation (Chung et al., 2011; Chapter 3). However, high phosphorylation levels of T166 are required for AvrRpm1-induced RPM1 activation (Mackey et al., 2002). So far, we detected RIN4 protein by mass

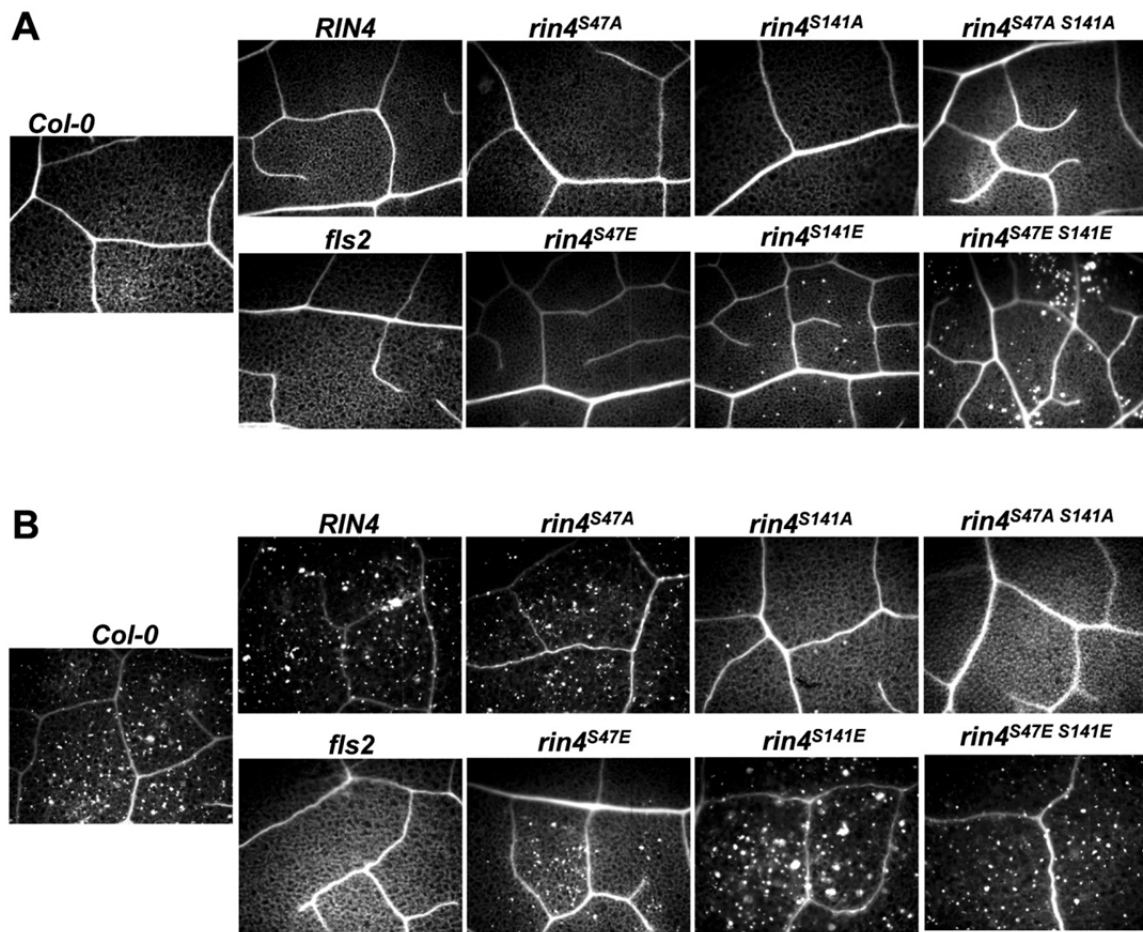


**Figure 4.3. PAMP-triggered phenotype of RIN4 phosphorylation mutants**

- (A) Callose deposition of RIN4 mutants without elicitation by flg22. Two possible flg22 dependent phosphorylation sites (S47 and S141) of RIN4 (Nushe et al., 2006) were mutated to alanine (phospho-dead) or glutamate (phospho-mimic) in one or both residues under the control of the RIN4 native promoter, and transformed into *rpm1 rps2 rin4* background to monitor the effect on PAMP-triggered immunity. Callose deposition of 5-week-old transgenic plants including positive (Col-0) and negative control (*fls2*) were monitored by aniline blue staining to visualize callose accumulation in each plant. Water was infiltrated with a needleless syringe. Samples were harvested 24 hours post infiltration.
- (B) Callose deposition of RIN4 mutants after elicitation by flg22. Same experiment as in (A) except for infiltration of the flg22 peptide (2 $\mu$ M).

spectrometry after enrichment by *Agrobacterium*-mediated transient assays in *Nicotiana benthamiana*. Therefore, identification of phosphorylation sites in RIN4 by co-infiltration with and without AvrB and AvrRpm1 is feasible and will provide evidence to dissect AvrB- and AvrRpm1-induced HR., Furthermore, it will allow us to examine how these two different effector proteins involved in PTI and virulence affect RIN4 phosphorylation.

Autoactive RPM1 alleles (D287A and D505V) were studied with my contribution (Gao et al., 2011). Each mutant exists in the NB domain of RPM1 where ATP binding and hydrolysis may occur. D287A, a mutation in the Walker B motif of RPM1, is a weak allele compared to the MHD mutant (D505V). The D129A mutant of the transcription factor MalT is analogous to D287A of RPM1, is constitutively active and binds to ATP without hydrolysis activity (Marquenet and Richet, 2007). The D505V variant is a strong allele which seems to be fully activated because HR from infiltration of D505V was comparable to HR obtained from co-infiltration of RPM1 wild type or D505V with RIN4 T166D (Figure 4.4). Both autoactive alleles are suppressed by RIN4 fully for D287A and partially for D505V. Strikingly, weak autoactivity of D287A or RPM1 can be increased with RIN4 T166D, and is suppressed by RIN4 T166A. However, autoactivity from D505V allele was not enhanced with RIN4 T166D mutant and not suppressed by RIN4 T166A, suggesting that D505V can be fully active allele of RPM1. This leads us to speculate that RIN4 can contribute to full activation of the D287A allele with respect to ATP hydrolysis, while D505V, the fully active allele, seems to by-pass the required contribution of

RIN4 to ATP hydrolysis. Thus, RPM1 may require ATP hydrolysis for its full activation.

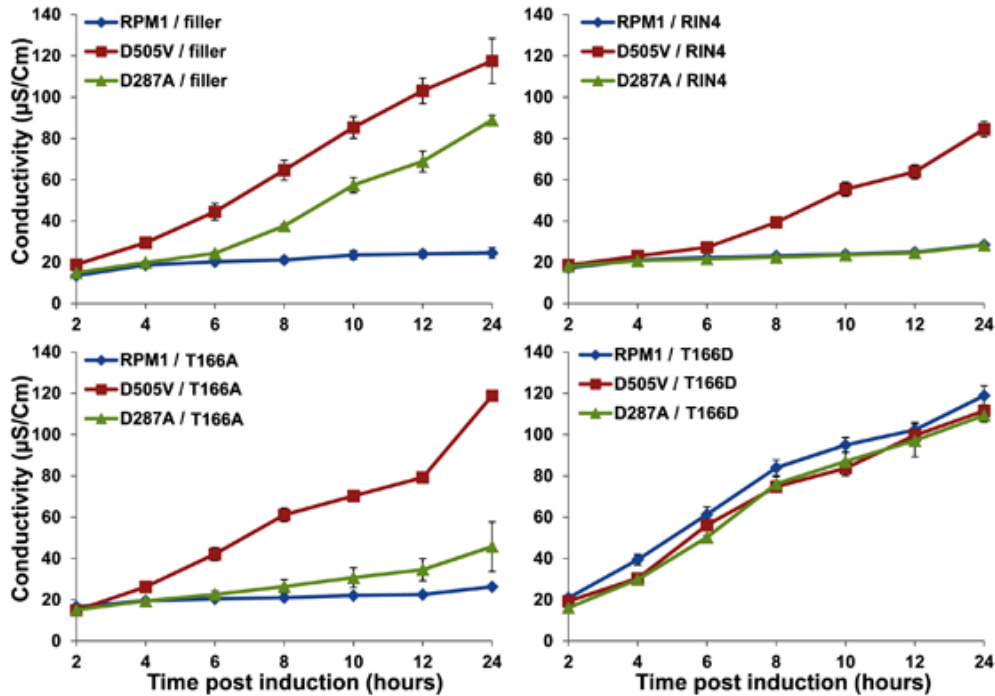


**Figure 4.4. Phenotypes of autoactive RPM1 alleles with RIN4 and RIN4 mutants**

Cell death (HR) was determined by conductivity measurement after infiltrating wt RPM1 and mutated RPM1 variants with or without RIN4 into *Nicotiana benthamiana*. The RPM1 Walker B mutant, D287A, exhibited a weak activation compared to the MHD variant, D505V (top left). RIN4 suppresses the autoactivity of D287A fully, and of D505V partially (top right). D505V is partial in top right. The loss of function mutant of RIN4 (T166A) for AvrB-triggered RPM1-mediated immune response (Chung et al., 2011; chapter 3) only suppresses D287A (bottom left). The RIN4 T166D mutant which can trigger effector-independent RPM1 activation (Chung et al., 2011; chapter 3) enhances D287A-mediated full activation and does not display additive activation for D505V mutant (bottom right). Agrobacteria containing RPM1 and RIN4 constructs were infiltrated at  $OD_{600} = 0.3$ . Estradiol ( $30\mu\text{M}$ ) was used to induce RPM1 variants two days post infiltration. All RIN4 constructs are expressed under control of their native promoter.

## **REFERENCES**

Benschop, J.J., Mohammed, S., O'Flaherty, M., Heck, A.J., Slijper, M., and Menke, F.L. (2007). Quantitative phosphoproteomics of early elicitor signaling in Arabidopsis. *Mol Cell Proteomics* 6, 1198-1214.

Camacho-Carvajal, M.M., Wollscheid, B., Aebersold, R., Steimle, V., and Schamel, W.W. (2004). Two-dimensional Blue native/SDS gel electrophoresis of multi-protein complexes from whole cellular lysates: a proteomics approach. *Mol Cell Proteomics* 3, 176-182.

Caspersen, M.B., Qiu, J.L., Zhang, X., Andreasson, E., Naested, H., Mundy, J., and Svensson, B. (2007). Phosphorylation sites of Arabidopsis MAP kinase substrate 1 (MKS1). *Biochimica et biophysica acta* 1774, 1156-1163.

Chung, E.H., da Cunha, L., Wu, A.J., Gao, Z., Cherkis, K., Afzal, A.J., Mackey, D., and Dangl, J.L. (2011). Specific Threonine Phosphorylation of a Host Target by Two Unrelated Type III Effectors Activates a Host Innate Immune Receptor in Plants. *Cell Host & Microbe* 9, 125-136.

Cui, H., Wang, Y., Xue, L., Chu, J., Yan, C., Fu, J., Chen, M., Innes, R.W., and Zhou, J.M. (2010). Pseudomonas syringae effector protein AvrB perturbs Arabidopsis hormone signaling by activating MAP kinase 4. *Cell Host Microbe* 7, 164-175.

Desveaux, D., Singer, A.U., Wu, A.J., McNulty, B.C., Musselwhite, L., Nimchuk, Z., Sondek, J., and Dangl, J.L. (2007). Type III effector activation via nucleotide binding, phosphorylation, and host target interaction. *PLoS Pathog* 3, e48.

Gao, Z., Chung, E.H., Eitas, T.K., and Dangl, J.L. (2011). Plant intracellular innate immune receptor RPM1 is activated at, and functions on, the plasma membrane. *PNAS* in press.

Kim, M.G., da Cunha, L., McFall, A.J., Belkhadir, Y., DebRoy, S., Dangl, J.L., and Mackey, D. (2005). Two Pseudomonas syringae type III effectors inhibit RIN4-regulated basal defense in Arabidopsis. *Cell* 121, 749-759.

Liu, J., Elmore, J.M., Lin, Z.J., and Coaker, G. (2011). A Receptor-like Cytoplasmic Kinase Phosphorylates the Host Target RIN4, Leading to the Activation of a Plant Innate Immune Receptor. *Cell Host & Microbe* 9, 137-146.

Mackey, D., Holt, B.F., 3rd, Wiig, A., and Dangl, J.L. (2002). RIN4 interacts with Pseudomonas syringae type III effector molecules and is required for RPM1-mediated resistance in Arabidopsis. *Cell* 108, 743-754.

Marquenet, E., and Richet, E. (2007). How integration of positive and negative regulatory signals by a STAND signaling protein depends on ATP hydrolysis. *Molecular Cell* 28, 187-199.

Moffett, P. (2009). Mechanisms of recognition in dominant R gene mediated resistance. *Adv Virus Res* 75, 1-33.

Nuhse, T.S., Bottrill, A.R., Jones, A.M., and Peck, S.C. (2007). Quantitative phosphoproteomic analysis of plasma membrane proteins reveals regulatory mechanisms of plant innate immune responses. *Plant J* 51, 931-940.

Nuhse, T.S., Stensballe, A., Jensen, O.N., and Peck, S.C. (2004). Phosphoproteomics of the Arabidopsis plasma membrane and a new phosphorylation site database. *Plant Cell* 16, 2394-2405.

Takken, F.L.W., Albrecht, M., and Tameling, W.I.L. (2006). Resistance proteins: molecular switches of plant defence. *Current Opinion in Plant Biology* 9, 383-390.